Capacitive Grounding for DC Distribution Grids with Multiple Grounding Points

F. Kenji Yáñez Martínez

Technische Universiteit Delft

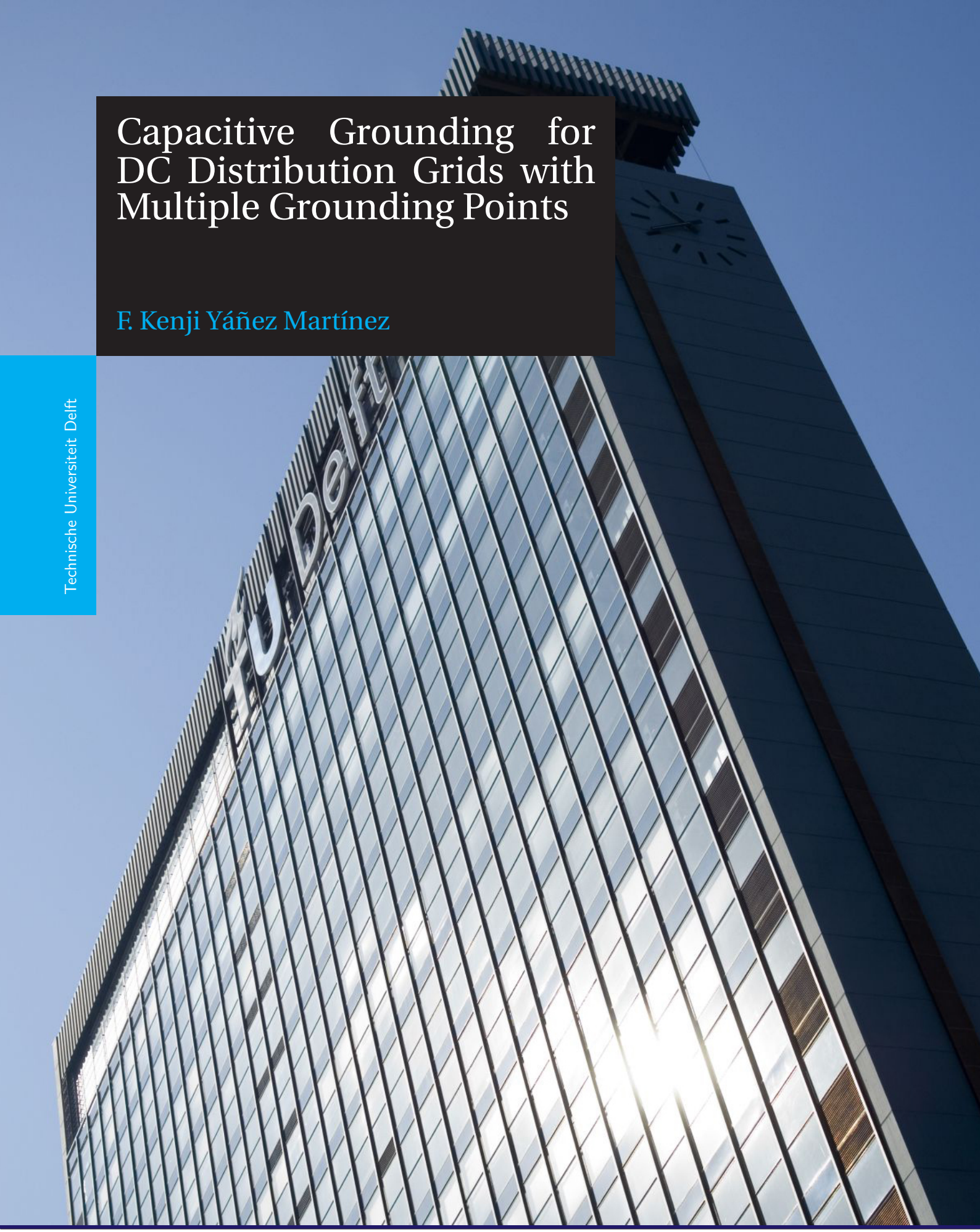

TU Delft Delft University of Technology

Challenge the future

Capacitive Grounding for DC Distribution Grids with Multiple Grounding Points

by

F. Kenji Yáñez Martínez

in partial fulfillment of the requirements for the degree of

Master of Science

in Sustainable Energy Technology

at the Delft University of Technology,

to be defended publicly on August 28th, 2017 at 13:00 h.

Student number:	4517431	
Project duration:	November 2nd, 2016 – August 28th, 2017	
Daily Supervisor:	Dr. ir. L. Ramirez Elizondo	
Advisor:	Laurens Mackay	
Thesis committee:	Prof. dr. eng. P. Bauer,	TU Delft
	Dr. ir. M. Popov,	TU Delft
	Dr. ir. M. Ghaffarian Niasan,	TU Delft

This thesis is confidential and cannot be made public until September 1st, 2018.

TU Delft Delft University of Technology

Abstract

DC Microgrids could play an important role in a renewable and sustainable future. Unfortunately, there are not enough standards or guidelines for the implementation of DC Microgrids or DC distribution grids in general. Nevertheless, reliability and security of such a system must be assured at all times. As a consequence, an important challenge lies in terms of protection.

This thesis project focuses on capacitive grounding and their respective ground fault detection and protection scheme for a general DC distribution grid. The protection scheme proposed aims to discriminate currents caused by load shifts from ground fault currents with as little communication between the protective relays as possible.

The safety requirements needed for a DC distribution system are analyzed and threshold values for current that may endanger the human body are derived from literature. A scheme using capacitive grounding is analyzed further through a sensitivity analysis for capacitor size. This analysis serves as a starting point to determine an important challenge for the discrimination of currents caused by load shifts and human faults. A detection scheme is proposed to differentiate these currents and demonstrated with Matlab Simulink.

An analysis showing the behavior of the system to increasing number of grounding points using this detection scheme is further discussed and studied by means of state space representation. This analysis helps as a starting point for the scalability of DC distribution systems with capacitive grounding.

Acknowledgements

Above all, I would like to thank my wife, Leslie, for her patience these last two years, for her relentless love and for always being there when I needed it the most.

I would like to thank Laurens Mackay, who helped me realize this project. Without his admirable attitude, advice, and vision I would not have been able to finalize this thesis.

F. Kenji Yanez Martinez, Delft, August 2017

CONTENTS

List of Figures

List of Tables

1

INTRODUCTION

1.1. MOTIVATION

Energy production and distribution will play a very important role in the upcoming years. Currently World's energy demand accounts for more than 20 TWh of energy, which according to Energy Information Administration [1] will increase up to 38 TWh [1] . Modern society depends on a steady supply of energy.

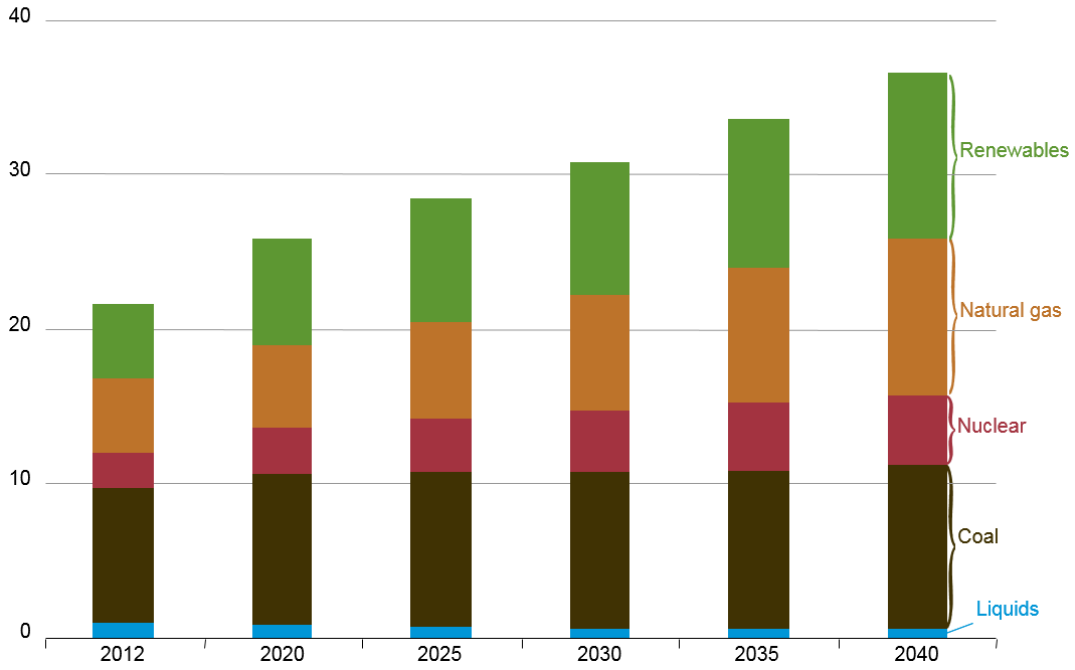

Figure 1.1: World net electricity generation by energy source in trillion watthours, 2012

If a renewable energy future is to be achieved, important changes have to be implemented to today's energy production and distribution systems. Energy has to be produced and transported ensuring stability and availability for all end users [2]. Renewable energies prove to be a feasible solution to future energy requirements but with their large scale implementation, new challenges appear.

Regardless of which renewable energy technology will be the most prominent, sun based renewable energies such as PV and Wind share one disadvantage: their stochastic behavior. These renewable technologies

[1] 1 trillion=10^{12}=1 Tera

unlike conventional energy generation systems cannot be controlled in terms of production. Nevertheless, their energy generation potential promises to overthrow conventional fossil fuels technologies with electricity as the main energy carrier. A match between consumption and production from stochastic energy resources has to be overcome if large scale renewable energy technologies are to be implemented.

Future electrical distribution grids have to cope with renewable energy technologies while ensuring the grid security, operation safety, protection, power quality and efficiency [2]. A relatively new concept emerges to solve this challenge: the Smart Grid. A smart grid is an electrical transmission network that by means of intelligent control can integrate the actions of energy generators and energy consumers whilst delivering sustainable, economic and secure electricity. This type of network can ease the integration of Distributed Generation, Renewable Energy Sources, and Energy Storage Systems [2]. Smart Grids are also a platform for new technologies and services that follow the main objective of linking power generation with power demand.

Moreover, as a result of the gradual improvement of renewable energy technology, microgeneration technologies such as home photovoltaic, micro wind power, domestic solar thermal systems and domestic combined heat and power have been steadily penetrating the low voltage energy market [3]. As a mean to integrate distributed generation on a low voltage level as a result of the increase in microgeneration units an adaptation of a Smart Grid on a low voltage scale demonstrates to be of great use. For the scope of this thesis project a Microgrid will be defined as the following according to [2],[4]:

"A Microgrid comprise a LV distribution system with distributed energy resources (micro-turbines, fuel cells, PV, etc.) together with storage devices (flywheels, energy capacitors and batteries) and flexible loads. Such systems can be operated in a non-autonomous way, if interconnected to the grid, or in an autonomous way, if disconnected from the main grid. The operation of microsources in the network can provide distinct benefits to the overall system performance, if managed and coordinated efficiently".

1.1.1. AC-MICROGRIDS VS DC-MICROGRIDS

In this Section a brief comparison between two system topologies which aim to integrate renewable based distributed generation units will be shown. First an overview of low voltage AC and low voltage DC Microgrid systems is provided. AC and DC topologies will be shown to exemplify the two systems.

AC MICROGRID SYSTEM

An AC microgrid system can be integrated by DC and AC systems with distributed generation units and electrical storage systems connected with the distribution network. Nevertheless, a part of the network which consists of the distributed units and loads form an AC Power System. In Figure 1.2 a general AC Microgrid system is shown.

As defined before these two networks can operate interconnected or if required in islanded mode. The main characteristic of an AC microgrid system is that during operation the network adopts the voltage and frequency standards applied in most conventional distribution systems which are clearly defined.

DC MICROGRID SYSTEM

Most of domestic LV equipments are inherently DC which have embedded power electronic devices (computers, cell phones, TVs, etc). Nevertheless, these devices need power electronic components in order to convert the AC power into DC power. As such, renewable distributed generation sources based on DC require also a conversion stage in order to be coupled with the existing AC Network. In Figure 1.3 a general topology of a DC Microgrid is shown.

In contrast with an AC microgrid the bulk of the network which consists of the DG units and loads form an isolated DC Power System with only DC/AC converters when AC loads have to be provided. Looking at Figure 1.3 the DC Microgrid is a simpler topology with a straightforward structure. Furthermore, the use of less power conversion stages increases the efficiency of the systems at by default lowers its cost.

The bipolar configuration enables the loads to be connected across the positive conductor and middle conductor which is neutral or between positive and negative conductor having increasing voltage for higher voltage loads. It is evident that in actual applications this could lead to asymmetric loading of the grid, causing increased voltage magnitudes for the nodes of the neutral conductor [6]. The low voltage DC links can be based on unipolar and bipolar configurations as shown in Figure 1.4.

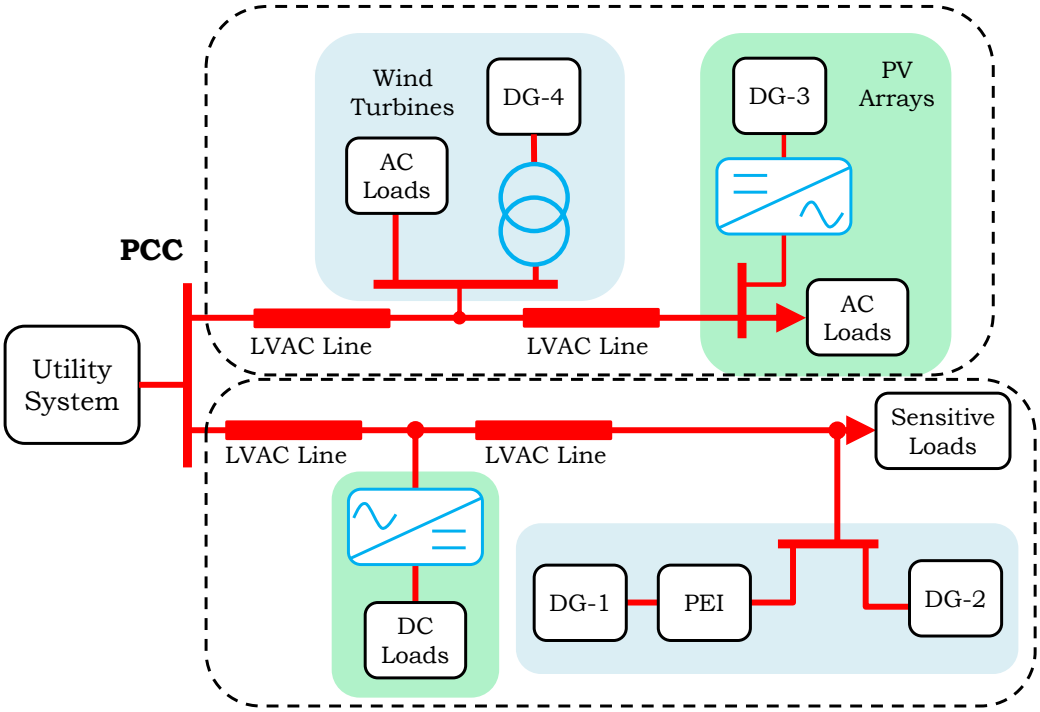

Figure 1.2: General AC Microgrid Topology. [5]

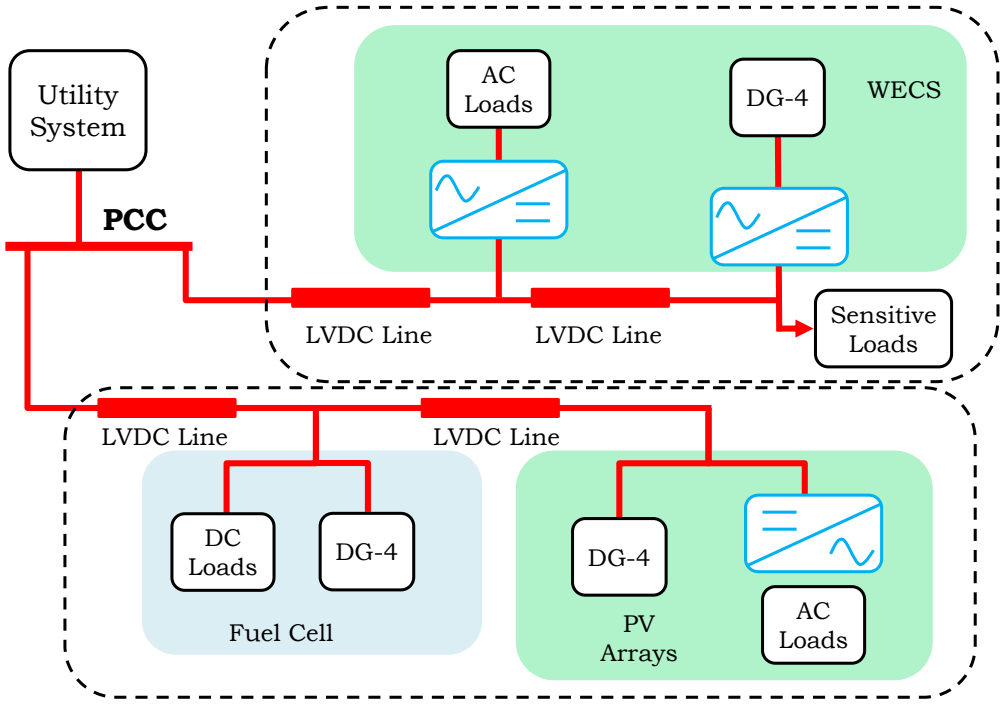

Figure 1.3: General DC Microgrid Topology. [5]

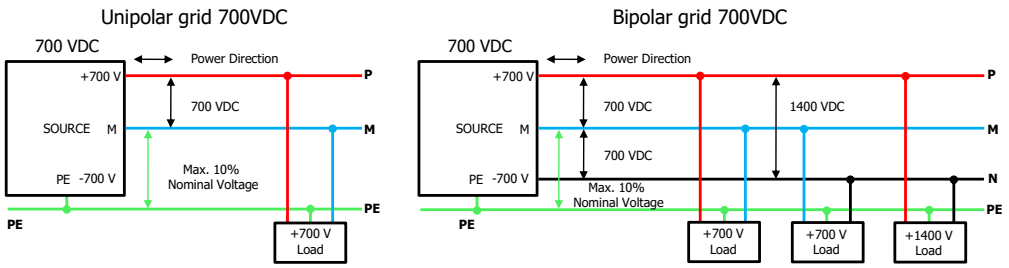

Figure 1.4: Unipolar and Bipolar Configuration of a DC Grid

1.2. PROBLEM DEFINITION

Although DC microgrids prove to be a solution for future energy systems many challenges have to be overcome. Potential areas of improvement are the grounding system, protection devices, power converters and battery protection methods [5]. Considering a DC bipolar network the main challenge as mentioned before is the protection scheme. Under this scope the grounding protection and its respective detection is of critical importance to ensure the system against ground faults and leakage currents. An interesting solution for grounding configuration is capacitive grounding. Since this is a new topic the literature is scarce, but still the requirements of such a scheme can be defined.

The grounding configuration analyzed through this thesis has the following restrictions:

- The grid can be meshed; it doesn't follow the standard radial distribution.
- The network is bipolar with +350 V on the positive conductor, 0 V (metallic return) on the middle conductor and -350 V on the negative conductor.
- The protection has to cope with the IEC Standard 60479 [7].
- The protection should not trip in case of load change or load unbalance.
- The protection should react fast enough to ensure safety of the users of the network.
- The network can be grounded at multiple locations.

1.3. OBJECTIVE

The objective of this Thesis is to determine a capacitive residual ground fault protection and detection scheme for a bipolar DC network that can discriminate between ground currents due to unbalance change and human touch. Thus, enabling normal operation of the network whilst ensuring safety of end users and equipment avoiding communication between protective relays when is not needed.

1.4. RESEARCH QUESTIONS

In order to exemplify the objective above mentioned the research questions intended to be solved by this thesis are the following:

- What is the effect of the capacitor size in the capacitive grounding scheme?

If capacitive grounding is to be implemented as a grounding scheme for a DC distribution grid its effects have to be known. The intention of this question is to determine the sensibility of a given DC distribution system to capacitor size.

- How can communication for fault triggering be omitted on a radial section of a DC distribution grid?

The intention of this question is to determine under which circumstances the communication between the protection devices can be omitted in order to optimize the system design and reduce costs.

- How can human ground faults and load changes be differentiated on a detection scheme for DC distribution grids?

The reason for communication is to be able to differentiate normal operating values from faulted values. The need of communication may be ommitted if the right conditions are met or if a proper detection scheme is implemented without the need of it.

- What would be a consequence of increasing the number of grounding points?

The intention of this question is to understand the consequences of increasing number of grounding points on a DC distribution grid. The reason of this question is to determine if the scalability of such a system is possible and under which considerations.

REPORT OUTLINE

At the outset of each chapter an introduction to the main topic will be given in order to explain the importance of protection in LVDC networks. At the end of each chapter a short conclusion summarizing the most important ideas is also given.

A more detailed description of the main challenges of a DC distribution system are introduced in Chapter 2 with an analysis of the requirements that such a system has to meet.The possible grounding configurations that could be used for a DC distribution grid are studied from literature. The effects of DC current flowing through the human body are analyzed to delimit threshold values that will be used in the following chapters for the protection and detection scheme. Capacitive grounding is explained from previous work done as an interesting choice to prevent corrosion on a DC grid.

Chapter 3 discusses in more detail capacitive grounding along with the grid configurations that are addressed throughout this thesis project. A sensitivity analysis by means of simulations done with software Matlab Simulink is presented to show the system behavior to different capacitance values. The focus is done to test the system when load power demand is changed suddenly and how the capacitance values affect the system response.

With the results presented in the previous Chapter the challenges of the protection scheme to discriminate ground faults from load change currents are described in Chapter 4. The approach for the system detection scheme studied by means of a filter is discussed with simulations done in Matlab Simulink. The filter is shown as a possible solution to discriminate ground fault currents from currents caused by load changes. A detection map is presented and compared with the threshold values of currents that may harm the human body that were discussed before.

Since the scalability of capacitive grounding is one of the main research questions, Chapter 5 is focused to study the behavior of a simple unipolar grid with increasing grounding points and with two different network arrangements. The analysis is done by means of state space representation and modeling load disconnection on the grid. The different results obtained and a comparison between current magnitudes for increasing grounding points is further debated in this Chapter.

Finally, in Chapter 6 the research questions presented at the beggining of the thesis are discussed. The questions are addressed with the results obtained in the previous Chapters. A brief conclusion summarizing the results shown is further presented.

2

PROTECTION OF DC GRIDS

As discussed in Section 1.2 one of the main challenges for DC Microgrids is how to properly suit it to protect sensitive loads and end users. Moreover, LVDC distribution systems primarily provide users who are unaware of certain aspects of the electric power utilization. Meantime, ground faults are one of the main threats to cause indirect contact risk[8].

In the first Sections of this chapter the relevance of system protection is addressed. A general design criterion from the literature is analyzed and the different possible grounding configurations for LVDC distribution are discussed. In these two Sections the focus is to set the starting point for the design of a residual ground fault protection scheme for a LVDC Grid. An analysis of the effects of current in the human body is presented in order to state the allowed threshold values for grounding currents. The standard *IEC60479* [7] is addressed to show the values and duration of current flowing through the human body which are hazardous to end users. Finally, the concept of capacitive grounding will be introduced as a interesting solution for the protection of LVDC grids.

2.1. ELECTRIC SYSTEMS OF THE FUTURE

The dominance of AC systems proves to be a difficult obstacle in the adoption of DC systems. Electrical AC systems are a well developed technology and widely adopted throughout the world. Nevertheless, there are several technologies that can benefit from the adoption of DC systems.

The USB Type-C and USB Power Delivery technologies can allow up to 100 W (5A at 20 V) to be transferred. This new protocol may be able to provide power to most consumer appliances under a DC network topology. As explained in the previous Chapter unnecessary power conversion steps may be omitted since most of the devices used by end users run on DC Power.

Furthermore, the adoption of public LED street lighting, greenhouse lighting and shipboard power systems [9] can benefit from the development of a DC distribution grid. On the other hand commercial buildings can benefit from these technologies enabling the adoption of these systems and as consequence the need and maturity of this technology.

In addition, residential DC houses are likely to become a feasible concept making use of the advantages of DC schemes such as the bipolar topology. As shown in Figure 2.1 the distribution systems for LV domestic could be able to provide enough power for high loads such as heat pumps, washing machines, cooking facilities and domestic lighting. The planning of future buildings and neighborhoods could be done thinking in this topologies and enabling the conversion of normal AC appliances into DC. The potential scalability of this components is shown in Figure 2.2.

A microgrid composed of multiple nano grids as a distributed energy source structure that can be coupled further with other microgrids may increase the adoption of RES and the scalability of DC systems. The connection between them may be more beneficial and natural to be done in DC in this case. Figure 2.3 shows a simple topology example connection of two microgrids as DES. This may be a future feasible option

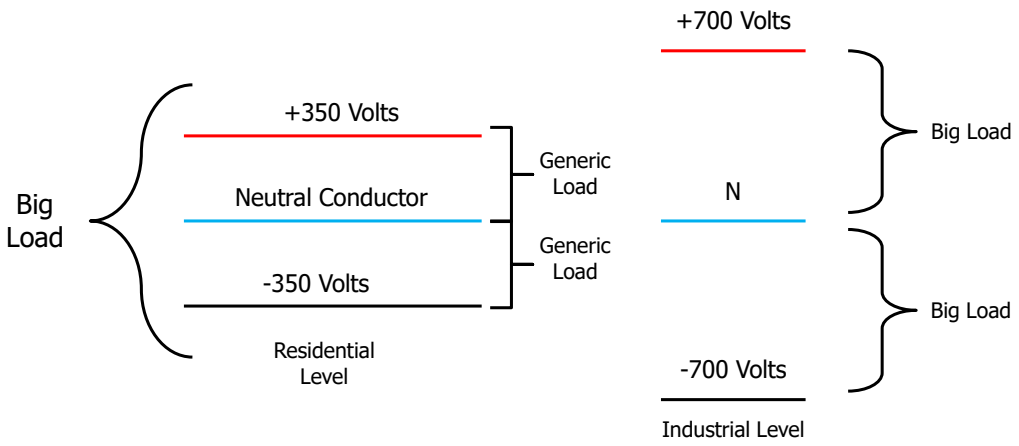

Figure 2.1: Modular Bipolar Voltage Levels. Adapted from [9].

for DES connection and large scale adoption.

Nevertheless, it is expected that AC and DC systems coincide in several locations during the transition and adoption of this new market. It is easy to understand that this change will not be easy and DC will only prove to be a tangible option to the well-established AC market when a DC market is also available and real infrastructure exists.

It is not the purpose of this thesis to prove that DC systems pose a better solution for energy distribution than AC systems but to exemplify that the conception of systems like this are the possible answers to the future challenges of energy usage and distribution that come along.

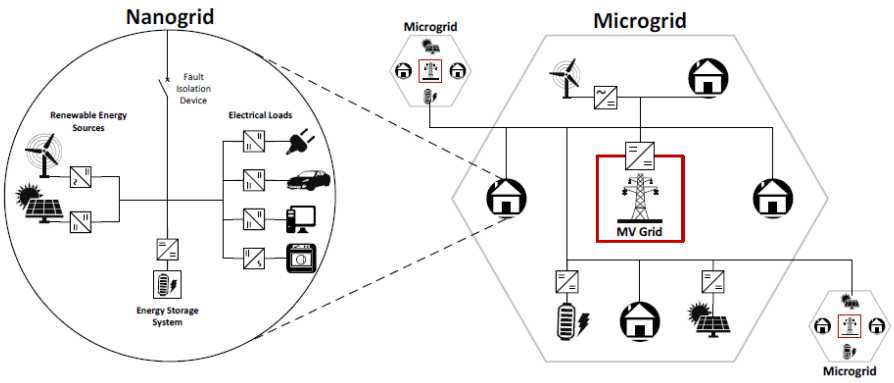

Figure 2.2: "On the right: a DC microgrid connecting a neighborhood with multiple DC nanogrids inside buildings and some larger distributed energy resources. It can be connected to other DC microgrids on the same voltage levels and/or to the medium voltage grid at the substation depicted in the center. On the left: a DC nanogrid inside a building with various energy resources is shown in detail. A fault isolation device can separate it from the microgrid".[9]

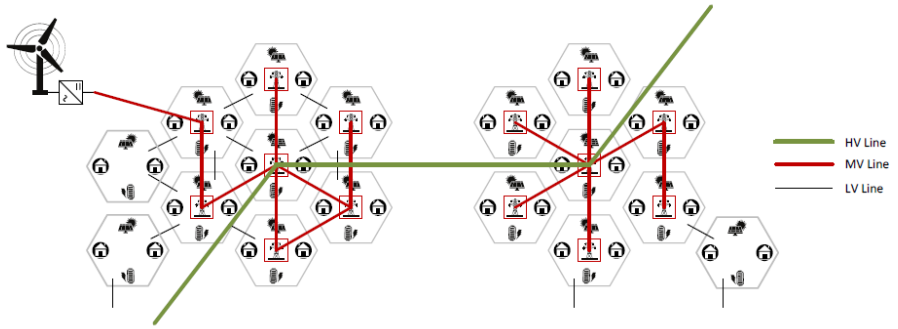

Figure 2.3: "An overview of a distribution area with multiple DC microgrids that are directly connected (black) to each other forming some meshes. On top of that, a medium voltage DC grid (red) connecting most of these microgrids at substations. Furthermore, a high voltage transmission system is depicted in green". [9]

2.2. REQUIREMENTS OF DC-MICROGRIDS PROTECTION SCHEME

Nowadays, AC systems continue to be preferred as opposed to DC systems due to the lack of available DC micro-grid protections schemes, standards and technologies. Likewise, the viability of the large scale implementation of DC micro-grids strongly depends on the right development of these standards and guidelines [10]. Nevertheless, protection is a complex parameter and there are many different means for its configuration in an electrical power system.

In order to establish how to properly protect a DC Grid the following key design criteria for any protective system have to be met according to [10]:

- Reliability: Right prediction of the protective system response to faults and dependability to not trip spuriously on transient or noise.
- Speed: Appropriate fault removal from the system and promptly restoration of operating voltages.
- Performance: Continuity of service to the loads; where lower performing system loses a significant portion of its loads when a fault occurs.
- Economics: Lowered installation and recurring costs; generally in opposition to performance.
- Simplicity: Quantity of parts, zones of protection to ensure its reliability.

A protection system in general terms consists of current interrupting protection devices, protective relays, measurement equipment, and grounding. Some commercially available components used on DC distribution systems depend on current interrupting devices which rely on the physical principle of clearing a current flow path upon an over-current condition. Moreover, fuse and breaker designs are enhanced with Zero Current Switching obtained by the natural zero current condition of AC systems. As a consequence, these devices are not properly designed for DC systems although can be used under special considerations [10].

For the case of distribution protection the main requirements for design criteria looking at a DC distribution system can be summarized in the following way according to [2]:

- Sensitivity: protection system should be able to identify an abnormal condition that exceeds a nominal threshold value.
- Selectivity: protection system should disconnect only the faulted part minimizing fault consequences.
- Speed: protective devices should respond to abnormal conditions in the least possible time in order to avoid damage to equipment/users and maintain the system stability.

- Dependability: protection system must operate correctly when required to operate and shall be designed to perform its intended function while itself experiencing a credible failure.
- Security: protection system must not operate when not required to operate and shall be designed to avoid unwanted operation while itself experiencing a credible failure.
- Redundancy: protection system has to care for redundant function in order to improve reliability. Redundant functionalities are planned and referred to as backup protection.

2.3. CONFIGURATIONS FOR LOW VOLTAGE DC

Electrical grounding is a safety practice implemented on electrical systems which consists in connecting a given electrical system to a common path for electrical current to flow or to a physical connection to earth's ground.

For safety and noise reduction nowadays electrical systems grounding connection is not intended to premeditate carry current but to safeguard users and property from risks arising from the use of electricity [11]. Nevertheless, the challenges facing DC systems protection are not only caused by the absence of standards and recommendations but also from the relative lack of practical experience [10].

Although LVDC systems are not fully developed HVDC connections have been implemented successfully in different countries. Knowledge from existing high power DC systems can be used as a starting point for a grounding protection outline for LVDC distribution systems. In [12] an overview and comparison for possible grounding configuration options for Meshed HVDC grids is given as base for LVDC grids. It is important to note that the grounding and grid configuration depend on each other and directly affect the grid design. Parameters like number of grounding points and their location affect the insulation requirements, fault behavior and fault response. Moreover, not all grid configurations are compatible for extensibility. In Tables 2.1 and 2.2 an analysis of HVDC grid configurations is presented according to [12].

Table 2.1: HVDC Grid Configurations: Unipolar Grid. Adapted from [12].

	Asymmetric monopolar grid	**Symmetric monopolar grid**
Operating voltages	-Un,0,Un	-Un/2,0,Un/2
Cables	2	2
Grounding Type	Low impedance	High impedance
Grounding points	Single grounding point Multiple grounding points	Multiple grounding points
Cable Voltage Rating	0,Un	-Un,Un
Steady-state fault current	Large	Zero
Protection requirements	Fast acting protection	Less stringent time constraints
Extensibility	Asymmetric monopoles Upgrade to bipolar grid	Symmetric monopoles High impedance grounded bipoles
Post-fault flexibility after loss of cable	Low	Low

Table 2.2: HVDC Grid Configurations: Bipolar Grid. Adapted from [12].

	Bipolar Grid	
Operating voltages	-Un,0,Un	-Un/2,0,Un/2
Cables	3/2	3
Grounding Type	Low impedance	High impedance
Grounding points	Single grounding point Multiple grounding points	Multiple grounding points
Cable Voltage Rating	Un,0,Un	-Un,+-Un/2,-Un
Steady-state fault current	Large	Zero
Protection requirements	Fast action protection	Less stringent time constrains
Extensibility	Low impedance grounded bipoles Asymmetric monopoles between metallic return and pole	High impedance grounded bipoles Asymmetric monopoles between metallic return and pole
Post-fault flexibility after loss of cable	High	High

2.3.1. STANDARD GROUNDING SYSTEMS

As discussed in Section 2.3 grounding scheme is important for the network design. Looking at ground faults the safety of users is a critical issue that has to be overcome for DC networks. In Chapter 1.2 the lack of standards and guidelines for DC networks acts as a counterweight on their adoption. Nevertheless, some currently defined standards can be used as a good guideline to achieve this.

First of all we have to acknowledge what the IEC is:

"The international Electrotechnical Commission (IEC) is a worldwide organization for standardization comprising all national electrotechnical committees (IEC National Committees). The object of IEC is to promote international co-operation on all questions concerning standardization in the electrical and electronic fields"[13].

According to the International standard IEC-60364, 3 grounding configurations are presented: TT, IT and TN systems. A brief explanation of each configuration will be given to put in perspective the impact on the grid design.

The standard IEC-60364 denotes the configurations with two letters. The first letter indicates the connection between the earth and the power source.

- T: Direct connection of a point with earth, from Latin terra.
- I: No point is connected with earth.

The second letter indicates the type of connection between earth and the power source.

- T: Earth connection is done by a local direct connection to earth.
- N: Earth connection is supplied by the power source either as a separate protective earth conductor or combined with the neutral conductor.

GROUNDING SYSTEMS

- TT-system: In the TT system the protective earth connection is provided by a local electrode whilst a separate conductor also grounds the power source. This system is preferred for telecommunications systems due to the lack of interference which is provided by the nature of this system. The TT grounding system is used throughout Japan, with RCD units in most industrial settings. This can impose added requirements on variable frequency drives and switched-mode power supplies which often have substantial filters passing high frequency noise to the ground conductor.
- IT-system: In the IT system the electrical distribution does not have a ground connection at all [8].

- TN-system: In the TN system at least one of the points of the power source is connected to earth. This is a very common system and is openly used for residential and industrial systems. Furthermore, TN systems can be classified further into TN-C, TN-S and TN-C-S. Figure 2.4 shows the different topologies described in the standard.

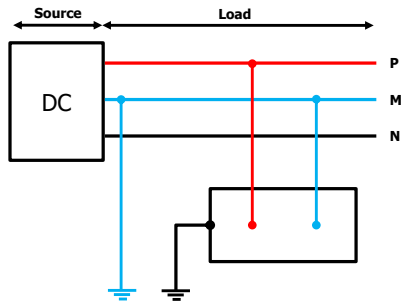

(a) TT Type

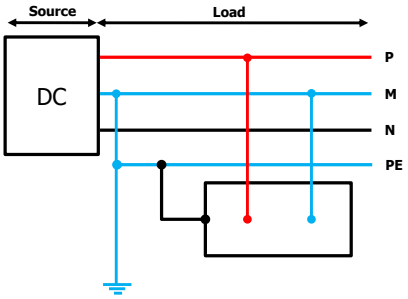

(b) TN-S Type

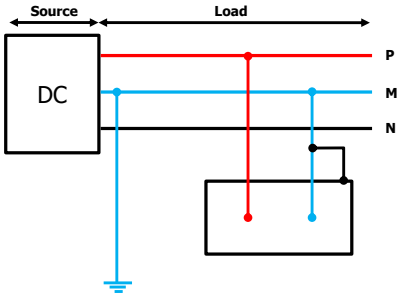

(c) TN-C Type

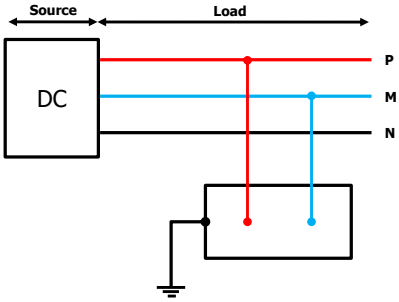

(d) IT Type

Figure 2.4: Possible grounding types on a LVDC network [14].

Significant voltage deviations on the cables are a hazard for network stability and as a consequence the nature of the IT systems becomes unrealistic for this type of networks. This also mean that the scalability of a DC distribution network cannot be achieved using an IT grounding system. On the other hand, a TT system requires the implementation of many grounding points if the network is to be scaled, which makes detection of ground faults a more demanding factor than needed. Therefore, as stated before the number of grounding points may be limited to an optimum amount.

Moreover, the TN system which may have the option to have a separate conductor enables a more stable grounding point which grounds the load and prevents current to flow through the grounding resistance. A TN system with a separate conductor proves to be a good option for DC distribution networks that may ensure both users and network stability.

2.4. EFFECT OF DC CURRENT ON THE HUMAN BODY

The IEC60479 standard *"Effects of current on human beings and livestock"* [7] helps to set a valuable basis of ground fault current limits that if surpassed may inflict permanent damage to end users. As its name indicates this standard provided by IEC describes the effect of electrical current passing trough human body. In this Section a brief explanation of the most relevant aspects for DC distribution systems under the view of a protection scheme is given. In addition, the relevance and usefulness that this standard implicitly has on DC distribution system protection is shown.

LET-GO AND PHYSIOLOGICAL THRESHOLDS

The Let-Go threshold is defined as the maximum value of electric current through the body of a person at which that person can release himself or herself. This value depends on multiple conditions such as the individual physiological attributes, contact area shape of the electrodes, etc. Figure 2.5 presents the Let-go thresholds for men, women and children for combinations of alternating current and direct current. The thresholds chosen by IEC are considered to be adequate to represent the entire population from inability to let go.

On the other hand, Figure 2.6 shows the physiological thresholds for AC and DC current flowing from both hands to both feet through the human body. This Figure delimits different values of DC current for different time duration and delimits 4 zones that have specific physiological effects for humans. A brief description of these zones and their physiological effects is presented below.

- DC-1: Slight pricking sensation when making, breaking or rapidly altering current flow.
- DC-2: Involuntary muscular contractions likely especially when making, breaking or rapidly altering current flow but usually no harmful electrical physiological effects.
- DC-3: Strong involuntary muscular reactions and reversible disturbances of formation and conduction of impulses in the heart may occur, increasing with current magnitude and time. Usually no organic damage expected.
- DC-4: Patho-physiological effects may occur such as cardiac arrest, breathing arrest, and burns or other cellular damage. Probability of ventricular fibrillation increases with current magnitude and time.

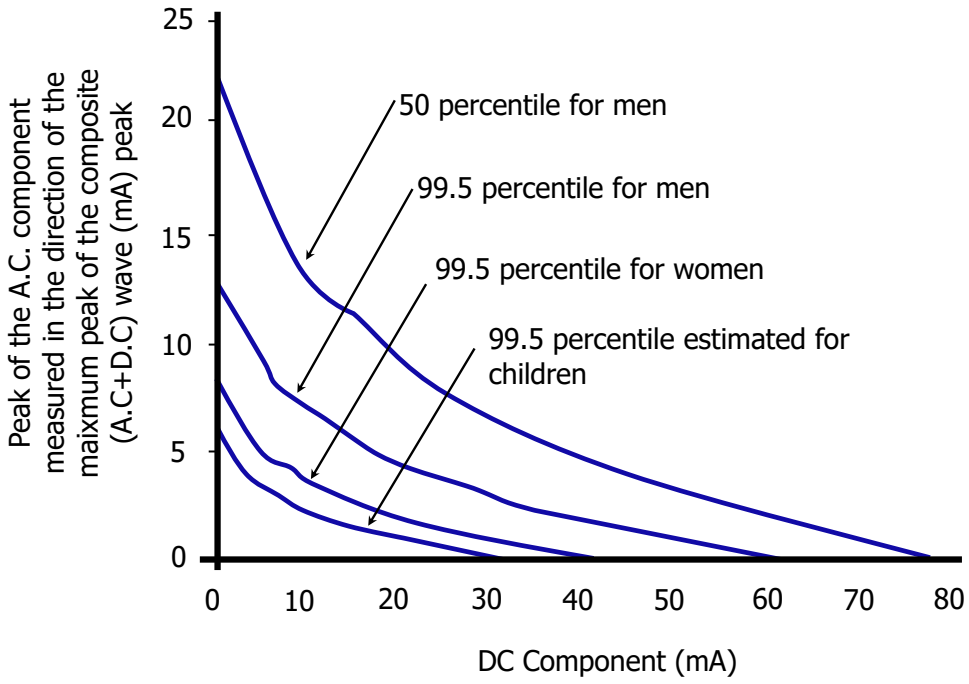

Figure 2.5: Let-go thresholds for men, women and children. Adapted from [7].

According to the IEC Standard IEC60479 2.6 the DC-3 and DC-4 zones pose a serious risk for end users and thus should be a safety requirement for the protection scheme. The time and current values that delimit these areas are in the order of mA which and have to be limited to values under 10 ms. This information also states that the detection and clearing of the faults have to be done under 10 ms which with current solid state technology can be easily achieved.

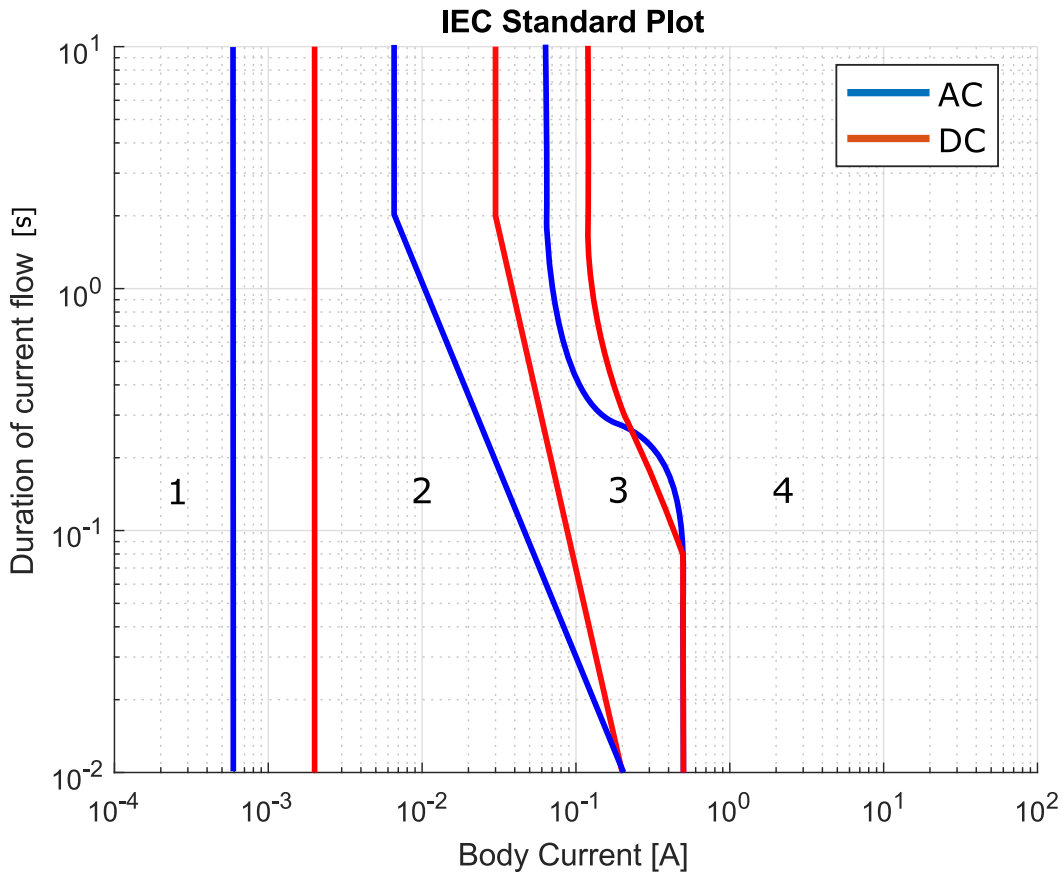

Figure 2.6: Time and current zones IEC standard [7]. Figure adapted from [8]

FAULT DETECTION

One of the most common methods for fault detection in electrical systems is the over current approach. As the name states faults are detected by measuring currents and comparing them with a threshold value. This approach is useful in systems that can provide enough fault current to reach the threshold limits. In the case of a domestic household exemplified as a nanogrid in Figure 3.1 this is the case when is interconnected to a large grid. Nevertheless, if operated in islanded mode current values may not be reached to ensure fault detection.

On the other hand, a relatively new approach based on fault transients emerges as a possible solution to this problem. By measuring the rate of change in current with respect to time $\frac{di}{dt}$ as a discriminating indicator even if the current limit may not be reached the slope could accurately indicate that indeed a fault is present. This type of detection can be very fast if applied properly. Since signal analysis is important, accurate measurements should be made with as few noise as possible.

As mentioned in Section 2.5 on a DC distribution grid one of the challenges is to differentiate between normal operation of the network and fault condition. However,this differentiation is not very obvious in terms of measurements. This in terms of clearance speed is critical and affects the detection method selection.

Furthermore, due to the nature of capacitive grounding inrush currents have to be considered. Inrush currents can surpass in 2 orders of magnitude the nominal current values causing a considerable problem in the protection scheme. With the purpose to solve this problem and avoid false positive detection standards regarding this type of systems have to be developed in detail.

Moreover, load shifts should not be done too fast in order to avoid transients causing false positive detections. As mentioned before guidelines and standards have to be developed to cover most cases by limiting the rate of change in load and thus ensuring system stability.

RESIDUAL CURRENT MEASUREMENT

As stated before, a ground fault is the flow of current in a path that was not designed for. There are many factors that may cause ground faults in electrical systems: aged infrastructure, poor insulation, etc. A ground fault occurs when an undesirable connection is made between one of the conductors and ground. In a DC system human error may cause ground faults and as part of the protection scheme it is relevant to analyze how to detect and prevent them.

Looking at a bipolar network under normal conditions in Figure 2.7 and applying Kirchoff's Current Law in node 1 when there are no fault conditions the sum of currents will account to 0 as shown in Eq. 2.1 .

$$I_{+} + I_{\text{m}} + I_{\text{-}} = I_{\text{gnd}} \implies I_{\text{gnd}} = 0 \tag{2.1}$$

On the other hand if the network is under a fault the sum of the currents will be different from 0 since there is current flowing through a path where is not supposed to. This simple method is applied to discriminate between normal conditions of operation and during faulted conditions[14].

$$I_{+} + I_{\text{m}} + I_{\text{-}} = I_{\text{gnd}} \implies I_{\text{gnd}} \neq 0 \tag{2.2}$$

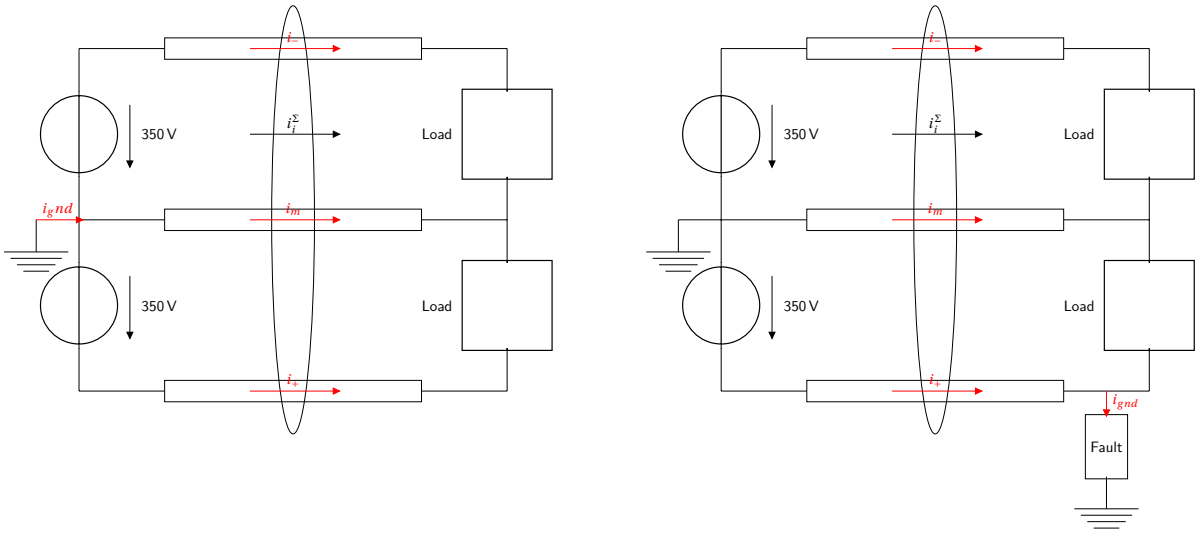

Figure 2.7: Bipolar dc grid with and without fault conditions. To the left Bipolar DC grid without fault conditions. To the right Bipolar DC grid with fault conditions.

2.5. CAPACITIVE GROUNDING

As discussed in Section 2.2 the bipolar system network proves to be the most preferred topology for LVDC grids. Nevertheless, when there is an unbalance on the poles, i.e. the power on each pole is not equal, a voltage deviation occurs on the middle conductor. This voltage deviation incites current to flow from the neutral conductor to ground. This is a normal effect on AC systems but is negligible since as a consequence of the alternating current this effect is canceled out. In a DC network this is not the case and the flow of this current to ground when unbalance exists will cause a constant current flowing to ground for a persistent period of time. This translates on the protection scheme since this current may be detected as a fault in the network which results on a poor designed protection system. Moreover, as stated in [14], this continuous current flow to ground will cause corrosion on the electrical infrastructure which ages prematurely the system and increases the likelihood of major failures. That is why on a DC distribution system this effect has to be taken into account properly when designing the protection scheme.

Capacitive grounding proves to be a simple yet efficient solution for grounding DC distribution networks and to avoid leakage currents on unbalanced operation. Capacitors prevent currents from flowing to ground

when a load unbalance is present on the network. Furthermore, due to their nature capacitors behave as open circuits at low frequencies (DC), and as short-circuit at high frequencies.

Due to the nature of the capacitors when load unbalance is present on the network current will start flowing to ground and start charging the capacitors. Once the capacitor is charged it behaves as an open circuit not allowing current to flow further. In Figure 2.9, the behavior of the two capacitive grounding points is proved when, in spite of the voltage unbalance, there is no current flowing to ground in steady state operation.

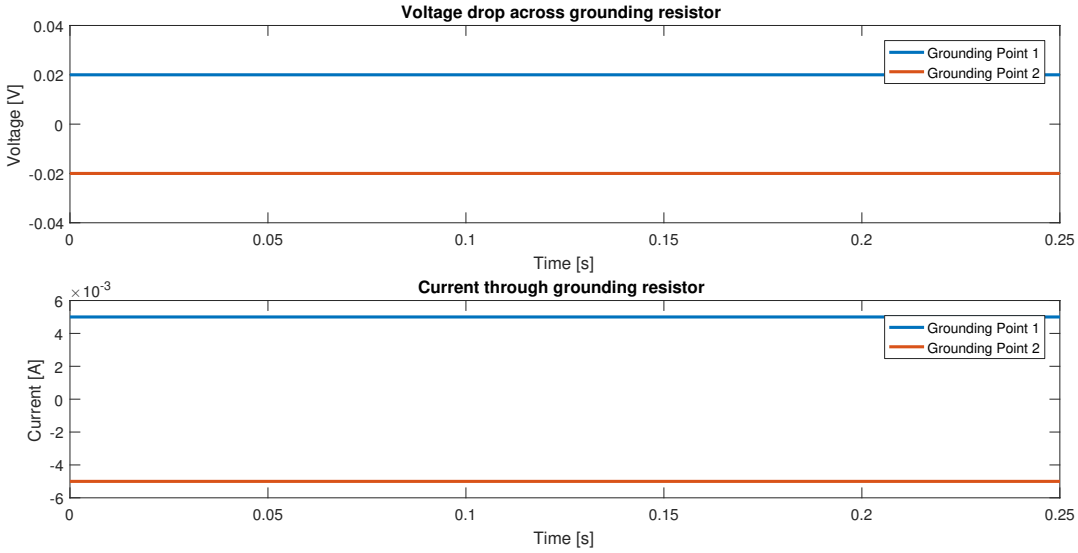

Figure 2.8: Plot of resistor grounding voltage and current when a load unbalance is presented[14].

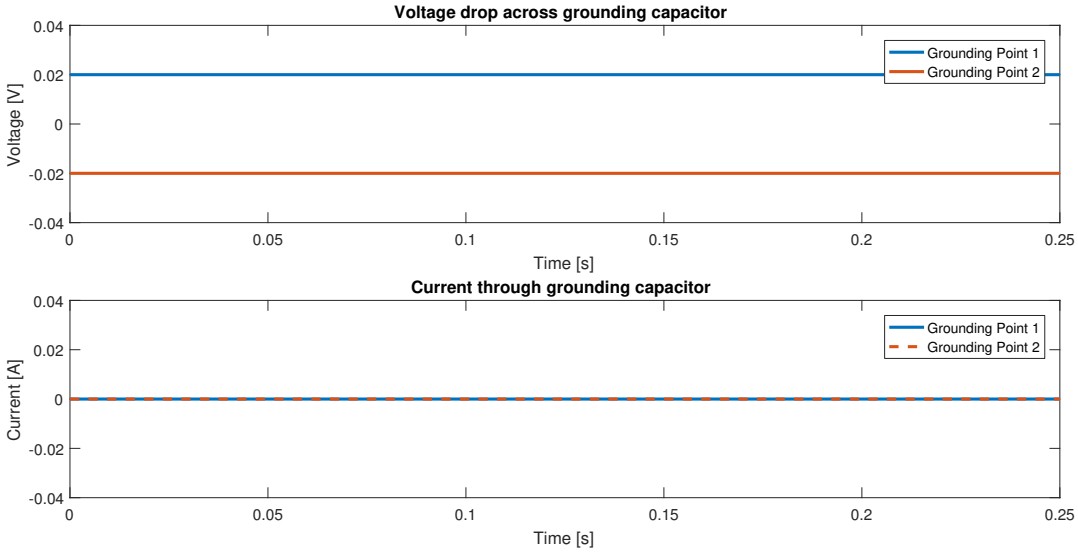

Figure 2.9: Plot of capacitive grounding voltage and current when a load unbalance is presented[14].

If a fault occurs most of the current would flow back to the network through them increasing the safety and stability of the grid. Nevertheless, the charge and discharge of the capacitors during ground faults remains a problem[14].

As discussed in [14] by means of RCM, ground faults can be detected in the system and determine their location. This enables the disconnection of the faulted section ensuring system selectivity. Nonetheless, this is only possible by means of efficient communication and multiple grounding points. Having a communication system between the protective relays in the grid configuration is imperative with this approach.

Every time a load is shifted, balancing current flows will leak through ground to enable capacitors reach steady state with the new voltage distribution. Ideally one would like to have a symmetric network but in real life applications this is hardly the case. The network is likely to be symmetrical causing a voltage drop across the capacitors that is directly related to the load distribution of the network. For balancing and circulating currents the order of magnitude is similar to that of fault current and protection is likely to be triggered if communication does not exist on the system. Communication between the protective relays ensures ground fault detection.

However, this approach implies a more expensive network due to the fact that in order to discriminate between balancing and circulating currents the protection device has to cover a considerable range of currents. Having such a robust protection device on the network may not be economically viable. Furthermore, since in order to avoid ground faults to reach critical values the clearance of the fault has to be done quite fast. This means that the communication system and protocol must be able to react in the order of ms or us.

As discussed in Section 1.4 one of the research questions of this thesis relates on how communication for fault detection be omitted on a radial distribution. A different approach will be considered in the following chapter which may enable the proper discrimination between ground faults and circulating currents avoiding having extensive communication all over the network.

2.6. CONCLUSION

In this Section the current status for the protection of DC grids was studied. A brief overview of the scope of DC distribution systems as a reality was presented. The potential of DC for LV systems and as a coupling technology with RES was discussed and different possibilities of implementation were mentioned.

Since the lack of standards and guidelines is one of the major problems for DC distribution systems the general safety requirements a system like this should meet were adressed. Different grounding configurations that standard AC systems use were also exemplified in a DC system. It was also concluded that the TN-S system is a good and stable configuration to be implemented on DC distribution systems and thus the following chapters base their topologies and analysis using this grounding configuration.

Furthermore, the effect of DC current was analyzed based on the IEC60479 standard *"Effects of current on human beings and livestock"*. The different physiological effects caused by different current magnitudes and durations were mentioned by the DC zones in the standard. This zones serve as design guideline for the DC protetcion scheme that is studied in the following chapters.

Finally, the concept of capacitve grounding as a mean of protection scheme for LV distribution grids was introduced. The advantages of this system to avoid leakage currents from load pole unbalance was mentioned. The current research done in this topic also shows that there are some aspects to be adressed such as the proper detection of fault currents. Moreover, the scalability of a system like this remains unkown. In summary this Section sets the requirements and guidelines from the knowledge taken from literature and previous research. For the following chapters the implementation of a capacitive grounding protection scheme are based on what has been mentioned in this chapter.

3

Capacitive Grounding for LV DC Grids

As explained in Chapter 2 ground fault protection is an important aspect for the adoption of DC distribution systems. Looking at this system, low impedance grounding does not avoid, the flow of DC ground currents which as discussed previously lead to corrosion and system degradation. On the other hand capacitive grounding was briefly discussed in Section 2.5 and may be a suitable solution for the protection of DC grids. In such a system the use of capacitive grounding promises to prevent ground faults whilst enabling normal operation on the grid.

However, in order to proper detect and clear faults the implementation of multiple grounding points all over the network and fast communication are required between the protective relays. This would increase the network costs making this system difficult to implement and not as attractive as more economical solutions.

The aim of this chapter is to further explain capacitive grounding as a mean of protection scheme applied on a DC distribution system. First, the scope of a DC distribution system grounding scheme is presented by discussing the way it could be implemented. Secondly, a description of the capacitive grounding implementations on a Unipolar and Bipolar configuration is discussed. An analysis done on each system is presented by means of a set of simulation results done with the software Matlab Simulink. These simulations are given to demonstrate the system sensibility to capacitor size. Finally, conclusions are made exemplifying the advantages, disadvantages and further research of this system.

3.1. Final Goal for Capacitive Grounding

In Section 2.2 an overview of how future DC distribution systems would look like was given. The different grounding schemes that could be adapted from AC systems were studied. This Section will focus in more detail on the protection system using capacitive grounding for DC distribution systems.

Figure 3.1 shows a schematic of capacitive grounding implemented on a LV Domestic street arrangement. The schematic shows a LV DC bipolar distribution network. At the point of interconnection each house serves as a nanogrid having a bipolar configuration and with their own capacitive grounding protection. The schematic shows a symmetric configuration with the possibility to load the two LV distribution poles with rows of houses lowering the poles voltage unbalances.

Multiple grounding points implementation like in Figure 3.1 are needed to island individual nanogrids. Nevertheless, multiple grounding points enable ground currents to flow and selective protection becomes more challenging. As a result the development of suitable grounding schemes is critical. In a configuration like this capacitive grounding could be an interesting alternative by providing low impedance for fault transients and preventing dc ground currents from flowing[15].

As described in the previous Section fast fault detection is essential to ensure fault clearance before reaching dangerous values. The response time of such a scheme would have to be in the order of a μs which is considerably faster than traditional protection strategies found on AC systems. In addition, if fast detection is achieved ensuring selectivity during fault clearance will become a more difficult task. In order

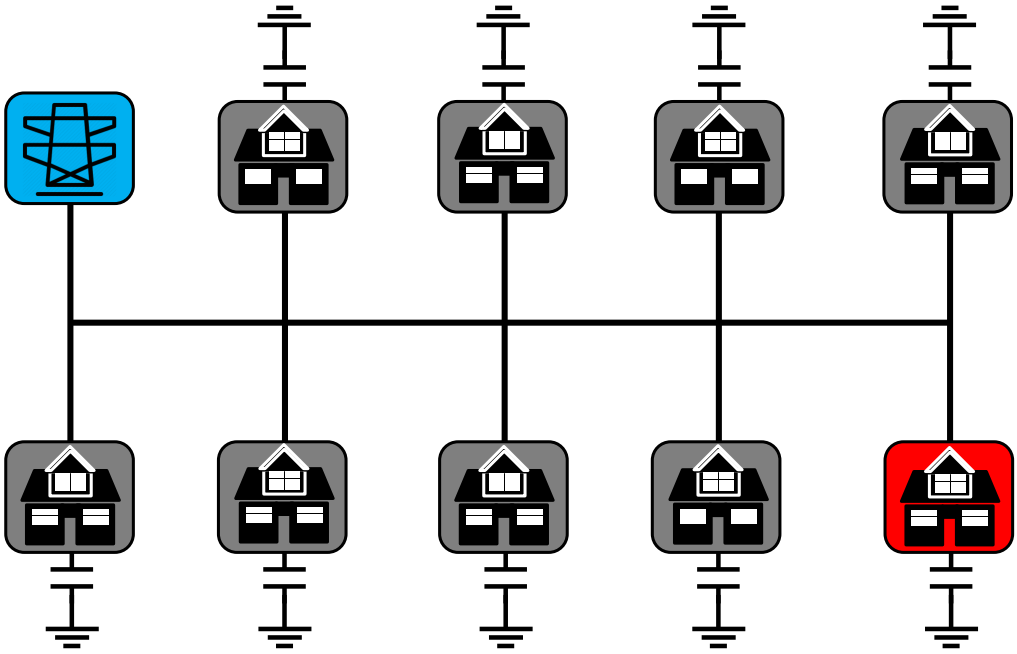

Figure 3.1: Schematic Capacitive Grounding DC Distribution Systems

.

to understand in which direction the capacitive protection scheme is to be stirred, different approaches to ensure the protection characteristics shown in Section 2.2 will be discussed.

3.2. UNIPOLAR TOPOLOGY

The Unipolar DC system consists of, DC sources and loads connected between the positive and negative pole of the DC bus voltage level. As shown in table 2.1 the voltage of the network would be the one of the source with the DC power transmitted on one level [16]. For capacitive grounding the neutral wire connected with a capacitor to ground. This is done in each place where otherwise solid grounding would be used, i.e., in each dc nanogrid that should be able to operate in islanding mode. Figure 3.2 shows a schematic of the unipolar configuration that is used on this thesis with two grounding points with capacitors C_1 and C_2 connected to the negative conductor.

The main advantage of this grounding configuration is that the impedance to ground is infinite in steady state $(s = 0)$. This means that no DC ground currents can flow. In this way corrosion can be avoided. For high frequencies the capacitor impedance $Z_C(s)$ decreases. Thereby it behaves similar to low impedance grounding for fast fault transients. Due to this fact selectivity and short circuit protection can be done similarly as with low impedance grounding.

The impedance of a capacitor in Laplace domain is

$$Z_C(s) = \frac{1}{sC}. \tag{3.1}$$

Capacitors are rated for a maximum voltage. A maximum neutral voltage should be specified, in order to limit the cost and size of the grounding capacitors. It is important that capacitors used do not have polarity. This is because the potential of the neutral conductor can go negative. Due to isolation leakage, or other means, the capacitors could charge over time to either their maximum or minimum voltage. As a consequence, the voltage across them has to be clamped.

A possible implementation that will be considered through this thesis project are two Zener diodes in

anti-series configuration as shown in Figure 3.2. For this thesis a value of ±5 % of 350 V is chosen, which results in a clamping voltage of ±17.5 V as can be seen in Figure 3.2.

A shielded cable with a length of 100 m length is assumed and modeled with a Π model, in order to consider the effect of the cable capacitance in the simulation. The Π model used for the unipolar schemes is detailed in Figure 3.3. The cable chosen is relatively thin, which is meant to show in principle a considerable voltage drop in order to make the load change more significant in the sensitivity simulations detailed in Section 3.5. The cable length is represented in the schematic as a series resistance-inductance with parameters described in Table 3.1. As discussed before Residual Current Measurement (RCM) is applied at both ends of the circuit to measure the grounding currents stated by i_{21}^{Σ} and i_{21}^{Σ}.

Table 3.1: Cable Parameters

Parameter	Value
Cable Resistance	4.61 Ω/km
Cable Inductance	360 μH/km
Cable Capacitance	260 μF/km
Capacitance ESR	10 Ω/km

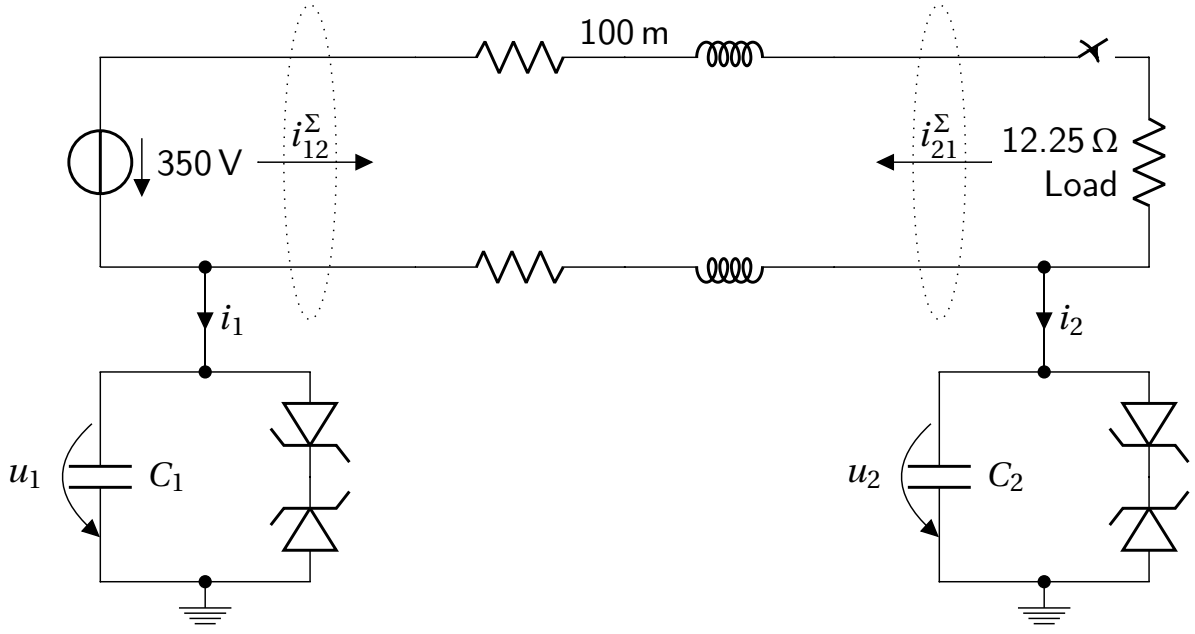

Figure 3.2: Unipolar DC grid with two capacitive grounding points with voltage clamping by zener diodes. Source on the left and load on the right [17].

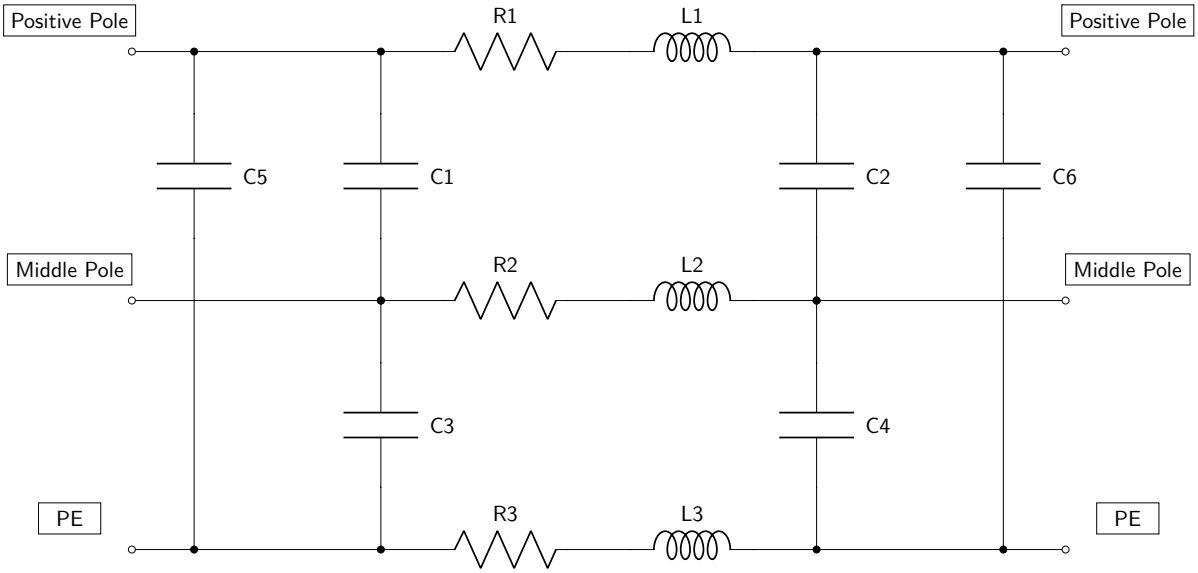

Figure 3.3: Detailed Π model used for unipolar cable simulations

3.3. BIPOLAR TOPOLOGY

The bipolar system as mentioned before has more flexibility than unipolar systems. A unipolar DC network consists of three wire bus system which has two voltage levels as illustrated in Figure 3.4. The clamping voltage configuration used in the unipolar scheme is also implemented here. The residual current measurement is applied including both poles at both ends of the circuit stated by i_{21}^{Σ} and i_{21}^{Σ}. The same Π model and cable parameters are included in this scheme as described in Table 3.1 and shown in Figure 3.5.

With such a configuration the system can provide +350 V,0 V, 350 V as shown in table 2.2. Having more voltage levels makes the system more flexible to the end users [16]. Nevertheless, as mention before the fact that with the connection of different potential levels and power demands on the poles can result on a system unbalance and these effects have to be taken into account for the protection scheme.

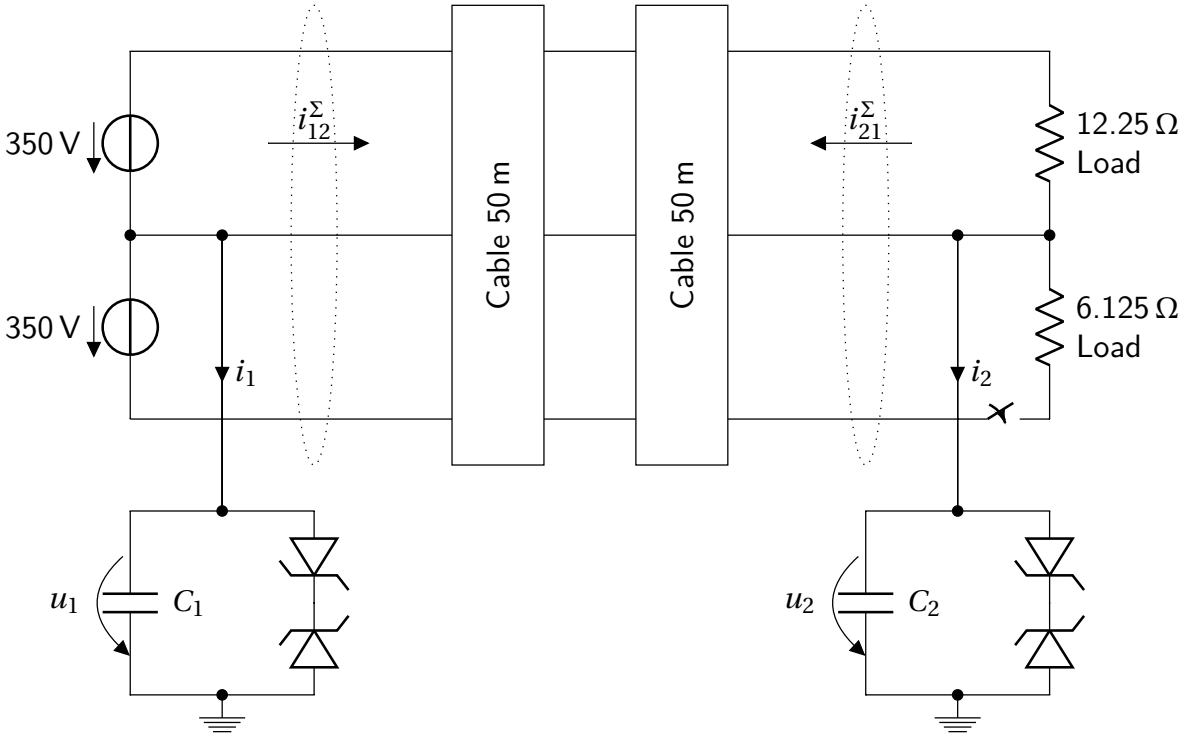

Figure 3.4: Bipolar DC grid with two capacitive grounding points with voltage clamping by zener diodes. Sources on the left and asymmetrical loads on the right [17].

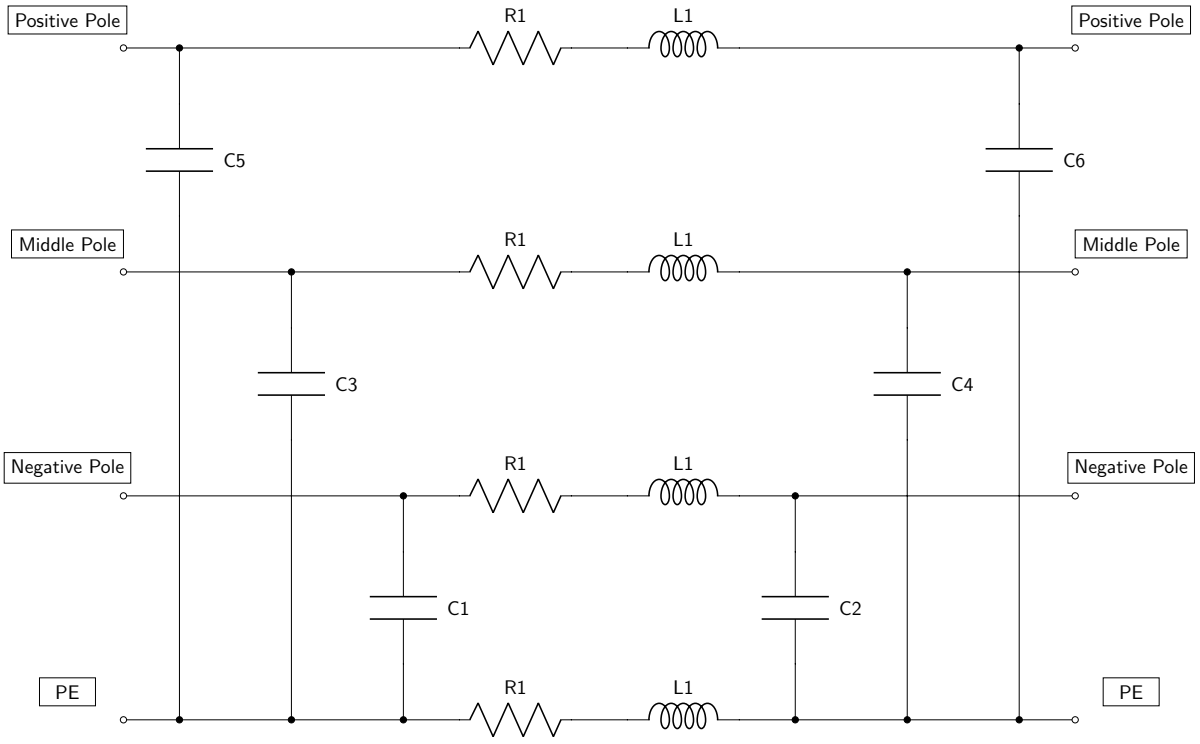

Figure 3.5: Detailed Π model used for bipolar cable simulations

3.4. CAPACITOR SIZING

It is easy to understand that capacitor size plays an important role in a capacitive grounding scheme. How capacitance affects the behavior and response of the system is the main topic for this Section. An important

event to take into consideration is that capacitors always need to be charged to the voltage potential of the neutral, respectively grounded wire. This voltage changes depending on the load in unipolar grids, likewise load balance in bipolar grids.

It is well know that the charge of a capacitor depends on its size and affects voltage and current as depicted in Eq. 3.2.

$$u_C(t) = \frac{q_C(t)}{C} = \frac{1}{C}\int_{t_0}^{t} i_C(\tau)\mathrm{d}\tau + u_C(t_0) \tag{3.2}$$

where $q_C(t)$ is the charge of the capacitor at time t.

Depending on the capacitor size and the amount of current provided to during load shifts the time for it to reach a steady state varies. As capacitance increases the time to reach steady state will also increase. This is important to understand what behavior is expected for load shifts as capacitance varies. For this a simple simulation is set up in order to asses the sensitivity of the system to capacitance values.

The capacitance values chosen are taken from the range of μF and are depicted in table 3.2

3.5. SYSTEM SENSITIVITY ANALYSIS

The previous Section shows the importance of capacitor size in the protection scheme. In this Section the results of simulations done in Matlab Simulink are presented. The simulations are done to analyze the system sensitivity to capacitor size for the unipolar and bipolar topologies. Since the goal is to model the behavior of the system at different capacitances a first simulation in with the unipolar scheme is presented. In order to model the worst case scenario for load shift and measure the system behavior the load is connected and disconnected. In addition, simulations showing capacitance value variations on the bipolar scheme are modeled using the same load shift.

SENSITIVITY UNIPOLAR GRID

A simple simulation of the Unipolar grid scheme shown in Figure 3.6 is made to show the behavior of the capacitors during worst case scenario of load change.

A capacitance value of 10μF was used for the grounding points C_1 and C_2. The grid is assumed in steady state at the beginning of the simulation with no load connected. The simulation duration is set to 0.7 s, at 0.2s a 10kW load is connected to the grid and at 0.4 s is then disconnected. The voltage (u_1, u_2) and currents (i_1, i_2) measured from C_1 and C_2 are respectively plotted in Figure 3.6.

This first simulation shows that the capacitors charge and discharge depending on the value of the neutral conductor with respect to ground which is shown in the voltage plot. There is a considerable peak that is caused mainly by the cable inductance reaching current values of 20A when the load is disconnected.

SENSITIVITY BIPOLAR GRID

Now that we know how in principle the capacitance behaves during load shifts it is relevant to simulate the behavior on a bipolar topology with increasing capacitance. For this reason, a simulation using schematic Figure 3.4 and cable parameters from Table 3.1 for different capacitance values is presented.

The schematic used consists of a bipolar dc grid system with a 350 V voltage source on each pole and two unbalanced loads of 10 kW on the positive and 20 kW on the negative pole. Two grounding points are included with a connection distance of 20 m both to source and load. A shielded cable with a length of 100 m is assumed and modeled with the Π model shown in Figure 3.5, in order to consider the effect of the cable capacitance in the simulation. The cable parameters used are listed in Table 3.1. The cable chosen is relatively thin, which is meant to show in principle a considerable voltage drop in order to make the load change more significant.

The capacitance values used in this simulation are considered in the range of μF and presented in Table 3.2.

Five simulations are made individually, each of them with a different capacitance value.The 20 kW load

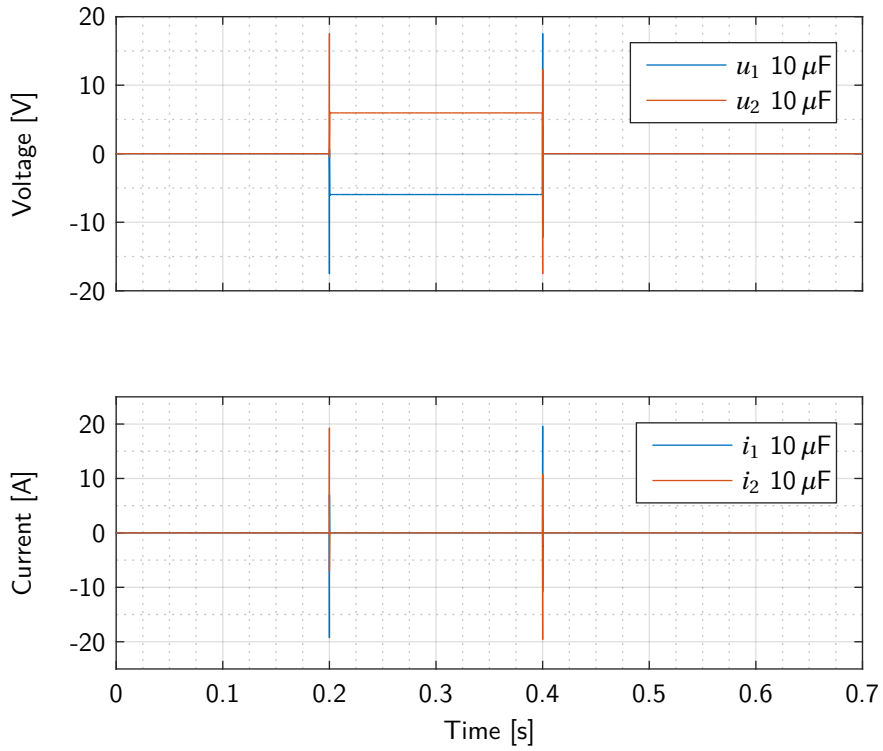

Figure 3.6: Unipolar dc grid with load connection (0.2 s) and disconnection (0.4 s). The capacitors are charged to the new voltage of the neutral line when connecting and discharged at disconnect. The voltages are clamped at 17.5 V and the balancing currents are in the magnitude of 20 A [17].

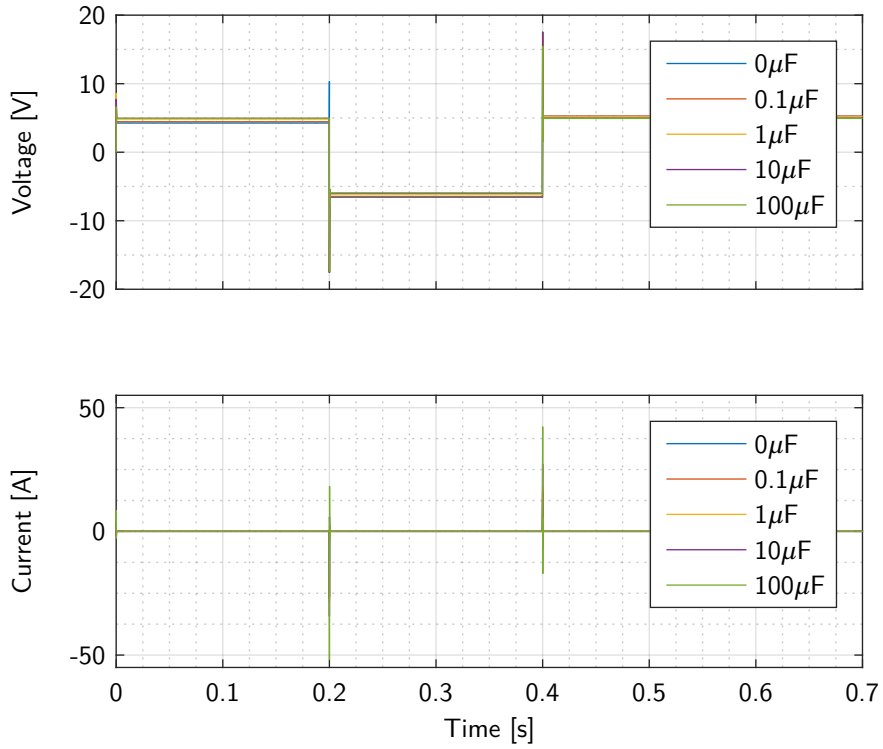

Figure 3.7: Sensitivity simulation results for different capacitance values. Top plot shows the voltage of C_1 shown on Figure 3.4. Bottom plot shows the current flowing through C_2 to ground as shown on Figure 3.4. Load is initially connected. At 0.2 s load is disconnected and reconnected at 0.4 s, human fault is omitted for this simulation [17].

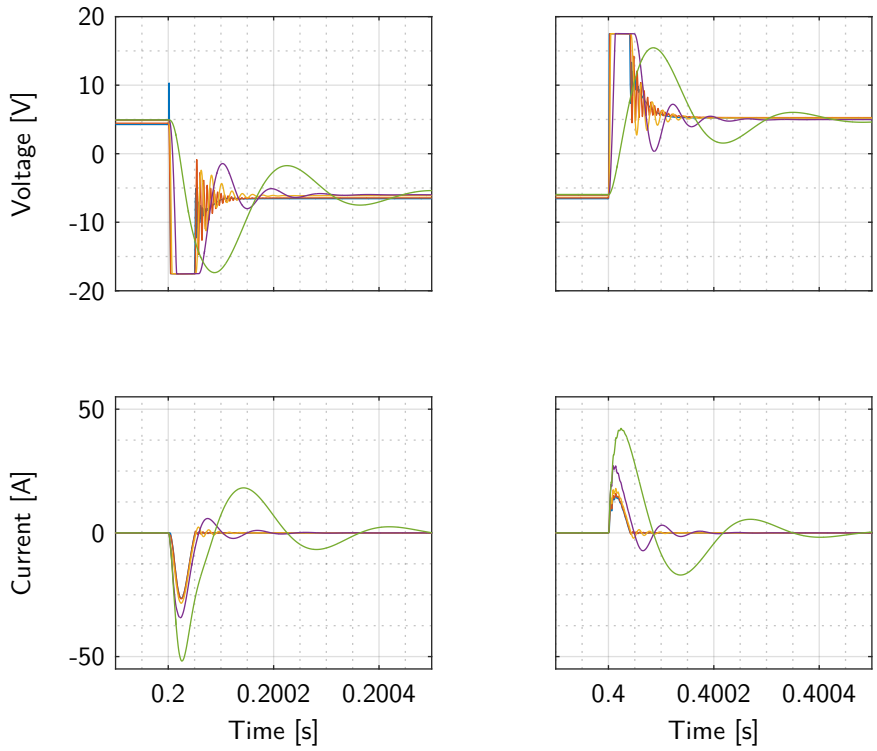

Figure 3.8: Zoom for connection and disconnection points of Figure 3.7 for both voltage and current. From top to bottom and left to right: zoom of voltage peak at 0.2 s (disconnection), zoom of voltage peak at 0.4 s (connection), zoom of current peak at 0.2 s (disconnection), zoom of current peak at 0.4 s (connection) [17].

Table 3.2: Capacitance Values chosen for bipolar sensitivity simulations

Run	Capacitance Value [μF]
1	0
2	0.1
3	1
4	10
5	100

at the negative pole is disconnected and connected again at 0.2 and 0.4 s respectively. Figure 3.7 shows the voltage and current values of C_1 shown on the schematic of Figure 3.4 for the different capacitance values with a total simulation time of 0.7 s.

A zoom on each peak for each plot (voltage and current) is shown in Figure 3.8. The color coding of the lines is the same as before. Looking at the 0 μF capacitance case the behaviour is similar to the capacitances of 0.1 and 1 μF, which is a consequence of the parasitic/snubber capacitance of the zener diodes which are modeled on the capacitive grounding points. Moreover, the voltage for the capacitance values of 1 and 10 μF shown in Figure 3.8 clamp at 17.5 V which corresponds to the breakdown voltage of the zener diodes.

Furthermore, the system becomes more stiff with increasing capacitance as it is shown for 1, 10 and 100 μF capacitance values. At the moment of connection/disconnection currents around 25 and 50 A corresponding to 1 and 10 μF flow through the capacitors to ground. It is important to note that low capacitance lower to 1 μF are in the order of the cable capacitance value shown in Table 3.1 which for further system sensitivity simulations can be omitted. The time it takes for the transients to be no longer relevant to the analysis is less than 0.5 ms which is relatively fast compared to the time it takes current flowing through the human body to cause irreversible damage [7]. The load disconnection served as extreme case scenario of load shift. Although load shift is a normal state of operation on a bipolar network as stated in Section 2.5 the transient

state may trigger protective relays.

3.6. CONCLUSION

This chapter discusses capacitive grounding as an interesting solution for the grounding scheme of DC distribution grids. Its advantages are the prevention of DC ground currents in steady state, while still showing low impedance behavior for fault transients. The importance of the capacitance values and the sensitivity of the system due to its variations was analyzed by means of simulations done in Matlab Simulink on the unipolar and bipolar schemes.

The magnitudes observed during load change were discussed and since the magnitude for currents caused from load shifts are considerably larger than the ones caused by human touch a discrimination scheme has to be developded to difference them. The boundaries of the applicability have to be identified and guidelines for capacitor size and line lenghts have to be derived.

4

Filter Design for Residual Ground Fault Detection

As shown in Section 3.5, relatively high currents occur at the moment of load change. Nevertheless, load changes are a normal behaviour in dc distribution grids and from the protection scheme point of view this needs to be taken into account. This current behavior poses a challenge for discrimitating load change currents from human fault currents, as the magnitude of the load change is much bigger than that of the fault.

For this reason a detection scheme is of great importance in order to safely implement capacitive grounding. The aim of this chapter is to describe a simple detection scheme by means of filtered current discrimination. This detection scheme is conceived to follow as accurately as possible the limits, times and thresholds defined by the IEC60479 [7] standard.

This chapter is organized as follows: in Section 4.1, the main approach for the protection design is presented and the main goal that is desired to achieve is discussed. Furthermore, in Section 4.2 the introduction of a simple first order filter aimed to describe the desired response of the system is given. Section 4.3 describes the methods to further synthesis the filter that could serve as tool for discrimination of human ground faults and load change currents. Finally, conclusions will be made in Section 4.4 discussing further work and important aspects to consider.

4.1. Approach

The approach relies on a relevant difference between human fault currents and load change currents. As mentioned in Section 3.5 load shifts take less than 0.5 ms to reach a steady state. This means that in a worst case load shift scenario looking at the values of capacitance used for the sensitivity simulations the maximum current values will not last more than 0.5 ms. On the other hand, according to the IEC60479 [7] standard the current duration that is likely to cause permanent damage to the human body is approximately of 10 ms. This means that the difference is at least one order of magnitude with a conservative approach. This meaningful characteristic is the base of the detection scheme that is presented on this chapter. The main objective of this chapter is to exemplify a detection scheme that can be useful for the implementation of capacitive grounding on DC distribution grids that is able to discriminate between load shift currents and human fault currents. If this approach is implemented properly the need of unnecessary communication that may be needed according to what is discussed in Section 2.5 between protective relays may be omitted.

4.2. First Order Filter

The frequency domain behavior of a filter is described mathematically in terms of its transfer function or network function. This is te ratio of the Laplace transform of its output and input signals [18]. Therefore, a first order low pass filter as shown in Figure 4.1 can be written as follows:

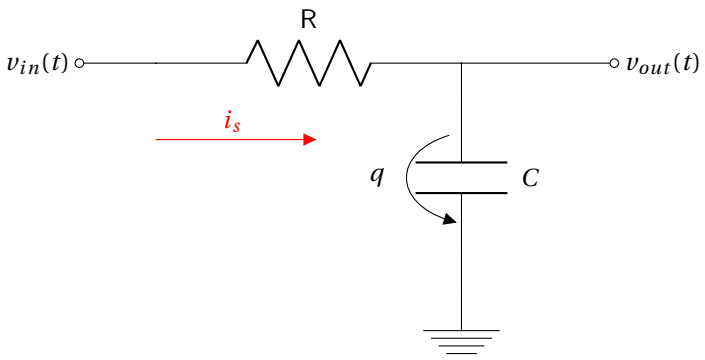

Figure 4.1: Circuit Schematic of a First Order Low Pass Filter.

Defining the input voltage of the circuit shown in Figure 4.1

$$v_{in}(t) = Ri(t) + \frac{q(t)}{C} \tag{4.1}$$

$$v_{in}(t) = Ri(t) + \frac{1}{C}\int_0^t i(u)du \tag{4.2}$$

Applying Laplace Transform to (4.2):

$$\mathcal{L}\left\{v_{in}(t)\right\} = \mathcal{L}\left\{Ri(t) + \frac{1}{C}\int_0^t i(u)du\right\} \tag{4.3}$$

$$V_{in}(s) = RI(s) + \frac{1}{Cs}I(s) \tag{4.4}$$

$$V_{in}(s) = \left(R + \frac{1}{Cs}\right)I(s) \tag{4.5}$$

Defining the output voltage of the circuit shown in Figure 4.1

$$v_{out}(t) = \frac{q(t)}{C} \tag{4.6}$$

$$v_{out}(t) = \frac{1}{C}\int_0^t i(u)du \tag{4.7}$$

Applying Laplace Transform to (4.7):

$$\mathcal{L}\left\{v_{out}(t)\right\} = \mathcal{L}\left\{\frac{1}{C}\int_0^t i(u)du\right\} \tag{4.8}$$

$$V_{out}(s) = \frac{1}{Cs}I(s) \tag{4.9}$$

Defining the Transfer Function using Equations (4.5) and (4.9)

$$\frac{V_{out}}{V_{in}} = \frac{\frac{1}{Cs}}{R + \frac{1}{Cs}} \tag{4.10}$$

$$G(s) = \frac{V_{out}}{V_{in}} = \frac{1}{RCs+1} = \frac{1}{\tau s+1} \tag{4.11}$$

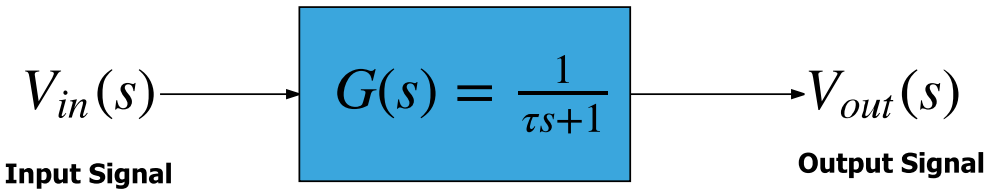

Figure 4.2: Block Diagram of a First Order Low Pass Filter

Where τ is defined as the time constant of the Transfer Function

(4.12)

The transfer function defines the filters response to any arbitrary input signal.

4.2.1. Analysis/Filter Performance

There are two types of faults that have to be considered. The first case is the residual ground fault which would occur when a subject touches a live wire. In this case currents are limited to values lower than 1 A by the relatively large fault impedance (more than 500 Ω). The fault will be cleared by residual ground fault protection within a reasonable time and should not pose a problem for the power limit of the Zener diodes.

In case of a low impedance fault currents would be naturally higher and could easily destroy both Zener diodes and grounding capacitors. Ground faults with potentially high currents would be cleared in the μs range by solid state breakers, such that the energy dissipation in the Zener diodes does not pose a problem.

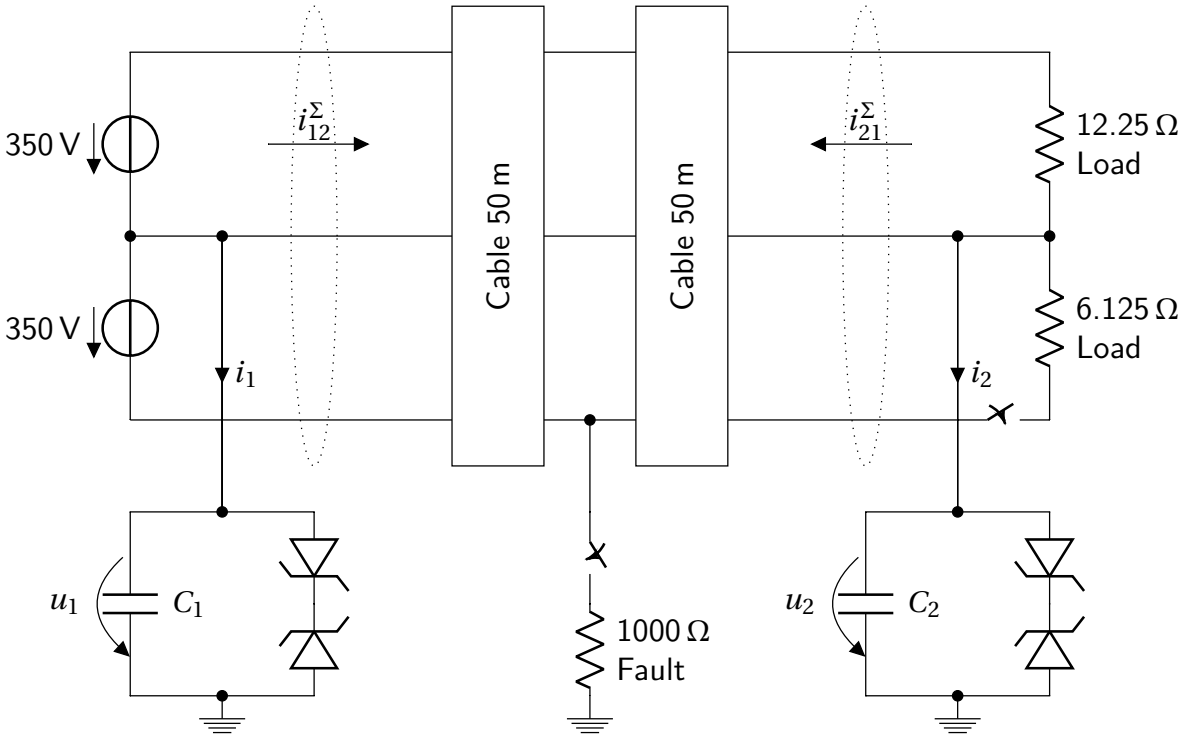

Figure 4.3: Bipolar dc grid with two capacitive grounding points with voltage clamping by zener diodes. Sources on the left and asymmetrical loads on the right. The 20 kW load on the negative pole is disconnected to change the load balance. Further a human ground fault can be generated in the middle of the cable of 100 m length [17].

A simulation for a grounding capacitance value of 1 μF is modeled using the schematic in Fig. 4.3. Additionally a ground fault on the negative pole is included to emulate a human ground fault. Human

impedance is by no means a constant value and depends on many factors. Nevertheless, a reasonable value of 1000 Ω is chosen according to the IEC Standard 60479-5 [7]. The human ground fault is only used in the next Section.The human ground fault is triggered at 0.5 s with a duration of 10 ms. The balancing current peaks can be seen in the top window of Fig. 4.4. The human ground fault can barely be seen at 0.5 s.

For discrimination the first order low pass filter from Eq. 4.11 is implemented to measure current for the sum of currents i_{12}^{Σ} shown in Fig. 3.4. A time constant $\tau = 100$ ms is choosen for this simulation. A fault is detected when the filtered value reaches the selected current threshold of 30 mA in both the positive and negative direction.

Looking at the simulation results shown on Fig. 4.4 it is easy to see that the duration for both the load change currents and the human fault current serves as discriminating variable for the protection scheme. The high peaks of the balancing currents are very short and thus have only a small effect on the filter output. The small magnitude of the human ground fault is compensated by the duration of 10 ms that is needed to cause considerable harm. In this simulation only the human ground fault filtered current peak the value is higher than the selected threshold value of 30 mA.

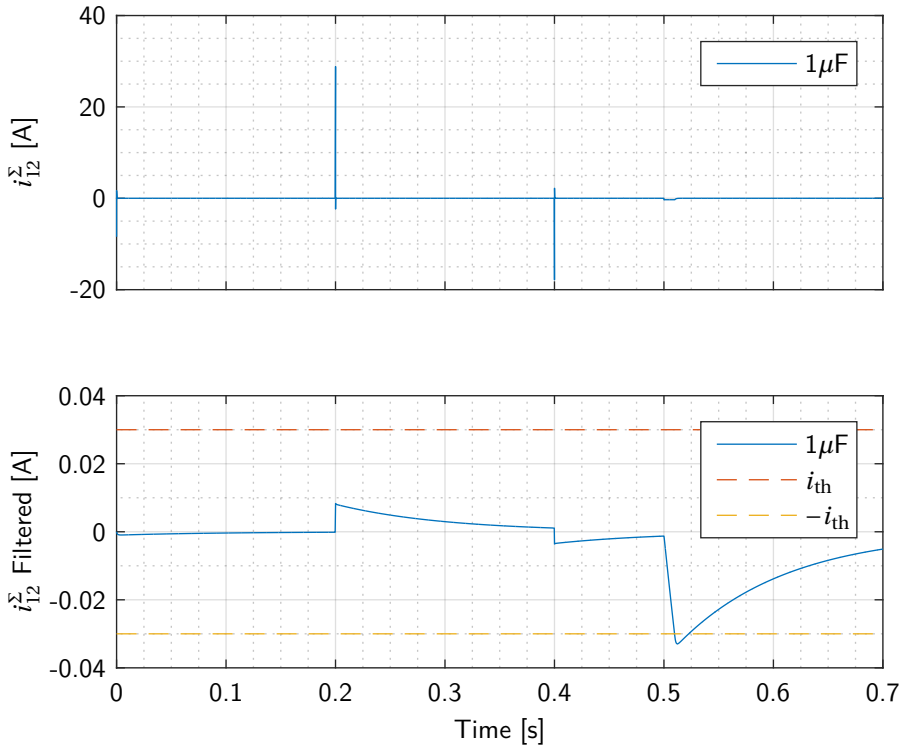

Figure 4.4: Current sum measurement and low pass filtered current sum with time constant $\tau = 100$ ms. The negative load is disconnected at 0.2 s and reconnected at 0.4 s. A 1000 Ω residual ground fault of 10 ms duration occurs at 0.5 s. It can be seen that the threshold is only reached for the residual ground fault and not for the balance changes, even though the raw magnitudes (on top) have the opposite relation [17].

4.2.2. Filter Detection Map

If a protection scheme for capacitive grounding were to be implemented using the aforementioned scheme, the filter should follow the IEC standard [7] in order to guarantee safety for all users. Therefore the residual ground fault protection filter is analized for different current magnitudes and fault durations. For this reason, a detection map is derived and shown in Figure 4.5.The map consists of currents between 100 μA and 10 A with durations ranging from 100 μs to 10 s. The first order low pass filter has a time constant $\tau = 100$ ms with a detection threshold of 30 mA.

For each value of current and time the filter is tested to compare allowed limits according to standard [7]. The IEC standard [7] limits are included on Figure 4.5 (red line) to make a proper comparison. The standard

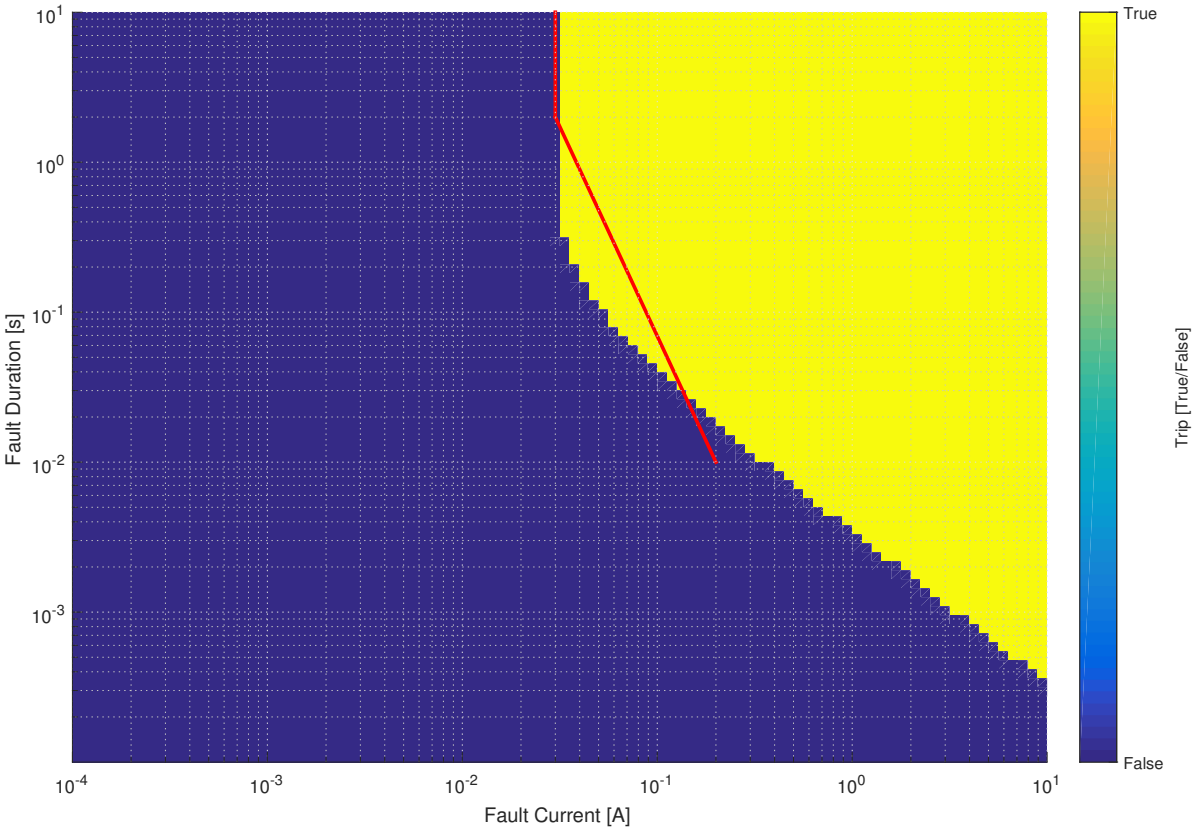

Figure 4.5: Detection map for first order low pass filter [17]. Blue color implies no detection from the filter whilst yellow color means favorable detection. Red line shows the limits for currents that may cause permanent damage to human body according to [7].

only defines the behavior above 10 ms as traditional AC circuitbreakers can not protect faster anyway. The filter follows approximately the sectors that the standard states for dangerous currents through the human body corresponding to values at the right of the red line. It can be seen that even though the filter detects most of the area located at the right side of the standard, it also has a considerable amount of detection to the left of it.

Furthermore, the time that the filter needed to detect the fault for each point in the map is shown as a detection time map in Figure 4.6. At the right side of the Figure a colored bar states the time it took to detect the fault. As a comparison with Figure 4.5, which can be considered as a Boolean map, this one states how much time it took to the filter to reach the threshold value and detect the fault. The blue color section means that the filter detected almost instantly the fault. This is a reasonable behavior since at higher currents the duration needed to reach the threshold values is considerably lower, while at low currents the filter may need more time to clear the fault. Nevertheless, the filter behavior as mentioned before follows the limits stated by the IEC standard.

The information given by these maps may be useful to determine whether a detection scheme goes according to the IEC standard or not. As means of standardization this can be implemented to state if the protection is fast enough to detect and thus clear the fault before it becomes a problem for the system or end users.

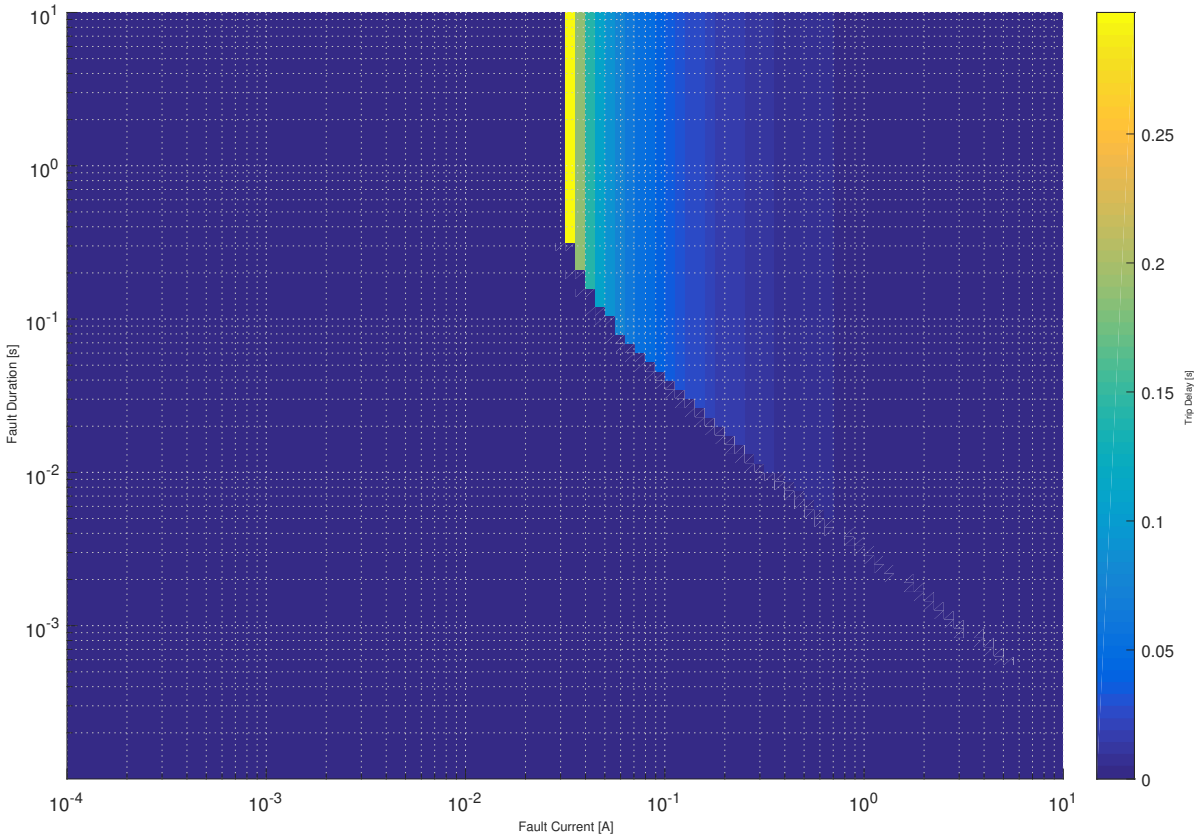

Figure 4.6: Time detection map for first order low pass filter.

4.3. FILTER SYNTHESIS

In the previous Section the detection maps of the first order low pass filter are shown to exemplify how the behavior of a detection scheme should look like and most importantly to establish a reference for future standards that may be used on the design of protection schemes for LV DC distribution grids. Nevertheless, this particular filter behavior is mainly determined by the time constant and threshold value chosen for the simulation. This Section focuses on the sensitivity of the filter to the current threshold and time constant parameters. The main objective is to determine how the detection behavior can be modified to adapt to new current threshold values and standardization guidelines.

To show the sensitivity of the first order low pass filter to changes in current threshold values and time constant a set of simulations is done. The filter simulations for different time constants and threshold values of the first order low pass filter are shown in Appendix C.1. The plots are presented as following: on the top leftt side the first simulation is presented with a current threshold value of 20 mA and a time constant of 1 ms. To the right side the simulation current threshold is increased per plot up to 100 mA. Furthermore, also from the top left side towards the bottom side the time constant is increased per plot up to a value of 10 ms. Every column increases towards the bottom side only in time constant values and every row increases towards the right side only in current threshold values.

These sets of simulations show an interesting behavior in the filter response. The "knee" shown in the plots follows the threshold and time constant values of the filter. This means that for synthesis and calibration purposes the filter can be adapted to follow the given behavior of the IEC or any relevant standard current thresholds. This is relevant since it shows that the detection scheme implemented could be easily adapted or modified if needed to address different detection requirements making it an interesting solution. Furthermore, as shown in Section 4.2 the filter used in the simulations follows a simple first order low pass filter transfer function stated by:

Figure 4.7: Filter sinthesis by means of filter's transfer function.

$$G(s) = \frac{1}{\tau s + 1} \tag{4.13}$$

Where τ is defined as the time constant of the Transfer Function.

Nevertheless, for practical real life applications this type of filter may also be adapted. For this reason and based in the results shown in Appendix C.1 it becomes interesting to simulate the behavior of the filter with different transfer functions. Therefore, a simulation with the same time constant and current threshold is done but with a filter transfer function with the form:

$$G(s) = \frac{\tau s + 1}{\tau s^2 + \tau s + 1} \tag{4.14}$$

The simulation results are shown in Figure 4.7.

As one may expect the filter response is not only affected by the current and threshold values but also by the filter's transfer function. Nonetheless, an interesting behavior is shown in Figure 4.7. The response of the filter also follows the bode plot of the transfer function as shown in Figure 4.8. The bode plot of a given transfer function can be further controlled by changing its poles and zeros. This enables the possibility of further implement detection schemes that may be able to follow any given behavior as stated by the IEC standard. Further filter synthesis can be done changing the poles and zeros of the filter's transfer function to test and ensure that the protection scheme will only be triggered by current values stated by relevant standards.

The further filter synthesis by means of this method stays out of the scope of this Thesis and remains as an importan aspect for further work and research.

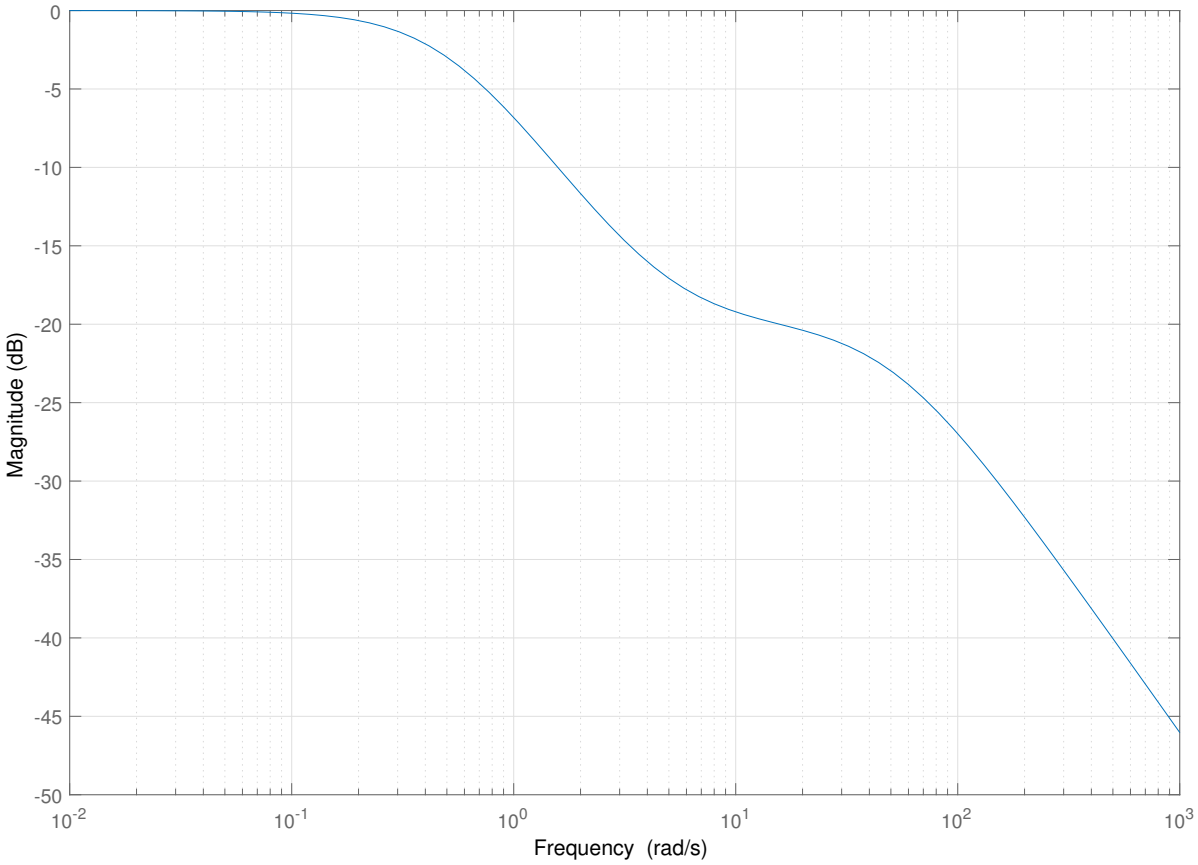

Figure 4.8: Bode plot for filter with transfer function shown in Eq. 4.14.

4.4. CONCLUSION

In this chapter a filter detection scheme implemented in a bipolar network was introduced. This simple filter is designed to detect as accurate as possible the ground fault currents that pose a hazard for the system and end users following the IEC standard current threshold limits. The filter though simple shows the potential of a detection scheme that can be implemented along capacitive grounding protection on a LV DC distribution grid.

Although the filter maps are only presented for a specific value of current threshold and time constant, the sensitivity to these two parameters is further analyzed. It is shown that the detection maps can be adapted by changing these two values.

The bode plots that correspond to the first order filter correspond to the detection curves in the maps shown. It was also shown that further filter synthesis can be achieved by controlling the poles and zeros of the transfer function in the frequency domain. This method may be very useful when designing new standards and guidelines for protection schemes in the LV DC systems.

5

Effect of Multiple Grounding Points

5.1. Mathematical Approach

In the previous Sections, the capacitive grounding scheme is analyzed on the unipolar and bipolar topologies. The importance of capacitance during load shifts is addressed and a sensitivity analysis is made to show the system behavior. A filter design is presented for residual ground fault detection which could discriminate between human ground faults and load shifts. The filter analysis and synthesis are shown and the importance standards like IEC60479 [7] is also discussed.

Nevertheless, the effect of increasing grounding points has not been addressed and the scalability of a system like this remains unknown. This Section will focus on the scalability of such a protection scheme by means of a mathematical analysis in state space representation on the unipolar topology applied on a street network with increasing grounding points.

5.1.1. State Space Model Representation

The state space representation of a system is a mathematical model as a set of input, output and state variables related by first-order differential equations. As such, the goal of this Section is to represent in the most simple yet accurate way the unipolar system we have discussed so far as a state space representation. This is done in order to study the sensibility of the system to increasing grounding points. The state space representation is based on the Unipolar scheme shown in Figure 5.1 with two grounding points.

Looking at Figure 5.1 the state space equations are derived by means of Kirchhoff's current law and Kirchhoff's voltage law applied on the 4 nodes of the schematic shown in Figure 5.1. The detailed derivation of the state space equations can be addressed in Appendix D.1.

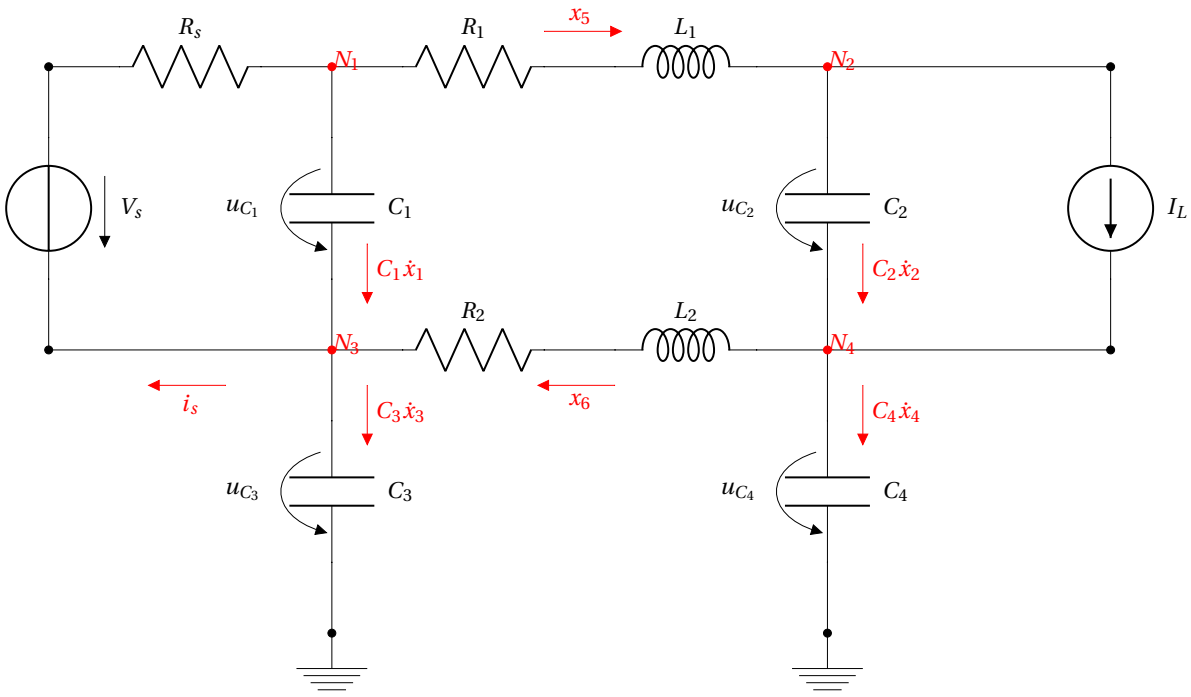

Figure 5.1: Unipolar DC grid with two capacitive grounding points model used to assemble state space equations.. Source on the left and load on the right represented as a current source. The cable length for both positive and negative poles is respresented by a series RL circuit (R_1,L_1 and R_2,L_2). The cable capacitance is represented by capacitors connected in parallel (C_1 and C_2) to both poles. Capacitive grounding points are represented as to capacitors connected to ground (C_3 and C_4). Currents and voltages on the pasive components are indicated

State Space Equations:

$$\dot{x} = Ax + Bu \tag{5.1}$$

$$\dot{x}_1 = \frac{V_s}{C_1 R_s} - \frac{1}{C_1 R_s} x_1 - \frac{1}{C_1} x_5 \tag{5.2}$$

$$\dot{x}_2 = \frac{1}{C_2} x_5 - \frac{1}{C_2} I_L \tag{5.3}$$

$$\dot{x}_3 = -\frac{1}{C_3} x_5 + \frac{1}{C_3} x_6 \tag{5.4}$$

$$\dot{x}_4 = \frac{1}{C_4} x_5 - \frac{1}{C_4} x_6 + I_L \tag{5.5}$$

$$\dot{x}_5 = \frac{1}{L_1} x_1 - \frac{1}{L_1} x_2 + \frac{1}{L_1} x_3 - \frac{1}{L_1} x_4 - \frac{R_1}{L_1} x_5 \tag{5.6}$$

$$\dot{x}_6 = -\frac{1}{L_2} x_3 - \frac{R_2}{L_2} x_6 + \frac{1}{L_2} x_4 \tag{5.7}$$

Once the state space equations are known they can be rearranged into a state space model representation [19](see Appendix E.1.)

$$\begin{cases} \dot{x}=Ax+Bu \\ y=Cx+Du \end{cases} \tag{5.8}$$

One equation per each energy storage element (capacitors and inductances) of the system was derived. In this way the state vector is given by:

$$\dot{x} = [\dot{x}_1 \quad \dot{x}_2 \quad \dot{x}_3 \quad \dot{x}_4 \quad \dot{x}_5 \quad \dot{x}_6]^T \tag{5.9}$$

The input vector in this case is defined as:

$$u = [V_s \quad I_L]^T \tag{5.10}$$

Finally the state space representation of the system is given by:

$$\begin{pmatrix} \dot{x_1} \\ \dot{x_2} \\ \dot{x_3} \\ \dot{x_4} \\ \dot{x_5} \\ \dot{x_6} \end{pmatrix} = \begin{pmatrix} -\frac{1}{C_1 R_S} & 0 & 0 & 0 & -\frac{1}{C_1} & 0 \\ 0 & -\frac{1}{C_2} & 0 & 0 & \frac{1}{C_2} & 0 \\ 0 & 0 & 0 & 0 & -\frac{1}{C_3} & \frac{1}{C_3} \\ 0 & 0 & 0 & 0 & \frac{1}{C_4} & -\frac{1}{C_4} \\ \frac{1}{L_1} & -\frac{1}{L_1} & \frac{1}{L_1} & -\frac{1}{L_1} & -\frac{R_1}{L_1} & 0 \\ 0 & 0 & -\frac{1}{L_2} & \frac{1}{L_2} & 0 & -\frac{R_2}{L_2} \end{pmatrix} \begin{pmatrix} x_1 \\ x_2 \\ x_3 \\ x_4 \\ x_5 \\ x_6 \end{pmatrix} + \begin{pmatrix} \frac{1}{C_1 R_S} & 0 \\ 0 & \frac{1}{C_2} \\ 0 & 0 \\ 0 & 1 \\ 0 & 0 \\ 0 & 0 \end{pmatrix} \begin{pmatrix} V_s \\ I_L \end{pmatrix} \tag{5.11}$$

Table 5.1: Fixed Parameters Values for Linear Street Topology

Parameter	Value
Voltage Source	385 V
ΔV (Source to Load)	70 V
Source/Load Resistance	1 Ω
Cable Length	0.3 km
Cable Resistance	0.265 $\frac{\Omega}{km}$
Cable Inductance	$680 \times 10^{-6} \frac{H}{km}$
Grounding Capacitance	10×10^{-6} F
Simulation Time	0.02 s
Load Disconnection Time	0.002 s

Now that the state space representation of the circuit shown in Figure 5.1 has been determined, it can be modeled in an easier way to assess its behavior. The system is now modeled to have a load disconnection at 0.002 seconds to assess the system behavior. The load disconnection is modeled by adjusting the input vector parameters. The voltage load is set to a fixed value of 385 V and the input current parameter is set in order to have a voltage drop of 70 V from load to source. The parameters for the passive components shown in Figure 5.1 are shown in Table 5.1.

The output signals before and after the filter are presenter in Figures 5.2 and 5.3. The response of the system without the filter shows high frequency oscillations and high current peaks (95 A). As discussed in the previous Chapters a load disconnection may be a normal operation of the grid and without a detection criteria this current value may trigger the protection scheme. Furthermore, the output signal is analyzed through the filter and shown in Figure 5.3. The filtered signal shows considerable lower values compared with the unfiltered signal with a maximum peak of 0.02 A. High frequency oscillations are further removed and the detection threshold could be easily adapted to allow current values like this.

The basic network topology serves as a first approach to determine the system behavior by means of the state space representation analysis. Nevertheless, further simulations have to be done to determine the scalability of such a system with a more detailed network topology.

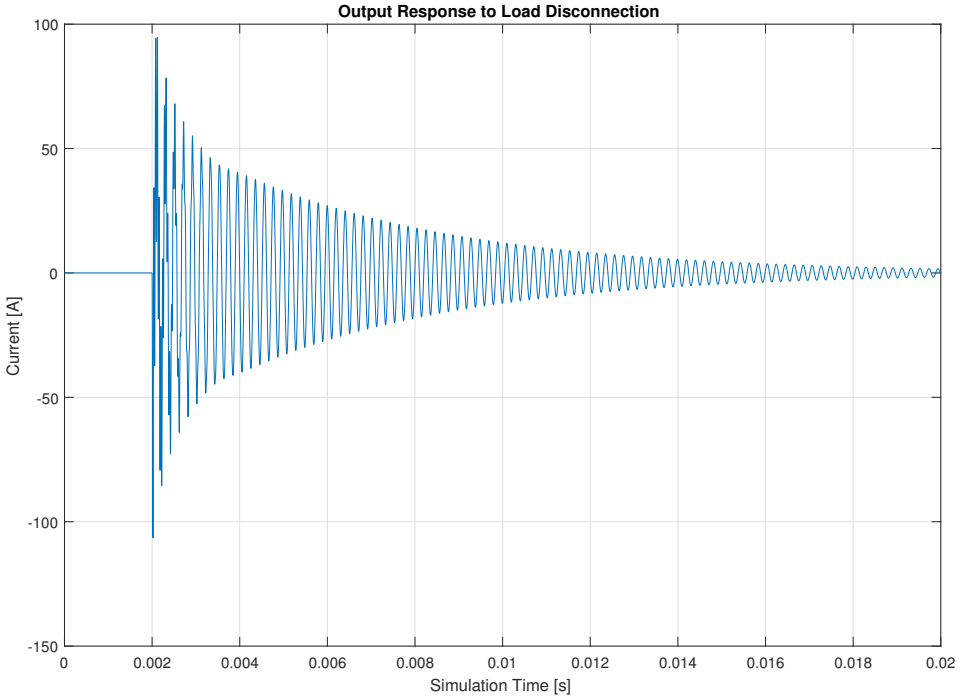

Figure 5.2: Response to load disconnection for the schematic shown in Figure 5.1 for 2 grounding points. The simulation time is set for 0.02 s with a load disconnection at 0.002 s. The resistance, inductance and capacitance are calculated by means of the length of the cable which is considered to be 300 m according to Table 5.1. The system response encounters high frequency oscillations with a peak current of 95 A approximately.

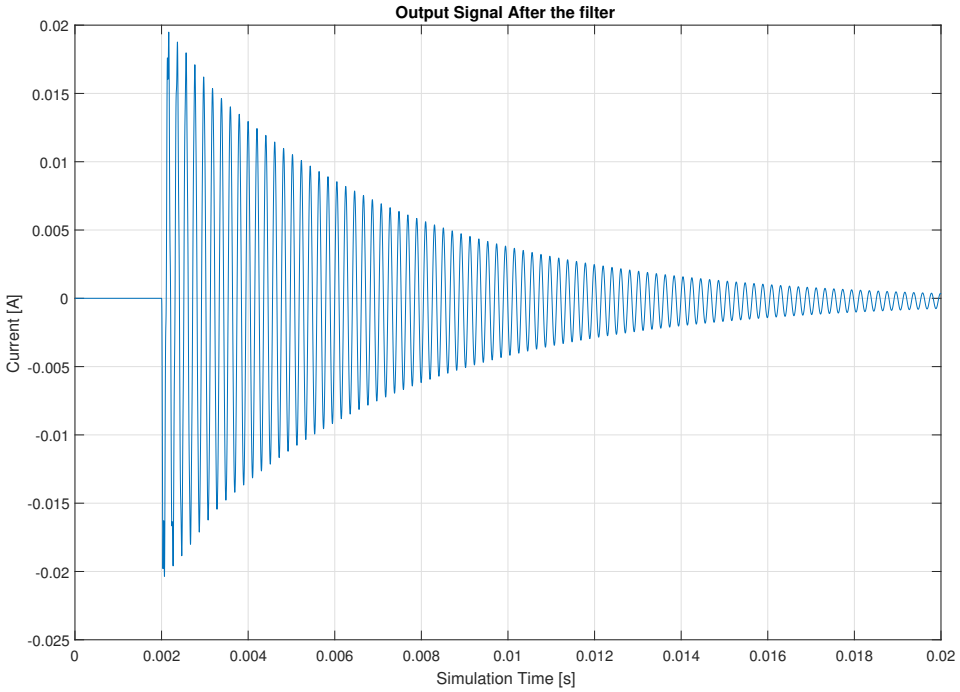

Figure 5.3: Response to load disconnection after filter for the schematic shown in Figure 5.1 for 2 grounding points. The simulation time is set for 0.02 s with a load disconnection at 0.002 s. The resistance, inductance and capacitance are calculated by means of the length of the cable which is considered to be 300 m according to Table 5.1. The system response after the filter has some higher frequency oscillations removed as a consequence of the filter with a considerably smaller peak current of 0.02 A approximately.

5.2. INCREASING GROUNDING POINTS: LINEAR NETWORK

Based on the simulation results on the previous Section the system topology is now adapted to a TN-S grounding configuration in order to make the simulations more realistic. The system schematic is shown in Figure 5.4.

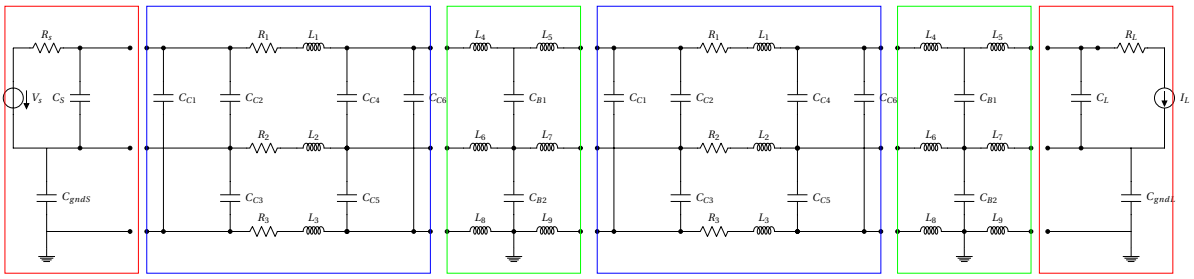

Figure 5.4: Schematic 2 grounding points unipolar network with PE. The schematic shows in colored squares the components of the grid. In red squares the load and source with their capacitive grounding points and the inherit capacitance on load and source modeled by capacitors C_S and C_L. In blue squares the cable representation with the TN-S grounding configuration. The cable capacitance is modeled by capacitors C_{C1}, C_{C2}, C_{C3}, C_{C4}, C_{C5} and C_{C6}. Furthermore, the cable length is modeled by a series RL circuit representented for each conductor by R_1-L_1, R_2-L_2 and R_3-L_3. Finally, in green squares a circuit breaker representation representing the grounding points. The breaker inductance and capacitance is modeled for each conductor by L_4-L_5, L_6-L_7, L_8-L_8 and C_{B1}-C_{B2} .

Furthermore, the topology that will be addressed on this Section is shown in Figure 5.5. The state space representation of the system is also derived from the circuit. For the sake of simplicity and due to the complexity of the following simulations the derivation of the state space representation are not described further. Nevertheless, the same principle is applied for all the following simulations to have consistent results.

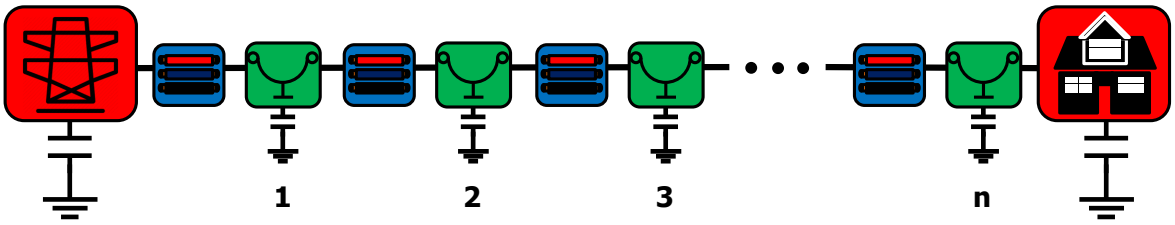

Figure 5.5: Linear Unipolar Distribution Network with increasing grounding points. This topology is used to analyze the behavior of the distribution LV unipolar DC grid to the effect of increasing grounding points. In red the load and source, in blue the cable model, in green a DC breaker on which the grounding points are present.

The system sensibility will be modeled on a Matlab Simulink script exemplifying a linear DC distribution system on a LV level for domestic households with increasing grounding points. Since the goal is to study the system behavior with increasing grounding points other variables in the system are fixed and exemplified in Table 5.2.

Furthermore, the system is modeled with a load disconnection at 3 ms in order to study the response to the system to load shifts with increasing grounding points. The input vector shown in Equation 5.10 is adapted to show a load disconnection by influencing the current source input variable while keeping the voltage source value at 385V at all time. This input vector current magnitude input is calculated in a way that guarantees that the voltage drop expected from load to source is exactly of 70 V which corresponds to a voltage drop from 385 V to 315 V ($\Delta V = 70\,V$).

In addition, the filter studied in Chapter 4 is also implemented in the analysis to show the current detection scheme implemented. This is done to give useful information on the detection scheme.The general flowchart of the modeled system is shown in Figure 5.6. The state space vector is obtained on each model i.e. the Unipolar schematic with 2, 4, 8, 16, 32 and 64 grounding points. Then a load disconnection is modeled to show the system behavior. The sums on the two conductors (positive and negative) between each grounding point are the outputs of the system. These individual outputs are plotted for each configuration and each number of grounding points. Furthermore, the outputs of this system go through the first order low pass

Table 5.2: Fixed Parameters Values for Linear Street Topology

Parameter	Value
Voltage Source	385 V
ΔV (Source to Load)	70 V
Source/Load Resistance	1 Ω
Cable Length	0.3 km
Cable Resistance	0.265 $\frac{\Omega}{km}$
Cable Inductance	$680 \times 10^{-6} \frac{H}{km}$
Breaker Inductance	47×10^{-6} H
Breaker Capacitance	10×10^{-6} F
Source Capacitance	100×10^{-6} F
Load Capacitance	100×10^{-6} F
Grounding Capacitance	10×10^{-6} F
Simulation Time	0.03 s
Load Disconnection Time	0.003 s

filter mentioned in Chapter 4 and with transfer function according to 4.13 with a time constant of 100 ms. The filtered output current signals are also plotted for each configuration and each number of grounding points.

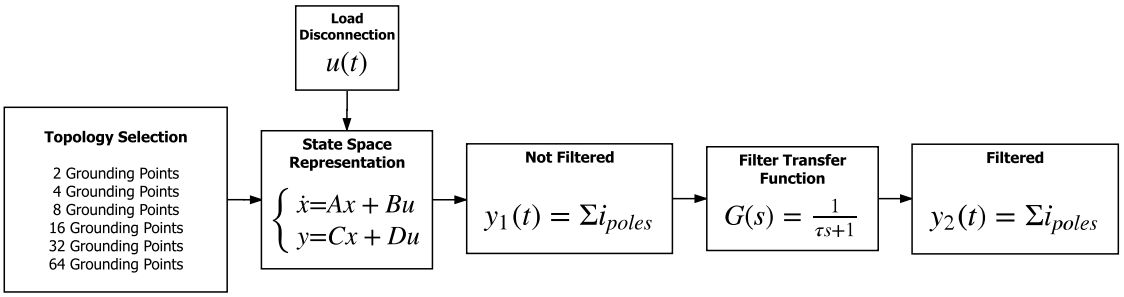

Figure 5.6: Simulation Flow Chart. The selection of the desired topology is translated to state space representation. The input vector simulates a load disconnection at a specific time and as ouput variables the sum of currents in the positive and negative poles is obtained (Σi_{poles}). This signal goes through the first order low pass filter with transfer function shown in Equation 4.13. The filtered and not filtered values are plotted for all the grounding points.

The output signal before and after the filter for 2 grounding points are shown in Figures 5.7 and 5.8. The load disconnection causes a disturbance in the system and as grounding points increase the current peaks are also incremented. On the other hand is important to note that the maximum current value is encountered approximately at the middle of the distribution line. This is because the inductance effect is increased resulting on a maximum current peak value at disconnection in the middle of the line. Look Figure 5.10

In addition to the information analyzed from the previous figures, the maximum peak current for every number of grounding points aefore the filter is shown in Figure 5.11.

It is interesting to mention that the maximum peak values after the filter seem to stabilize to 0.04 A. This could mean that the effect of added inductance may be limited to a certain value and the load changes on the scalability of the system may not increase up to dangerous values for the system or end users. Moreover, the system may be able to work properly and not detect these current values if filter synthesis is applied as mentioned in Chapter 4. Since the values are still on a reasonable threshold value this could be easily implemented on the detection scheme to avoid detection when load shifts occurs whilst detecting human ground faults according to the IEC standard [7]. Nevertheless, further research has to be done with different topologies and variables in order to prove this observation right.

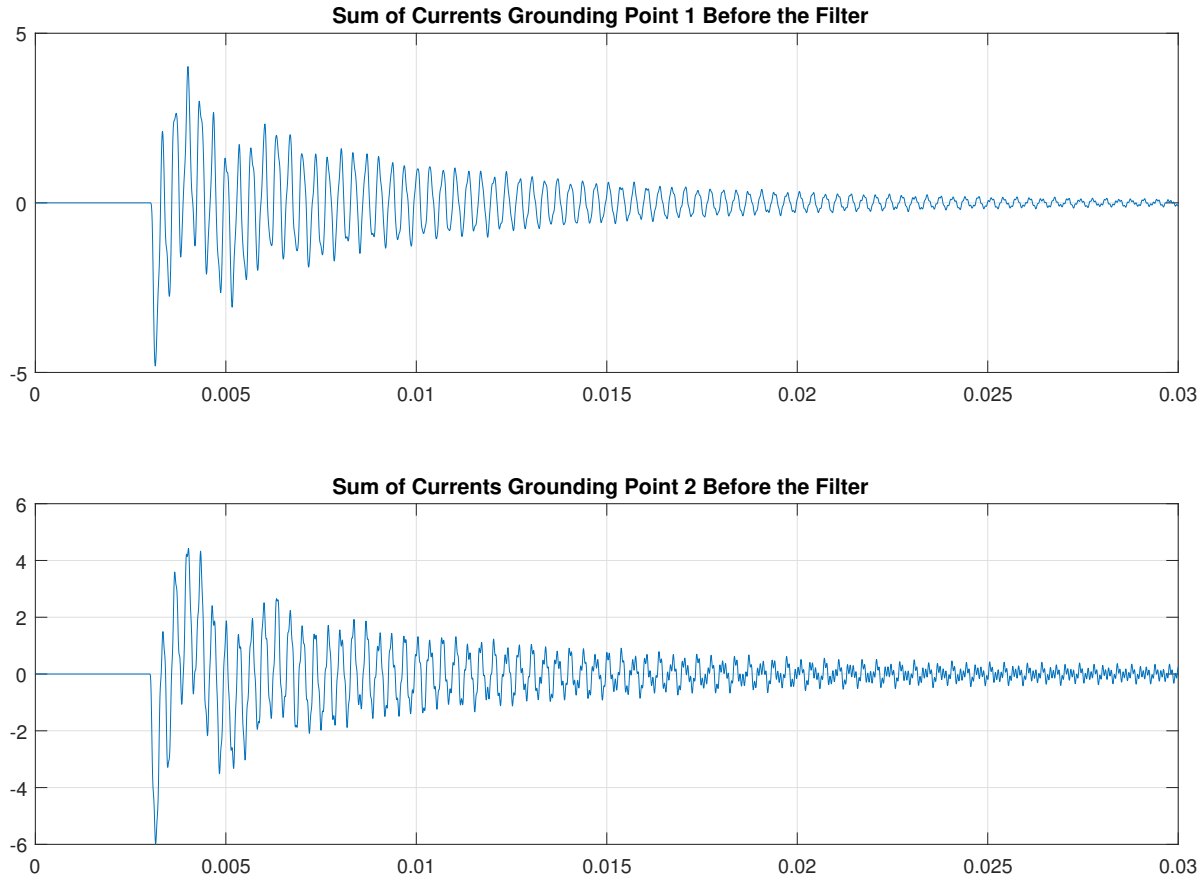

Figure 5.7: Output Signal for 2 grounding points before filter. The signal corresponds to the sum of the currents on the positive and negative pole. The load disconnection is modeled after 0.003 seconds.

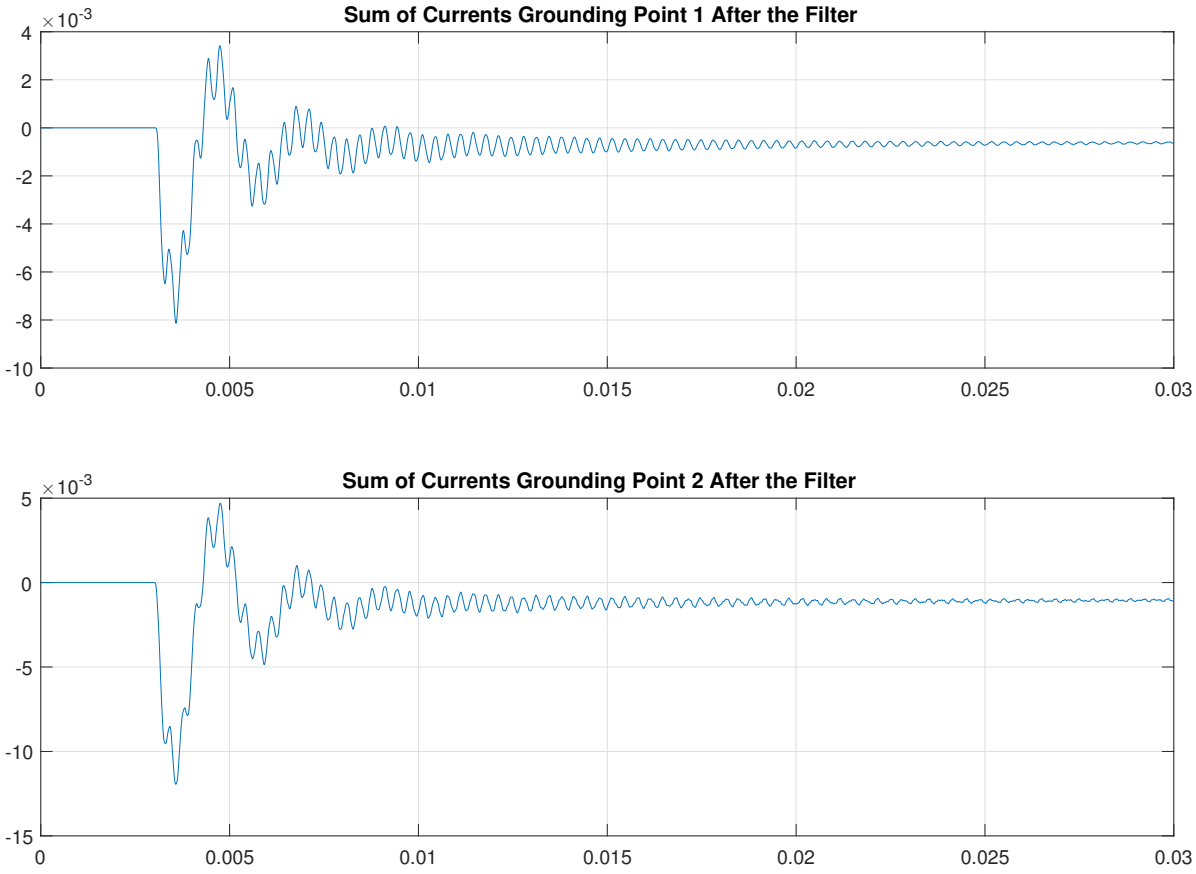

Figure 5.8: Output signal for 2 grounding points after filter. The signal corresponds to the sum of the currents on the positive and negative pole. The load disconnection is modeled after 0.003 seconds.

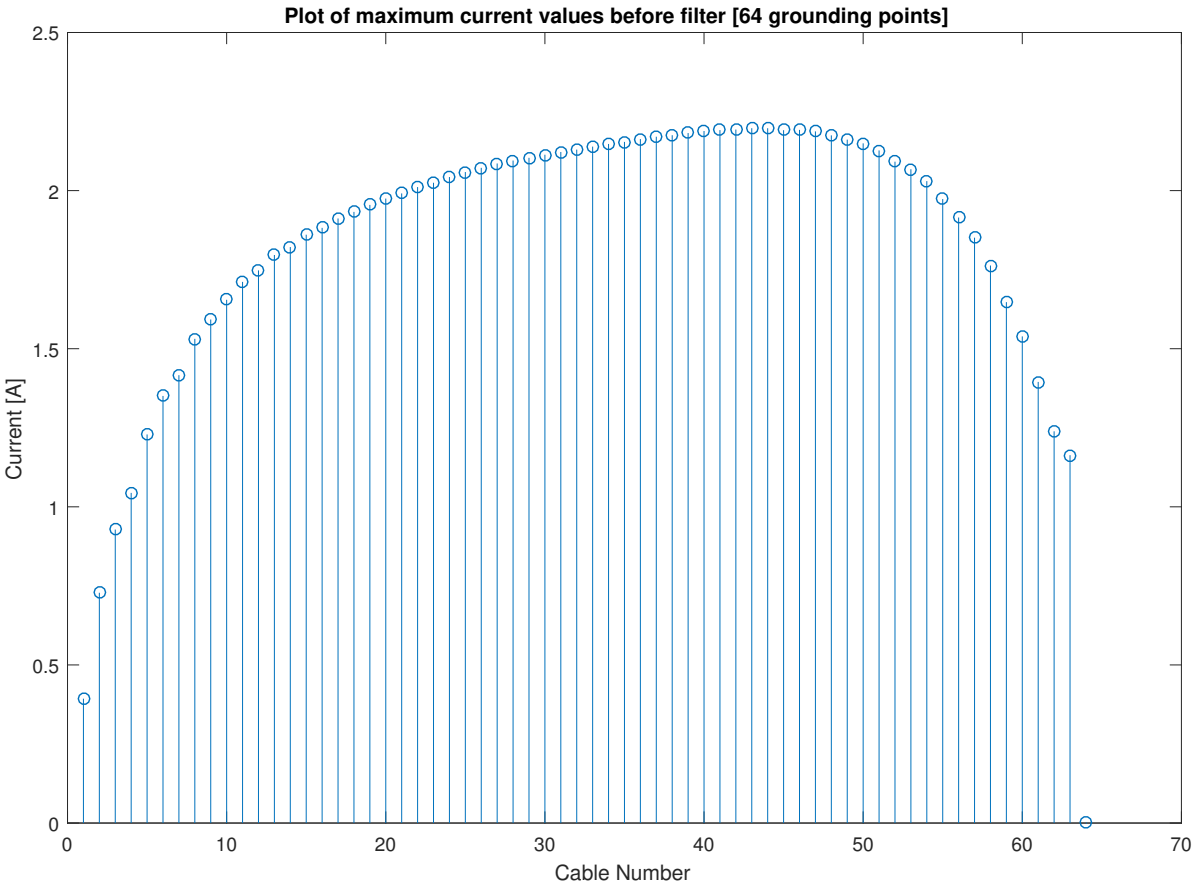

Figure 5.9: Output signal for 64 grounding points before the filter. The signal corresponds to the sum of the currents on the positive and negative poles for each grounding point.

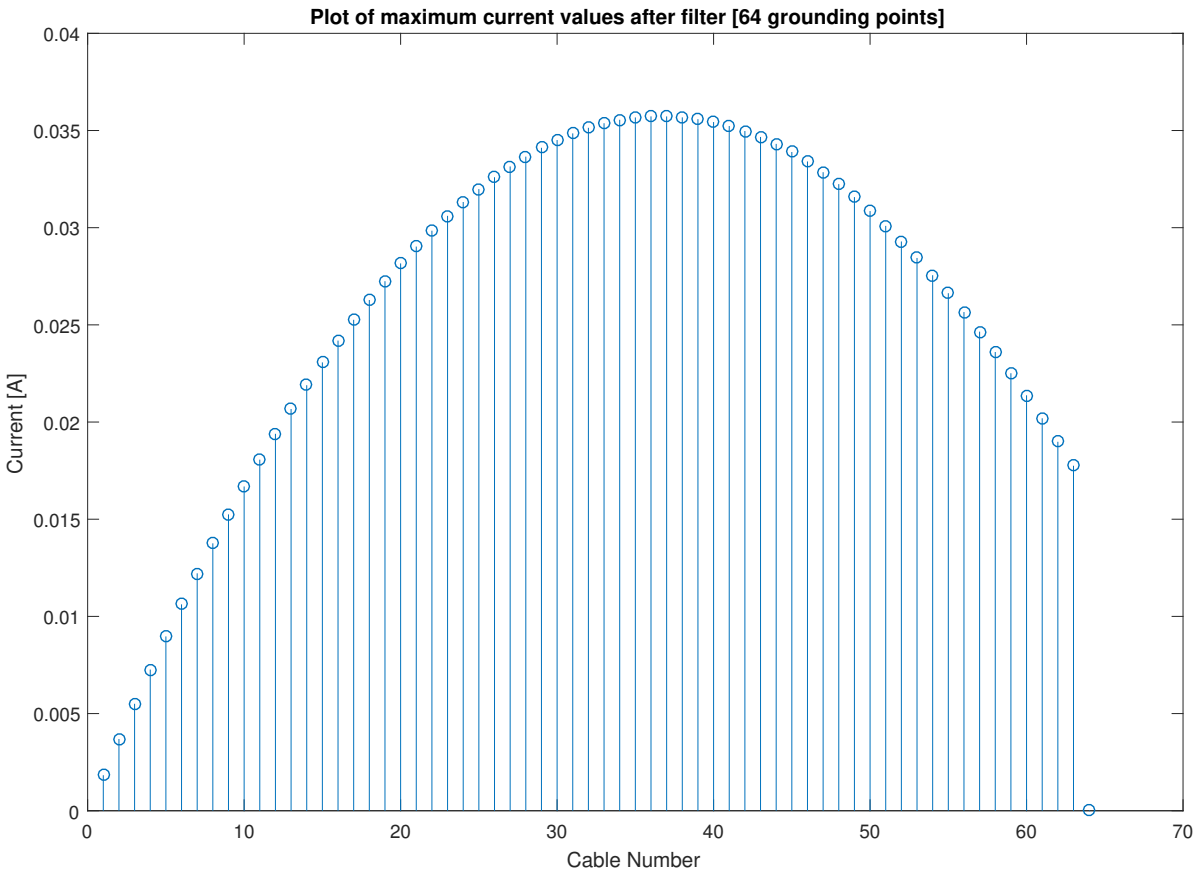

Figure 5.10: Output signal for 64 grounding points after the filter. The signal corresponds to the sum of the currents on the positive and negative pole for each grounding point.

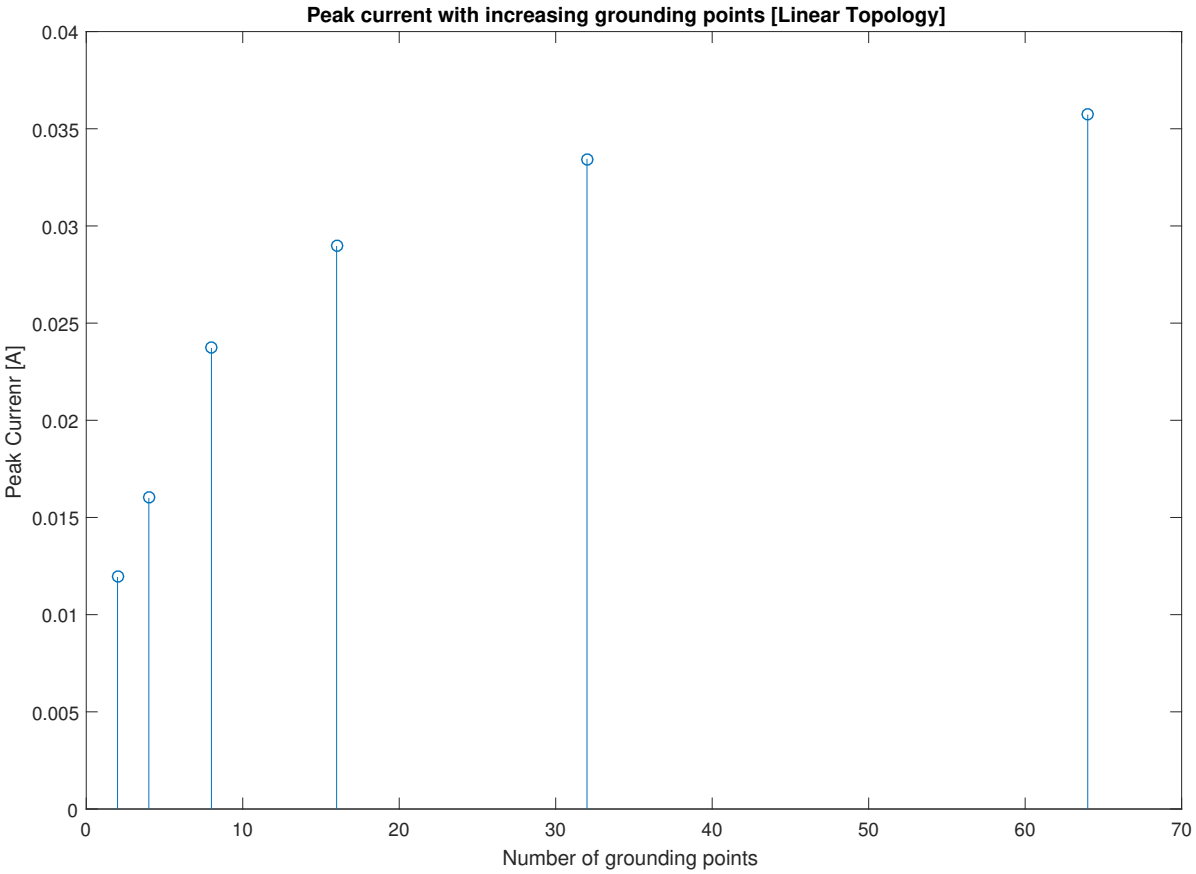

Figure 5.11: Maximum peak current values for each grounding simulation on the linear topology. On the X axis the number of grounding points simulated, on the Y axis the maximum current measured in A. The current values with increasing grounding points seems to have a limit tending to 0.04 A.

5.3. INCREASING GROUNDING POINTS: HOUSE NETWORK

Now that the behavior of the system to load unbalance with increasing grounding points was discussed in Section 5.2, it is now interesting to analyze a different network arrangement. Keeping the same grounding configuration as in Section 5.2 (TN-S), the schematic that will be addressed on this Section is shown in Figure 5.12.

The system is also simulated for 2, 4, 8, 16, 32 and 64 grounding points following the topology shown in Figure 5.13. The same flow diagram as mentioned in Figure 5.6 is also implemented so the simulation results are consistent with each other. In the same way as in Setion 5.2 the input vector shown in 5.10 is adapted to show a load disconnection by influencing the current source input variable while keeping the voltage source value at 385V at all time. This input vector current magnitude input is calculated in a way that guarantees that the voltage drop expected from load to source is exactly of 20% which corresponds to a voltage drop from 385 V to 315 V. The fixed system variables are modified for a symmetric LV domestic network as shown in Table 5.3.

In Figures 5.14 and 5.15 the output signals for 2 grounding points modelated with this topology are shown. The load disconnection causes a peak current value at 0.004 ms and the current presents high frequency oscilations. This effect is mainly due to the parasitic capacitance that is included in the cable. The peak current for every number of grounding point configuration is shown in Figures 5.18. In contrast with the linear network results this plot shows no convergence towards a specific value. The peak encountered

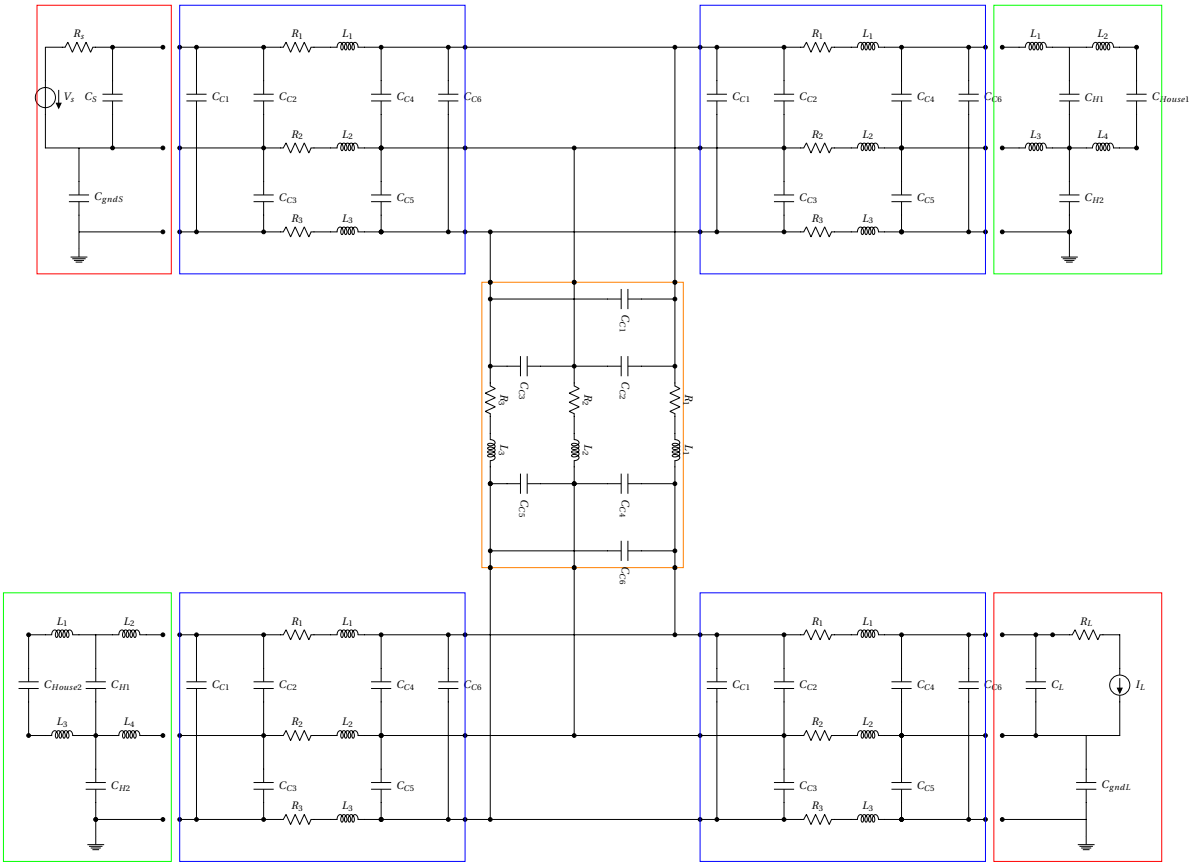

Figure 5.12: Unipolar DC grid with two capacitive grounding points on a symmetric network. The schematic shows in colored squares the grid components. In red squares the load and source with their capacitive grounding points and the inherit capacitance on load and source is modeled by capacitors C_S and C_L. In blue squares the cable representation with the TN-S grounding configuration. The cable capacitance is modeled by capacitors C_{C1}, C_{C2}, C_{C3}, C_{C4}, C_{C5} and C_{C6}. In orange and located at the center of the Figure the street distribution cable line is shown. This orange squared section represents a different cable parameters than the ones squared in blue. The distance for these cables blocks is not equal and thus a differentiation has to be made. Finally, in green squares the LV household representation with its own grounding point. This LV household is modeled as a load which is not consuming power from the grid. For this reason the current source encountered in the normal operating LV household is not present in this case.

in the 32 grounding point simulation is higher than the one of 64 grounding points. Since the peak current plot in this Figure is the result of the sum of currents in both conductors (Positive and Negative) the current fluctuations caused by the capacitance may not be the same and the peak shown may be a consequence of this.

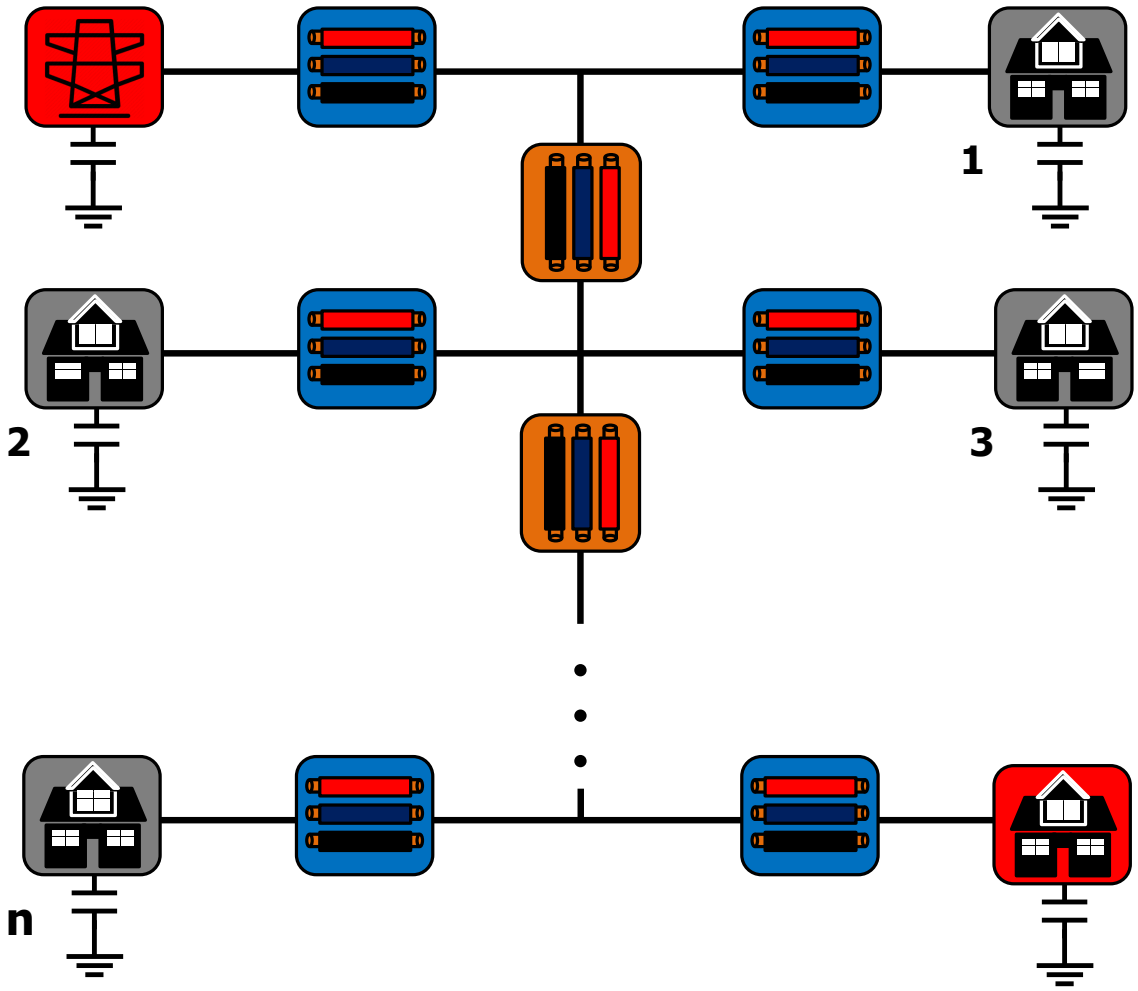

Figure 5.13: Symmetric Unipolar Distribution Network with increasing grounding points. This topology is used to analyze the behavior of the distribution LV unipolar DC grid to the effect of increasing grounding points with a symmetric network of houses. In red the load and source, in blue the cable model that represents the cable connected from the distribution line to the house, in orange the cable model that represents the cable connection for the distribution line, in green a LV household model connected to the distribution grid but with no load demand.

Table 5.3: Fixed Parameters Values for Symmetric Street House Topology

Parameter	Value
Voltage Source	$385\ V$
ΔV (Source to Load)	$70\ V$
Source/Load Resistance	$1\ \Omega$
Street Length	$0.03\ km$
House Length	$0.02\ km$
Cable Resistance	$0.265\ \frac{\Omega}{km}$
Cable Inductance	$680 \times 10^{-6}\ \frac{H}{km}$
Breaker Inductance	$47 \times 10^{-6}\ H$
Breaker Capacitance	$10 \times 10^{-6}\ F$
Source Capacitance	$100 \times 10^{-6}\ F$
Load Capacitance	$100 \times 10^{-6}\ F$
Grounding Capacitance	$10 \times 10^{-6}\ F$
Simulation Time	$0.4\ s$
Load Disconnection Time	$0.04\ s$

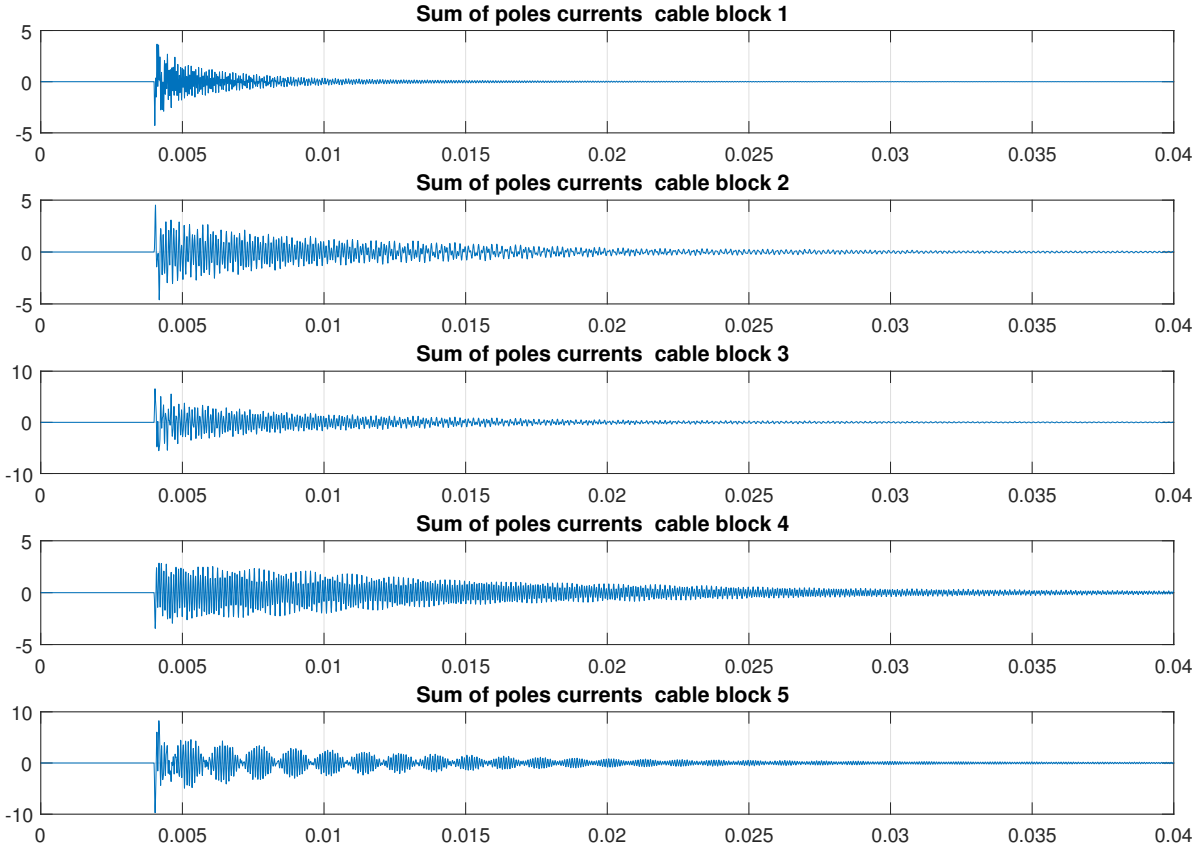

Figure 5.14: Output signal for 2 grounding points before filter symmetric network. From top to bottom the sum of currents on the cable conductors for the cable blocks explained in Figure 5.12 are shown. The signals show high requency oscilations due tothe parasitic capacitance modeled in the cable blocks.

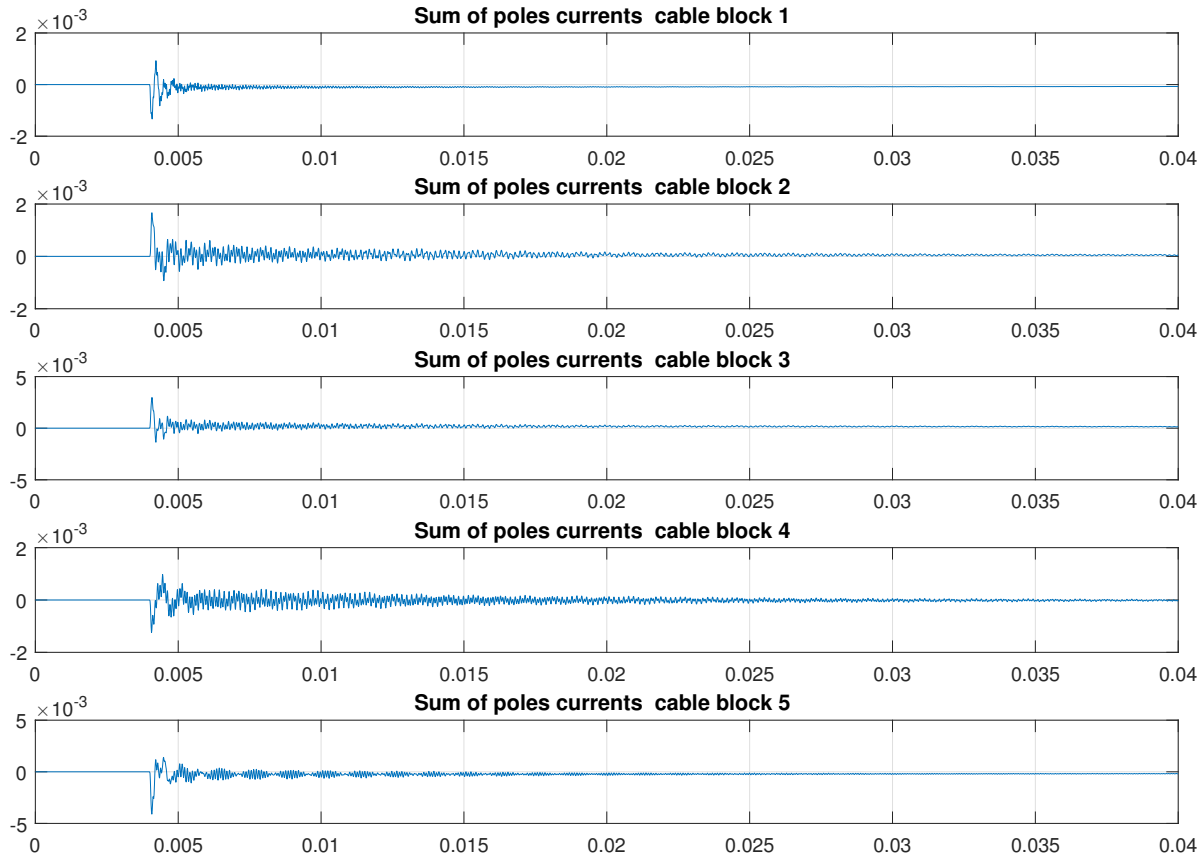

Figure 5.15: Output signal for 2 grounding points after filter symmetric network. From top to bottom the sum of currents on the cable conductor for the cable blocks explained in Figure 5.12 are shown. The magnitude for this signals is due to the fact of the filter effect and in comparison with the output signals in Figure 5.14 this are not present.

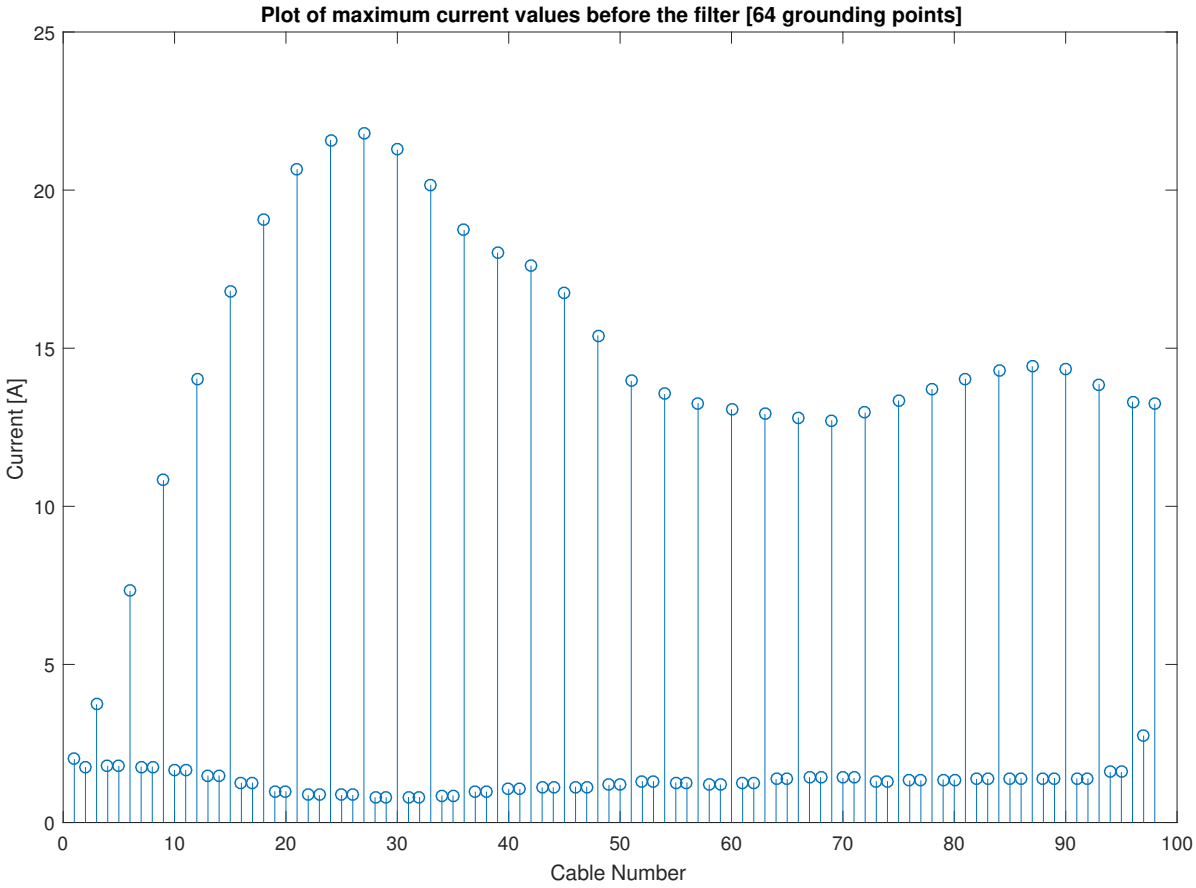

Figure 5.16: Maximum current values before the filter [64 grounding points]. For every cable model under the topology explained in Figure 5.13 the sum of currents in the poles is shown. The current values seem to increase to a global maximum in the first sections of the distribution line. On the other hand a local maximum is also present on the end line of the distribution line. Since the simulation was done with 2 different distance for the cable connected to the houses and the transmision cable of the street, the highest current values are encountered in the transmision cable. The lower current values are reasonable steady and represent the curent flowing through the cable houses.

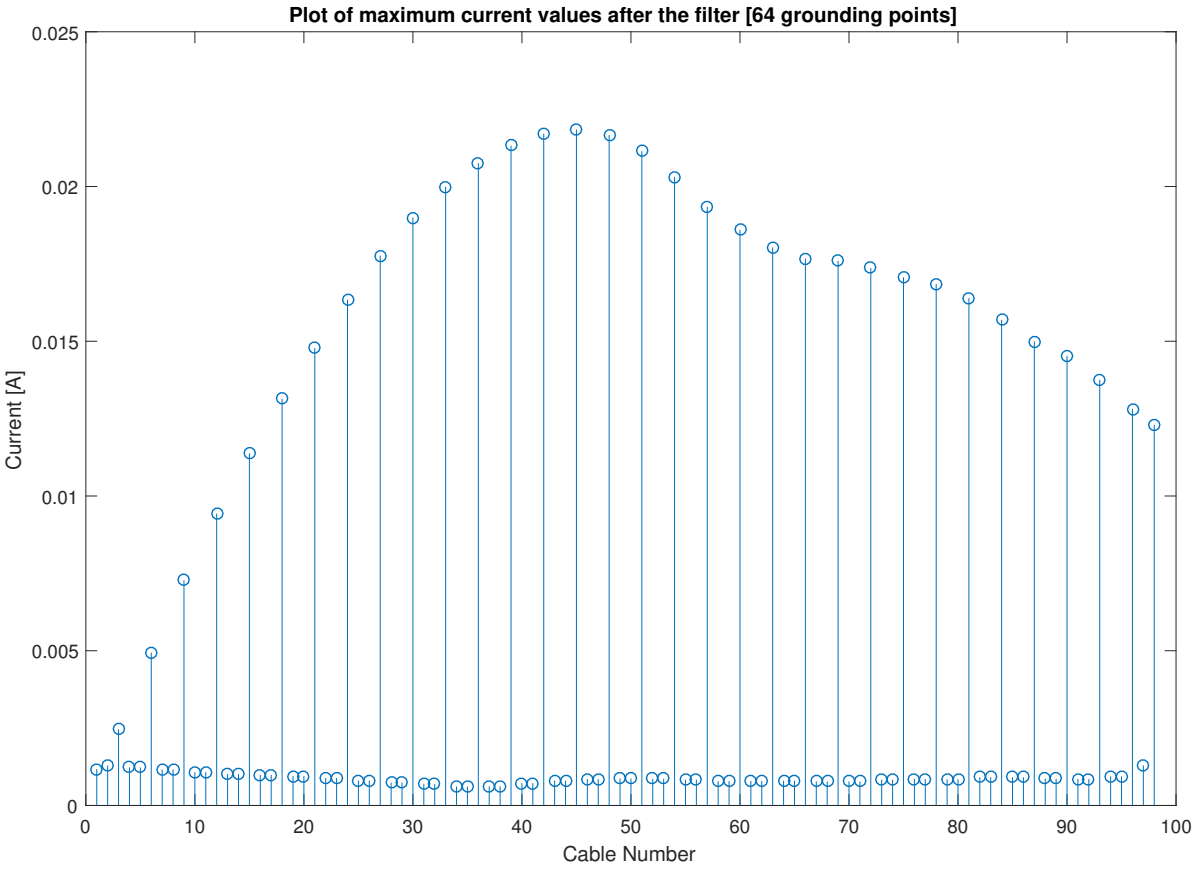

Figure 5.17: Maximum current values aftter the filter [64 grounding points]. For every cable model under the topology explained in Figure 5.13 the sum of currents in the poles is shown. The current values seem to increase to a global maximum approximately at the middle section of the distribution line which in comparison with the signals before the filter only have a global maximum. Since the simulation was done with 2 different distance for the cable connected to the houses and the transmision cable of the street, the highest current values are encountered in the transmision cable. The lower current values are reasonable steady and represent the curent flowing through the cable houses.

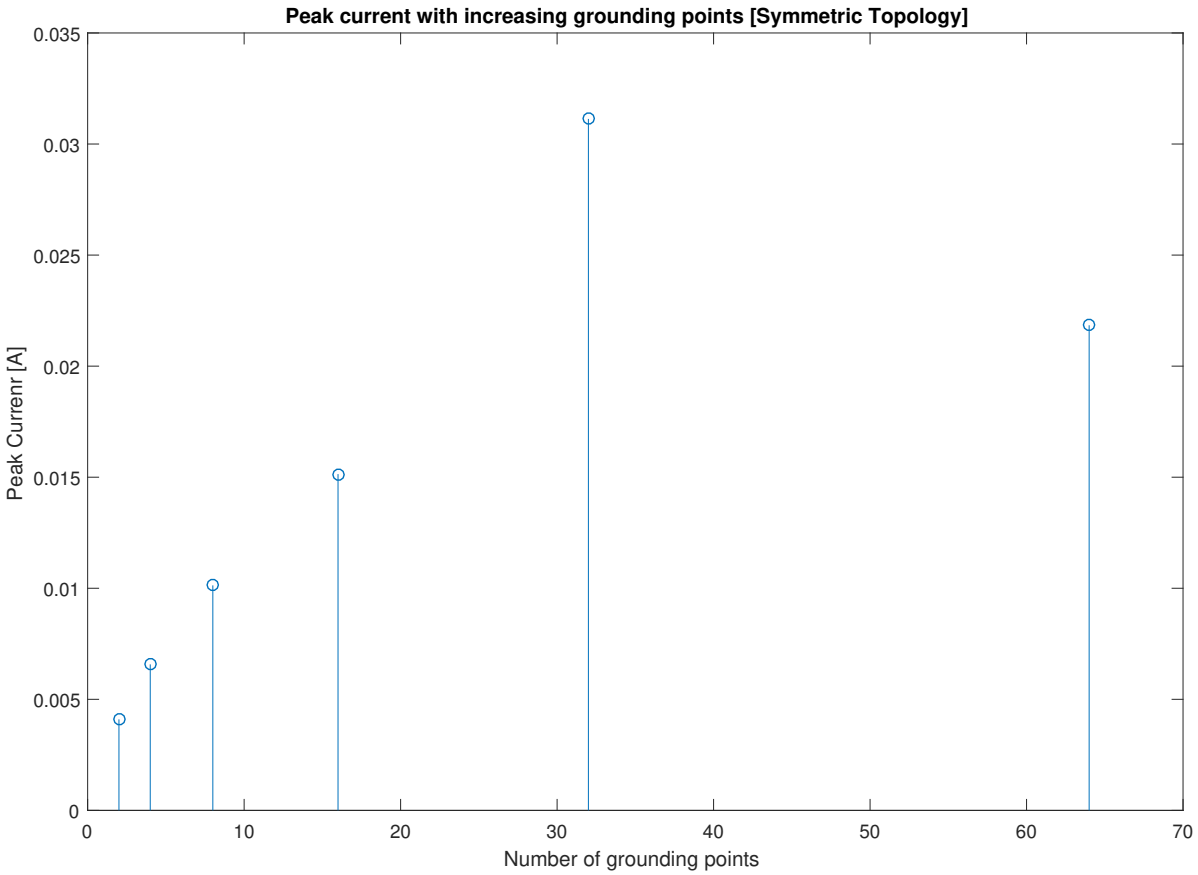

Figure 5.18: Peak Current with increasing grounding points (Symmetric Network). The maximum value of current for each simulation under the symmetric topology shown in Figure 5.13 are presented. In comparison with the linear topology shown in Section 5.2 the current values does not seem to tend to a specific value. There peak encountered at 32 grounding points (0.033 A) is higher than the one encountered at 64 grounding points (0.023 A).

5.4. CONCLUSIONS

In this Section the behavior of increasing grounding points on a unipolar topology with a sudden load change was studied. It is shown that the effect of added capacitive grounding points may not be a disadvantage to the detection scheme. The results for the linear configuration shown in Section 5.2 show that with increasing grounding points the maximum current encountered when the load change happens tends to converge to a maximum value. This value is also in a reasonable limit if filter detection is implemented. This behavior could be easily adapted to the protection scheme in order to keep normal operation and not detect currents due to load shifts while detecting current caused by human ground faults.

On the other hand, it is also shown that this behavior is not present in all the topologies. The results shown in Section 5.3 show that the peak current values not seem to converge to a specific value. In order to properly determine the reason of such an invariance further research has to be done. It would be useful to analyze the individual current behavior for each pole individually and not as a sum. This could help determine if indeed the peak may be caused by the addition of both currents in the poles.

6

Conclusion

Throughout this thesis the capacitor grounding scheme for a LV DC distribution grid was studied. From the literature studied in Chapter 2 requirements for a ground fault current detection and protection scheme were derived. It was shown that using information of standards such as IEC Standard 60479 [7] current limits that ensure human safety can be applied for a protection scheme. In Chapter 3 the effect of capacitive size in the capacitive grounding scheme mainly affect the transient behavior during load changes. The current values encountered during sudden load changes pose a danger for human users. Therefore, it was concluded that a detection scheme has to be implemented to ensure normal operation while detecting ground faults caused by humans. This detection scheme was analyzed demonstrated with Matlab Simulink and detection maps were derived from it. The detection maps show that such a detection scheme may be implemented to follow limits set by the standards. Finally, in Chapter 5 the scalability for increasing number of grounding points was addressed. It was shown that with increasing cable lengths the current peaks encountered when load changes occurred increased as well. Furthermore, it was shown that for some specific topology cases this current increase tend to a limit thus showing system scalability without endangering end users.

6.1. Answer to Research Questions

- What is the effect of the capacitor size in the capacitive grounding scheme?

As discussed in Chapter 3 the effect of capacitor value affects primarily the transient behavior during load shifts. Simulations were done to determine how sensitive the system is to this capacitance value and how does affect the protection system. It was determined that the capacitance values should not be smaller than μF since it will have no effect compared with the line capacitance.

Furthermore, since every system may be different it is important to state that if capacitance increases current peaks are also increased in consequence. This means that the protection has to be designed to withstand the peak value of current and consider it in the protection scheme. Moreover, system response to transients and load shifts is also determined by how large the capacitance value is. A higher capacitance value means the system will be more stiff to load shifts but higher current values are likely to happen for more time until steady state is reached again. The most important point for capacitor size may be that load shifting is likely to be limited by a standard value according to the voltage levels on which the capacitive grounding scheme is to be implemented. That is to ensure stability of the system and avoid sensibility problems that may arise due to effects caused by capacitance.

- Can communication for fault triggering be omitted on a radial section of a DC distribution grid?

Fast communication is considered on a radial section in order to improve system sensibility. This because in order to discriminate between ground currents and circulating currents the direction and magniitude of the currents had to be measured in several points of the grid. In addition the device has to be able to read a wide range of values and manufacturing of this protective devices may be hard to achieve.

Communication may be omitted if enough information of the current values can be obtained without the need of another point of information. This can be done in a radial section of a DC distribution grid by means of a detection scheme.

- How can human ground faults and load changes be differentiated on a detection scheme for DC distribution grids?

The approach presented on this thesis is that communication may be needed at some points in the grid but less information may be required if filter devices are installed at the grounding points. It was proven that the filter is able to follow the curve of the IEC standard for DC current flowing through the human body. Furthermore, it was determined that the filter syntheiss to follow other current profiles can be achieved which could make this approach flexible to more system requirements that may be determined from future standards.

- What would be a consequence of increasing the number of grounding points?

As discussed in Chapter 5 with increasing grounding points and longer distribution lines the inductance and capacitance of the cables and grounding points adds up. As a consequence the currents encountered when load changes occur increase as well. Nevertheless, it was shown that depending on the network topology the maximum current peaks may have a limit although further research with different topologies and a higher number of grounding points is needed. Capacitive grounding with their respective detection and protetcion scheme may be a solution for grounding DC distribution grids since the effects of scalability may be overcomed with the right parameters of the detection filter.

APPENDIX A

A.1. SIMULINK SCHEMATICS USED FOR SIMULATIONS

In order to understand the results and simulations a brief overview of the system components will be given. The networks presented are kept as simple as possible in order to exemplify certain parameters at a time. The poles of the networks studied in this thesis are modeled as 350 V.

SOURCE UNIPOLAR

The Unipolar source consists of one DC voltage source with a series resistor modeling the source internal resistance. Figure A.1 shows the block diagram made in Simulink and its internal components.

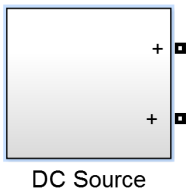

(a) DC Source Block

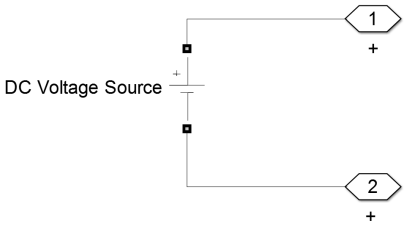

(b) Internal Schematic of the DC Source Block

Figure A.1: Overal DC Unipolar Source Block

BLOCK MEASUREMENT (RCM)

The measurement block implemented in Matlab Simulink its based on the RCM. Figure XX shows the measurement block and its internal components.

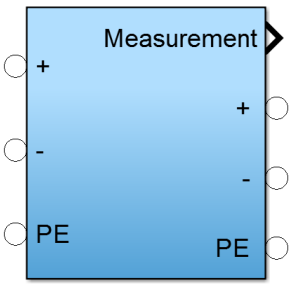

(a) Measurement Block

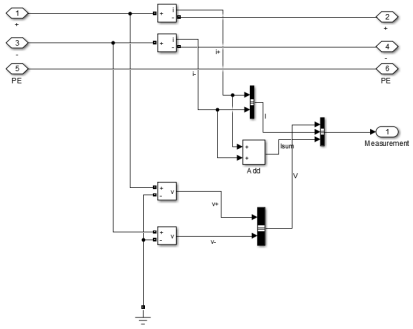

(b) Internal Schematic of the Measurement Block

Figure A.2: Overal Measurement Block

SOURCE BIPOLAR

The source consists of two DC voltage sources arranged in series with a middle conductor in between them. The positive and negative poles have a voltage of 350V with the middle conductor having 0 Volts with respect to ground under normal conditions. Figure A.3 shows the block diagram made in Simulink and its internal components.

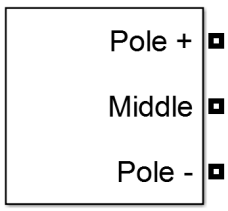

(a) DC Bipolar Source Block

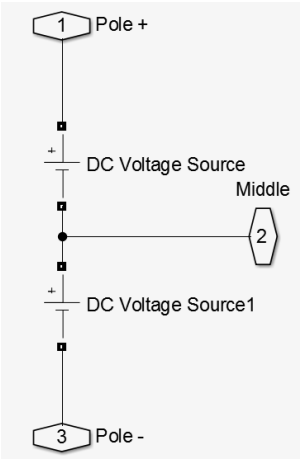

(b) Internal Schematic of the DC Bipolar Source Block

Figure A.3: Overal DC Bipolar Source Block

CABLE

Figure A.4

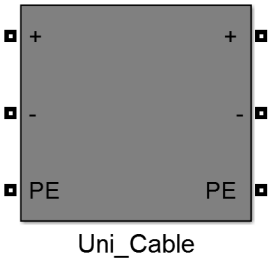

(a) Cable Block

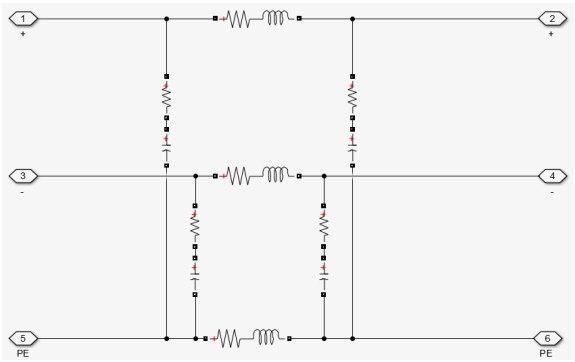

(b) Internal Schematic of the Cable Block

Figure A.4: Overal DC Cable Block

CAPACITIVE GROUNDING

For the capacitive grounding block the schematic consists on a capacitor block with additional mesurement blocks that enable to obtain voltages and current with respect to ground. Look Figure A.5.

Inside the capacitor block a capacitor with two Zener diodes in anti-series configuration as shown in Fig. A.6 The use of this diodes will be further explained on the next sections.

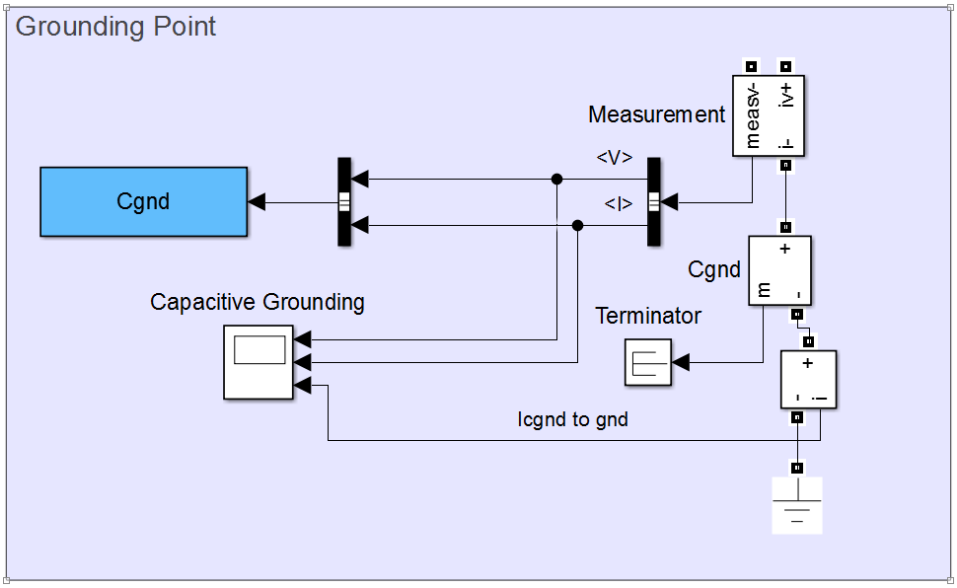

Figure A.5: Capacitive Grounding Simulink Scheme

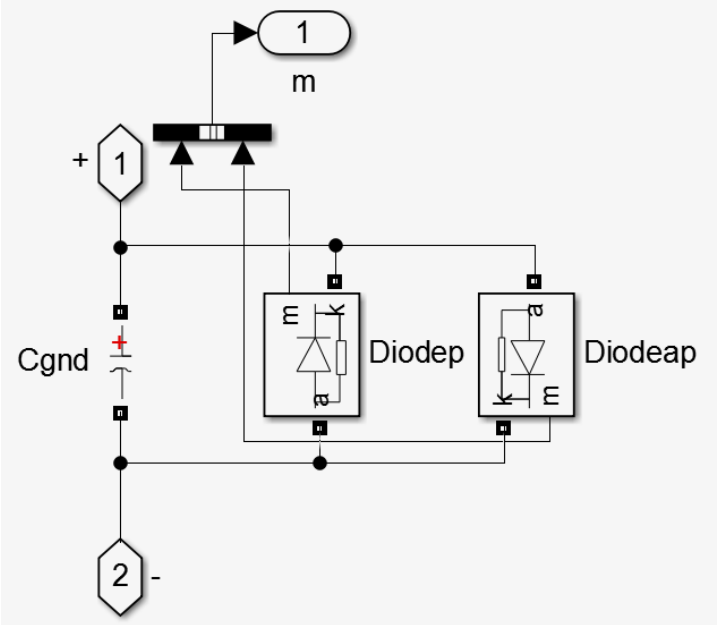

Figure A.6: Iinternal Capacitive Grounding Simulink Scheme

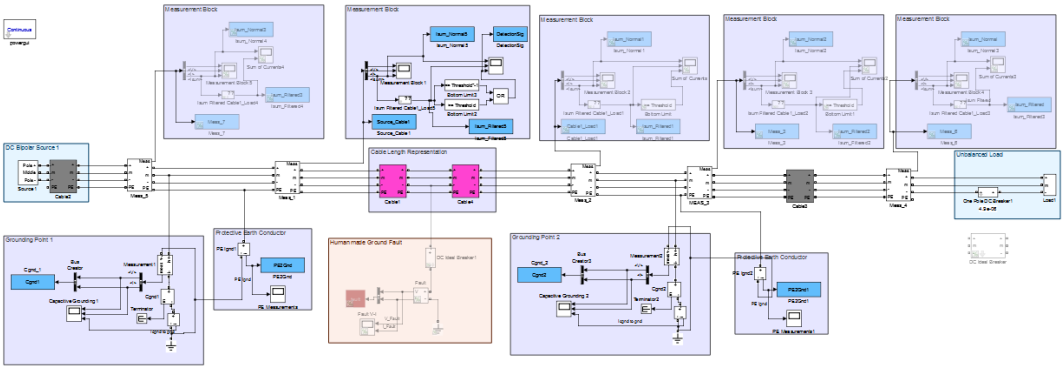

Figure A.7: Bipolar Schematic Simulink

Appendix B

B.1. Conference Paper Capacitive Grounding for DC Distribution Grids with Two Grounding Points

Done in colaboration with Laurens Mackay, Elisabeth Vandeventer, Laura Ramirez Elizondo and Pavol Bauer at the TU Delft University of Technology, Netherlands

Capacitive Grounding for DC Distribution Grids with Two Grounding Points

Laurens Mackay, Kenji F. Yanez Martinez, Elisabeth Vandeventer, Laura Ramirez-Elizondo and Pavol Bauer
Delft University of Technology, the Netherlands
l.j.mackay@tudelft.nl

***Abstract*—Connecting large dc distribution grids on the same voltage level can allow superior utilization of infrastructure. Selective ground fault protection is necessary and can be done using low impedance grounding. Distributed energy resources would allow for higher resilience of the grid if islanding operation of dc microgrids is allowed. For safety, grounding is essential in these islanded microgrids so individual grounding points are needed. Multiple low impedance grounding points would cause dc ground currents that lead to corrosion.**

This paper introduces capacitive grounding which is high impedance in steady-state effectively eliminating ground currents but is low impedance for fault transients and thus can allow for selective ground fault protection. The sensitivity of the capacitor sizing for two grounding points is shown. Further an initial filter for ground fault discrimination is analyzed.

I. Introduction

The emergence of distributed energy resources suggest changes to the traditional ac power system. Most of these resources are dc inherently, or use a dc bus internally, and a majority of the loads connected to the low voltage grid nowadays directly rectify ac to dc before converting the voltage levels using dc/dc power electronic converters. DC distribution grids could remove unnecessary conversion steps and increase the utilization of the components. This can be done inside buildings, but higher benefits could be gained if the complete low voltage distribution grid would be operated on dc. In this case it would still be beneficial if dc nanogrids inside buildings could operate independently in islanding mode in case of faults in the grid [1]. These dc nanogrids may be galvanically connected and only separated by protection devices [2], [3].

Grounding is an important aspect of the protection system of a distribution grid. DC microgrids that are galvanically isolated can have various grounding schemes [4]. High impedance grounding or floating is used often for critical loads such as data centers in order to allow continuous operation in case of a single ground fault [5]. This can be done because the single ground fault current is very low. Ground faults are detected by isolation monitoring. A problem with this approach that fault localization and selectivity is difficult/not possible. Low impedance grounding allows for residual ground fault detection and selectivity using the current sum in the conductors. This is commonly applied for residual ground fault protection in ac grids.

For dc distribution grids each islanded dc nanogrid should have a low impedance grounding point to allow local selectivity. This would result in multiple grounding points in connected (non-islanding) mode and dc ground currents would flow due to difference in neutral potential. This can cause corrosion in metallic structures, e.g, reinforcement steel in concrete and has to be prevented [6].

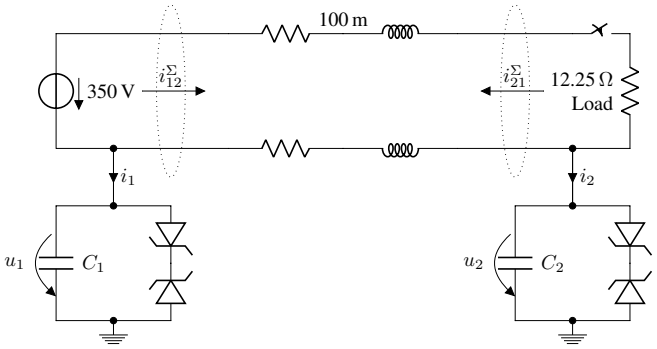

Fig. 1. Unipolar dc grid with two capacitive grounding points with voltage clamping by zener diodes. Source on the left and load on the right.

This paper proposes capacitive grounding for dc distribution grids to prevent dc ground currents in steady state while still providing low impedance during fault transients [7]. The general properties and challenges are described. Additionally a sensitivity analysis regarding the grounding capacitor size for two grounding points is done. Initial filter design to discriminate balancing current from residual ground faults is presented.

The remainder of this paper is organized as follows: In Section II the concept of capacitive grounding is introduced and a unipolar example grid is shown. Further the properties and challenges are described. In Section III a sensitivity analysis is done on the size of the capacitors. The challenges of residual ground fault discrimination are discussed in Section IV and finally conclusions are drawn and future work is indicated in Section V.

II. Capacitive Grounding

For capacitive grounding the neutral wire connected with a capacitor to ground. This is done in each place where otherwise solid grounding would be used, i.e., in each dc nanogrid that should be able to operate in islanding mode. Fig. 1 shows an unipolar example of such a configuration with two grounding points with capacitors C_1 and C_2 connected

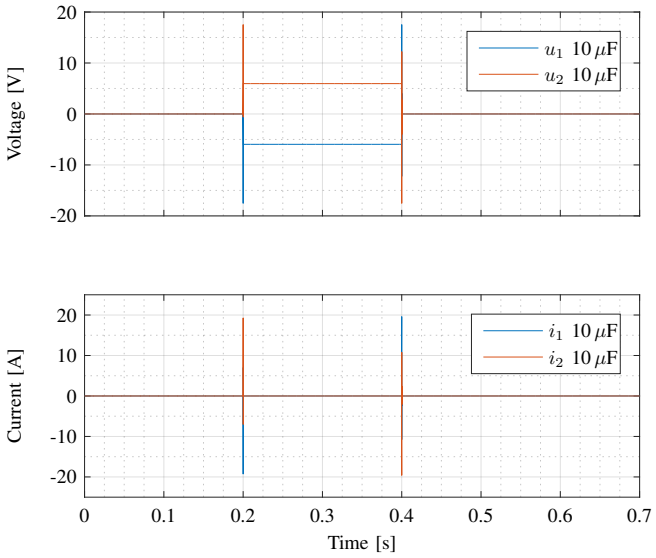

Fig. 2. Unipolar dc grid with load connect (0.2 s) and disconnect (0.4 s). The capacitors are charged to the new voltage of the neutral line when connecting and discharged at disconnect. The voltages are clamped at 17.5 V and the balancing currents are in the magnitude of 20 A.

to the negative conductor. The impedance of a capacitor in Laplace domain is

$$Z_C(s) = \frac{1}{sC}. \tag{1}$$

The main advantage of this grounding configuration is that the impedance to ground is infinite in steady state ($s = 0$). This means that no dc ground currents can flow. In this way corrosion can be avoided. For high frequencies the capacitor impedance $Z_C(s)$ decreases. Thereby it behaves similar to low impedance grounding for fast fault transients. Due to this fact selectivity and short circuit protection can be done similarly as with low impedance grounding.

A. Load Change – Balancing Currents

One challenge that occurs is that the capacitors always need to be charged to the voltage potential of the neutral, respectively grounded wire. This voltage changes depending on the load in unipolar grids, likewise load balance in bipolar grids. In order to charge the capacitors, ground currents will flow at load changes. The charge is depending on the size of the capacitors and relates to voltage and current as

$$u_C(t) = \frac{q_C(t)}{C} = \frac{1}{C}\int_{t_0}^{t} i_C(\tau)\mathrm{d}\tau + u_C(t_0) \tag{2}$$

where $q_C(t)$ is the charge of the capacitor at time t. The current is further dependent on the impedance of the ground loop. In Fig. 2 the simulation of the unipolar grid of Fig. 1 is shown. The load is connected at 0.2 s and disconnected at 0.4 s. The capacitors charge and discharge to the respective neutral voltage potentials. There is a significant overshoot which is caused by the cable inductance. It can be seen that the currents reach values of almost 20 A.

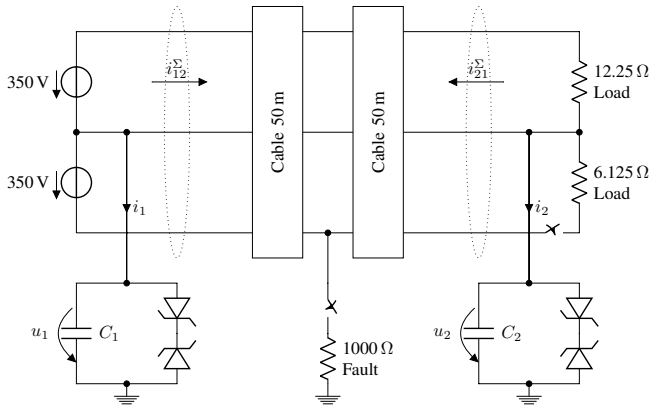

Fig. 3. Bipolar dc grid with two capacitive grounding points with voltage clamping by zener diodes. Sources on the left and asymmetrical loads on the right. The 20 kW load on the negative pole is disconnected to change the load balance. Further a human ground fault can be generated in the middle of the cable of 100 m length.

B. Voltage Clamping

Capacitors are rated for a maximum voltage. A maximum neutral voltage should be specified, in order to limit the cost and size of the grounding capacitors. It is important that capacitors used do not have polarity. This is because the potential of the neutral conductor can go negative. Due to isolation leakage, or other means, the capacitors could charge over time to either their maximum or minimum voltage. Therefore, the voltage across them has to be clamped. A possible implementation are two Zener diodes in anti-series configuration as shown in Fig. 1. For this paper a value of ±5 % of 350 V is chosen, which results in a clamping voltage of ±17.5 V as can be seen in Fig. 2 on the top.

C. Ground Faults

There are two types of faults that have to be considered. The first case is the residual ground fault which would occur when a subject touches a live wire. In this case currents are limited to values lower than 1 A by the relatively large fault impedance (more than 500 Ω). The fault will be cleared by residual ground fault protection within a reasonable time and should not pose a problem for the power limit of the Zener diodes.

In case of a low impedance fault currents would be naturally higher and could easily destroy both Zener diodes and grounding capacitors. Therefore, this grounding scheme is only applicable with a low short-circuit current protection philosophy [8]. Ground faults with potentially high currents would be cleared in the µs range by solid state breakers, such that the energy dissipation in the Zener diodes does not pose a problem.

III. Capacitor Sizing Sensitivity

One of the challenges when using capacitive grounding is the proper sizing of the capacitors. The capacitance will determine the current behaviour during load changes. Therefore,

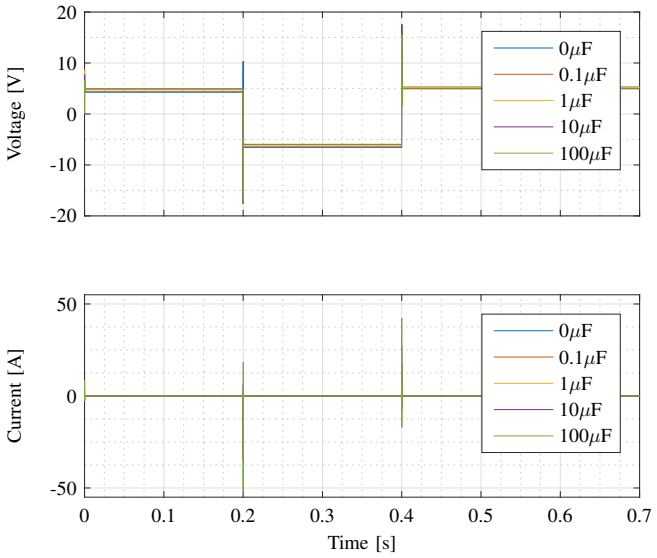

Fig. 4. Sensitivity simulation results for different capacitance values. Top plot shows the voltage of C_1 shown on Figure 3. Bottom plot shows the current flowing through C_2 to ground as shown on Figure 3. Load is initially connected. At 0.2 s load is disconnected and reconnected at 0.4 s, human fault is omitted for this simulation.

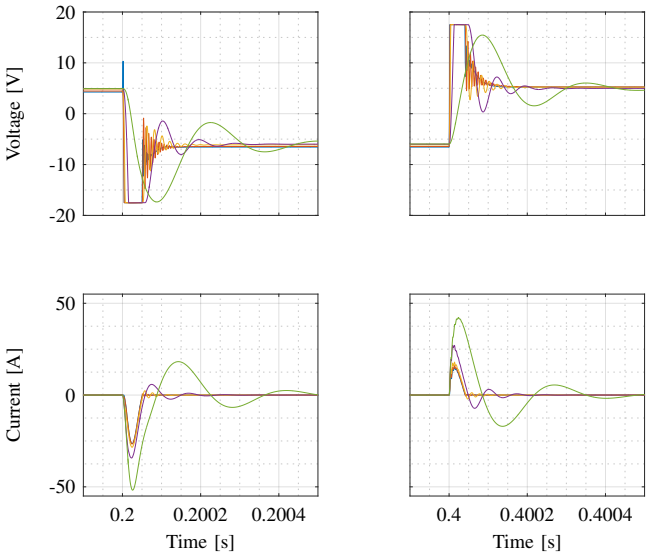

Fig. 5. Zoom for connection and disconnection points of Fig. 4 for both voltage and current. From top to bottom and left to right: zoom of voltage peak at 0.2 s (disconnection), zoom of voltage peak at 0.4 s (Connection), zoom of current peak at 0.2 s (Disconnection), zoom of current peak at 0.4 s (donnection).

TABLE I
CABLE PARAMETERS

Parameter	Value
Cable Resistance	4.61 Ω/km
Cable Inductance	360 μH/km
Cable Capacitance	260 μF/km
Capacitance ESR	10 Ω/km

a simulation is made in order to test the system sensitivity to different capacitance values. Fig. 3 shows the schematic used which consists of a bipolar dc grid system with a 350 V voltage source on each pole and two unbalanced loads of 10 kW on the positive and 20 kW on the negative pole. Two grounding points are included with a connection distance of 20 m both to source and load. A shielded cable with a length of 100 m is assumed and modeled with a Π model, in order to consider the effect of the cable capacitance in the simulation. The cable parameters used are listed in Table I. The cable chosen is relatively thin, which is meant to show in principle a considerable voltage drop in order to make the load change more significant.

Additionally a ground fault on the negative pole is included to emulate a human ground fault. Human impedance is by no means a constant value and depends on many factors. Nevertheless, a reasonable value of 1000 Ω is chosen according to the IEC Standard 60479-5 [9]. The human ground fault is only used in the next section.

Five simulations are made individually, each of them with a different capacitance value. The capacitance values are 0, 0.1, 1, 10 and 100 μF. The 20 kW load at the negative pole is disconnected and connected again at 0.2 and 0.4 s respectively. Fig. 4 shows the voltage and current values of C_1 shown on the schematic of Fig. 3 for the different capacitance values with a total simulation time of 0.7 s.

A zoom on each peak for each plot (voltage and current) is shown on Fig. 5. The color coding of the lines is the same as before. Looking at the 0 μF capacitance case the behaviour is similar to the capacitances of 0.1 and 1 μF, which is a consequence of the parasitic/snubber capacitance of the zener diodes which are modeled on the capacitive grounding points. Moreover, the voltage for the capacitance values of 1 and 10 μF shown on Fig. 5 clamp at 17.5 V which corresponds to the breakdown voltage of the zener diodes.

Furthermore, the system becomes more stiff with increasing capacitance as it is shown for 1, 10 and 100 μF capacitance values. At the moment of connection/disconnection currents around 25 and 50 A corresponding to 1 and 10 μF flow through the capacitors to ground. It is important to note that low capacitance lower to 1 μF are in the order of the cable capacitance value shown on Table I which for further system sensitivity simulations can be omitted. The time it takes for the transients to be no longer relevant to the analysis is less than 0.5 ms which is a relatively fast compared to the time it takes current flowing through the human body to cause irreversible damage [9].

IV. RESIDUAL GROUND FAULT DETECTION FILTER DESIGN

As shown in Section III, relatively high currents occur at the moment of load change. Nevertheless, load changes are a normal behaviour in dc distribution grids and from the protection scheme point of view this needs to be taken into account. This current behavior poses a challenge for

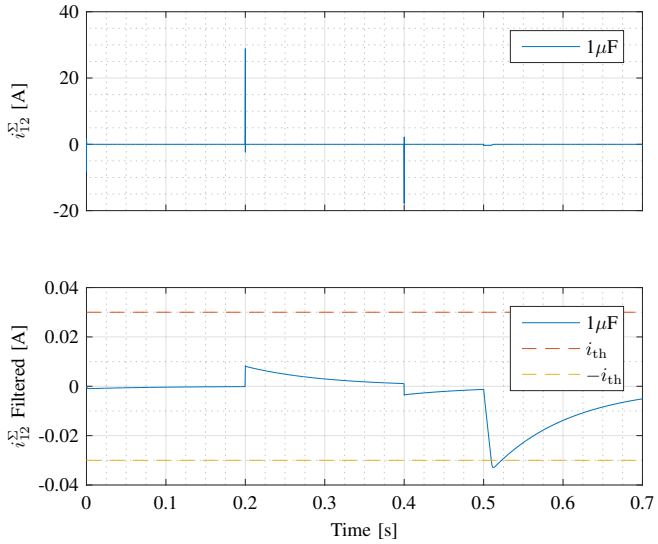

Fig. 6. Current sum measurement and low pass filtered current sum with time constant τ = 100 ms. The negative load is disconnected at 0.2 s and reconnected at 0.4 s. A 1000 Ω residual ground fault of 10 ms duration occurs at 0.5 s. It can be seen that the threshold is only reached for the residual ground fault and not for the balance changes, even though the raw magnitudes (on top) have the opposite relation.

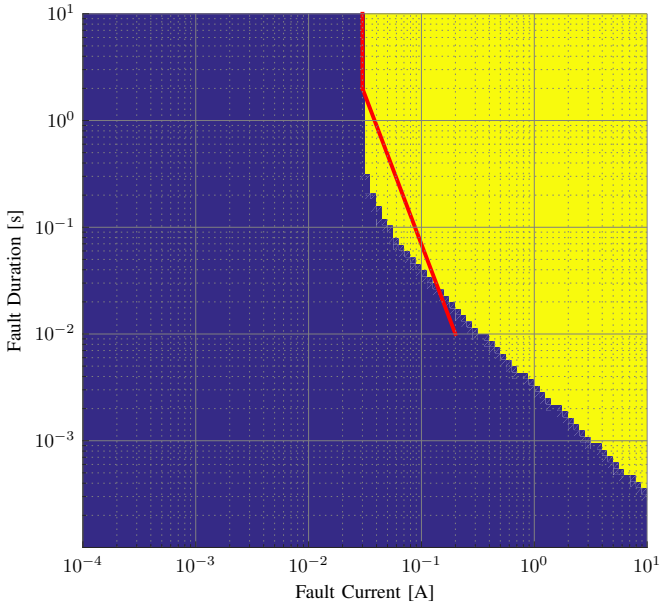

Fig. 7. Detection map for first order low pass filter. Blue color implies no detection from the filter whilst yellow color means favorable detection. Red line shows the limits for currents that may cause permanent damage to human body according to [9].

discrimitating load change currents from human fault currents, as the magnitude of the load change is much bigger than that of the fault. A simulation for a grounding capacitance value of 1 μF is modeled using the schematic in Fig. 3 and including the human ground fault at 0.5 s with a duration of 10 ms. The balancing current peaks can be seen in Fig. 6 on top. The human ground fault can barely be seen at 0.5 s.

For discrimination these measurements are filtered. A first order lowpass filter with transfer function

$$H(s) = \frac{1}{1+\tau s} \tag{3}$$

is used for the sum of currents i_{12}^{Σ} shown in Fig. 3. A time constant $\tau = 100$ ms is choosen for this simulation. A fault is detected when the filtered value reaches the selected current threshold of 30 mA in both the positive and negative direction. Looking at the simulation results shown on Fig. 6 it is easy to see that the duration for both the load change currents and the human fault current serves as discriminating variable for the protection scheme. The high peaks of the balancing currents are very short and thus have only a small effect on the filter output. The small magnitude of the human ground fault is compensated by the duration of 10 ms that is needed to cause considerable harm. In this simulation only the human ground fault filtered current peak the value is higher than the selected threshold value of 30 mA.

If a protection scheme for capacitive grounding were to be implemented using the aforementioned scheme, the filter should follow the IEC standard [9] in order to guarantee safety for all users. Therefore the residual ground fault protection filter is analized for different current magnitudes and fault durations. Thereby a detection map is derived that is shown in Fig. 7. The map consists of currents between 100 μA and 10 A with durations ranging from 100 μs to 10 s. The first order low pass filter has a time constant $\tau = 100$ ms with a detection threshold of 30 mA. For each value of current and time the filter is tested to compare allowed limits according to standard [9]. On Fig. 7 the detection map for the given filter is shown. The IEC standard [9] limits are included on Fig. 7 (red line) to make a proper comparison. The standard only defines te behaviour above 10 ms as traditional ac circuitbreakers can not protect faster anyway. The filter follows approximately the sectors that the standard states for dangerous currents through the human body corresponding to values at the right of the red line. It can be seen that even though the filter detects most of the area located at the right side of the standard, it also has a considerable amount of detection to the left of it.

V. Conclusion

In this paper capacitive grounding was introduced as a possible grounding scheme for dc distribution grids with multiple grounding points. Its advantages are the prevention of dc ground currents in steady state, while still showing low impedance behavior for fault transients. The challenging magnitudes of load change and balancing currents were shown in a sensitivity analysis on the capacitor size for two grounding points. A filter was shown which can discriminate between residual fault currents and balancing currents.

Future work comprises the extension to a multitude of grounding points in order to generalize the system. Further filter synthesis should be done in order to prevent false positives. The boundaries of the applicability have to be identified

and guidelines for capacitor size and line lenghts have to be derived.

REFERENCES

[1] I. S. 142-2007, *Ieee Recommended Practice for Grounding of Industrial and Commercial Power Systems.*, 2007, vol. 142-2007.

[2] L. Mackay, T. G. Hailu, G. R. Chandra Mouli, L. Ramirez-Elizondo, J. A. Ferreira, and P. Bauer, "From DC Nano- and Microgrids Towards the Universal DC Distribution System A Plea to Think Further Into the Future," in *PES General Meeting*. IEEE, 2015.

[3] L. Mackay, N. H. van der Blij, L. Ramirez-Elizondo, and P. Bauer, "Towards the Universal DC Distribution System," *Electric Power Components and Systems, Taylor and Francis*, 2017.

[4] L. Li, J. Yong, L. Zeng, and X. Wang, "Investigation on the system grounding types for low voltage direct current systems," *2013 IEEE Electrical Power and Energy Conference, EPEC 2013*, vol. 6, pp. 1–5, 2013.

[5] T. R. de Oliveira, A. S. Bolzon, P. F. Donoso-Garcia, T. R. de Oliveria, A. S. Bolzon, and P. F. Donoso-Garcia, "Grounding and safety considerations for residential DC microgrids," *Industrial Electronics Society, IECON 2014*, 2014.

[6] R. W. Revie and H. H. Uhlig, *Corrosion and Corrosion Control: An introduction to corrosion science and engineering, 4th ed.*, 2008.

[7] J. Nelson, "Safety through proper system Grounding and Ground Fault Protection," 2015.

[8] L. Mackay, N. Gouvalas, T. Hailu, H. Stokman, L. Ramirez-Elizondo, and P. Bauer, "Low Short-Circuit Current Protection Philosophy for DC Distribution Grids," 2017.

[9] IEC, "TR 60479-5:2007 - Effects of current on human beings and livestock - Part 5: Touch voltage threshold values for physiological effects," 2007.

APPENDIX C

C.1. FILTER SYNTHESIS WITH TC AND THRESHOLD VALUES

The filter simulations for different time constants and threshold values of the first order low pass filter are shown in this section. The plots are presented as following: on the top leftt side the first simulation is presented with a current threshold value of 20 mA and a time constant of 1 ms. To the right side the simulation current threshold is increased per plot up to 100 mA. Furthermore, also from the top left side towards the bottom side the time constant is increased per plot up to a value of 10 ms. Every column increases towards the bottom side only in time constant values and every row increases towards the right side only in current threshold values.

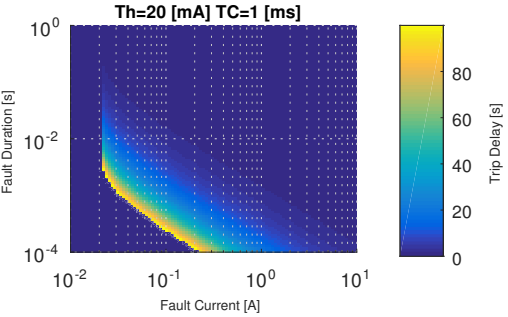
Th=20 [mA] TC=1 [ms]
Fault Duration [s]
Fault Current [A]
Trip Delay [s]

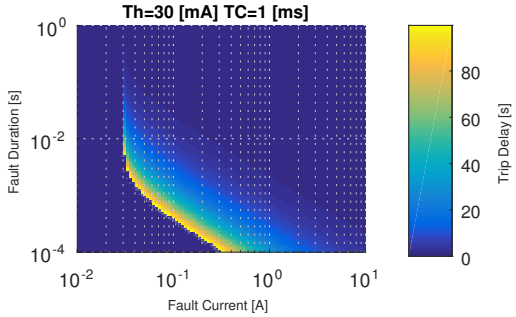
Th=30 [mA] TC=1 [ms]
Fault Duration [s]
Fault Current [A]
Trip Delay [s]

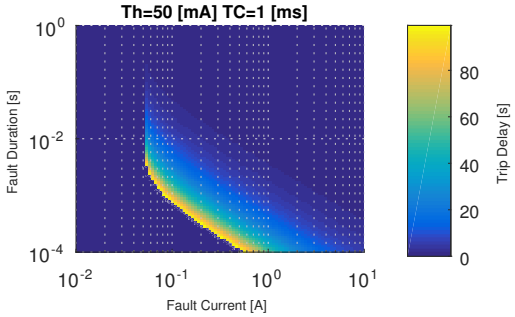
Th=50 [mA] TC=1 [ms]
Fault Duration [s]
Fault Current [A]
Trip Delay [s]

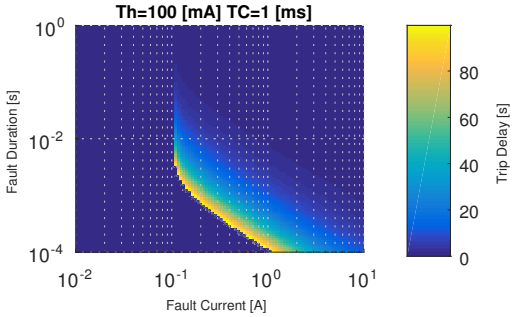
Th=100 [mA] TC=1 [ms]
Fault Duration [s]
Fault Current [A]
Trip Delay [s]

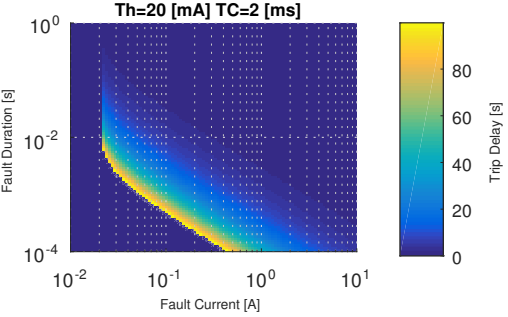
Th=20 [mA] TC=2 [ms]
Fault Duration [s]
Fault Current [A]
Trip Delay [s]

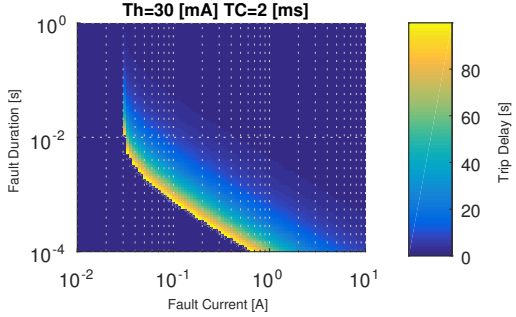
Th=30 [mA] TC=2 [ms]
Fault Duration [s]
Fault Current [A]
Trip Delay [s]

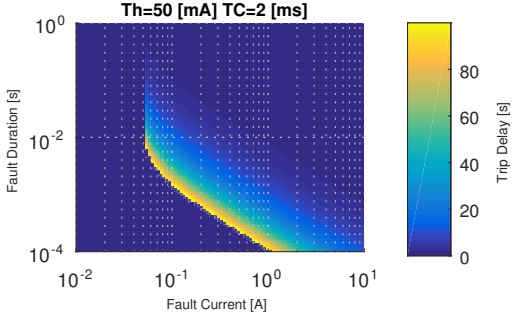
Th=50 [mA] TC=2 [ms]
Fault Duration [s]
Fault Current [A]
Trip Delay [s]

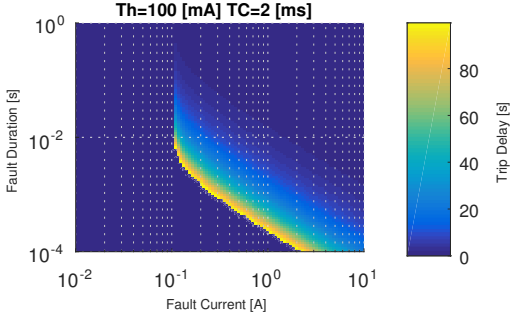
Th=100 [mA] TC=2 [ms]
Fault Duration [s]
Fault Current [A]
Trip Delay [s]

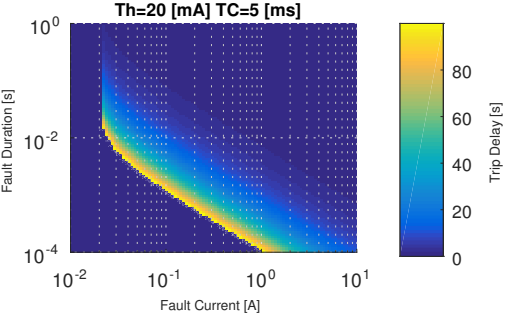
Th=20 [mA] TC=5 [ms]
Fault Duration [s]
Fault Current [A]
Trip Delay [s]

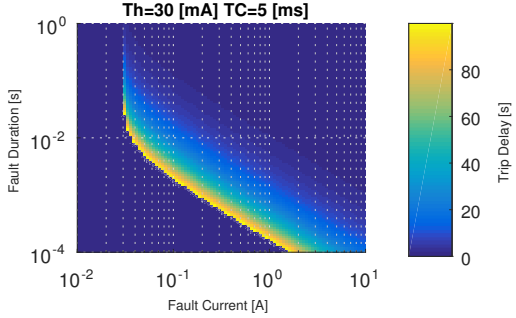
Th=30 [mA] TC=5 [ms]
Fault Duration [s]
Fault Current [A]
Trip Delay [s]

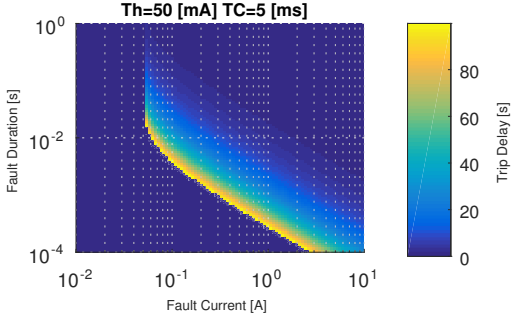
Th=50 [mA] TC=5 [ms]
Fault Duration [s]
Fault Current [A]
Trip Delay [s]

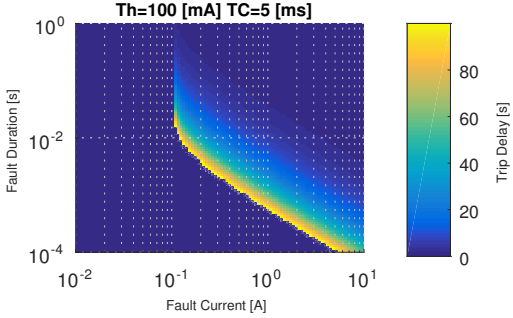
Th=100 [mA] TC=5 [ms]
Fault Duration [s]
Fault Current [A]
Trip Delay [s]

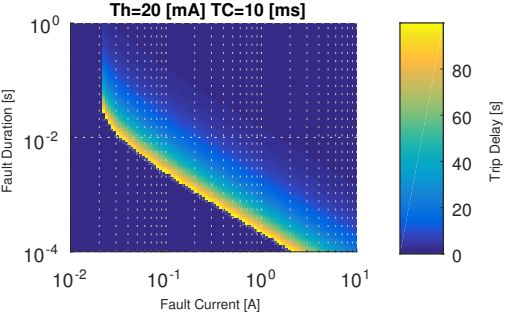
Th=20 [mA] TC=10 [ms]
Fault Duration [s]
Fault Current [A]
Trip Delay [s]

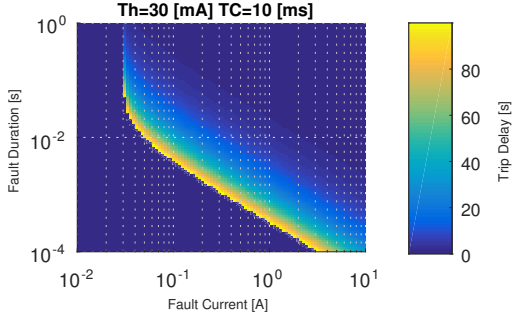
Th=30 [mA] TC=10 [ms]
Fault Duration [s]
Fault Current [A]
Trip Delay [s]

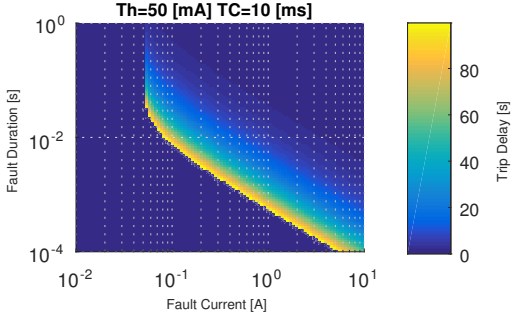
Th=50 [mA] TC=10 [ms]
Fault Duration [s]
Fault Current [A]
Trip Delay [s]

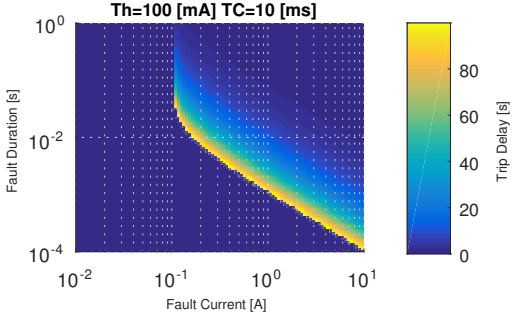
Th=100 [mA] TC=10 [ms]
Fault Duration [s]
Fault Current [A]
Trip Delay [s]

APPENDIX D

D.1. STATE SPACE EQUATIONS DERIVATION UNIPOLAR CIRCUIT

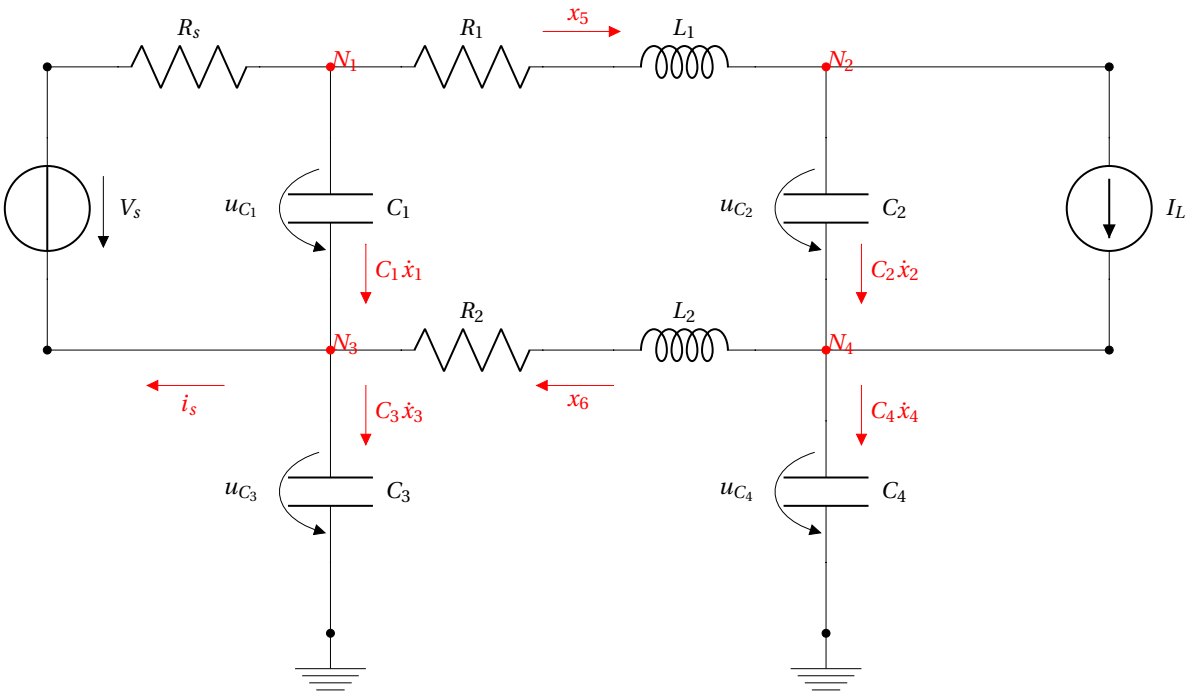

Figure D.1: Unipolar DC grid with two capacitive grounding points model used to assemble state space equations.. Source on the left and load on the right represented as a current source. The cable length for both positive and negative poles is respresented by a series RL circuit (R_1,L_1 and R_2,L_2). The cable capacitance is represented by capacitors connected in parallel (C_1 and C_2) to both poles. Capacitive grounding points are represented as to capacitors connected to ground (C_3 and C_4). Currents and voltages on the pasive components are indicated

KCL for Node 1:

$$i_s = C_1\dot{x}_1 + x_5 \tag{D.1}$$

knowing that:

$$i_s = \frac{V_s - x_1}{R_s} \tag{D.2}$$

Solving for $\dot{x}_1$:

$$\frac{V_s - x_1}{R_s} = C_1\dot{x}_1 + x_5 \tag{D.3}$$

$$C_1\dot{x}_1 = \frac{V_s - x_1}{R_s} - x_5 \tag{D.4}$$

$$\dot{x}_1 = \frac{V_s}{C_1 R_s} - \frac{1}{C_1 R_s}x_1 - \frac{1}{C_1}x_5 \tag{D.5}$$

KCL for Node 2:

$$x_5 = C_2\dot{x}_2 + I_L \tag{D.6}$$

Solving for $\dot{x}_2$:

$$C_2\dot{x}_2 = x_5 - I_L \tag{D.7}$$

$$\dot{x}_2 = \frac{1}{C_2}x_5 - \frac{1}{C_2}I_L \tag{D.8}$$

KCL for Node 3:

$$C_1\dot{x}_1 + x_6 = C_3\dot{x}_3 + \frac{V_s - x_1}{R_s} \tag{D.9}$$

$$C_3\dot{x}_3 = C_1\left(\frac{V_s}{C_1R_s} - \frac{1}{C_1R_s}x_1 - \frac{1}{C_1}x_5\right) + x_6 + \frac{x_1 - V_s}{R_s} \tag{D.10}$$

substituing $\dot{x}_1$ and solving for $\dot{x}_3$:

$$C_3\dot{x}_3 = C_1\dot{x}_1 + x_6 + \frac{x_1 - V_s}{R_s} \tag{D.11}$$

$$C_3\dot{x}_3 = C_1\left(\frac{V_s}{C_1R_s} - \frac{1}{C_1R_s}x_1 - \frac{1}{C_1}x_5\right) + x_6 + \frac{x_1 - V_s}{R_s} \tag{D.12}$$

$$C_3\dot{x}_3 = -x_5 + x_6 \tag{D.13}$$

$$\dot{x}_3 = -\frac{1}{C_3}x_5 + \frac{1}{C_3}x_6 \tag{D.14}$$

KCL for Node 4:

$$x_5 + I_L = C_4\dot{x}_4 + x_6 \tag{D.15}$$

$$C_4\dot{x}_4 = x_5 - x_6 + I_L \tag{D.16}$$

$$\dot{x}_4 = \frac{1}{C_4}x_5 - \frac{1}{C_4}x_6 + I_L \tag{D.17}$$

KVL for Bottom Mesh:

$$-x_5 - R_2x_6 - L_2\dot{x}_6 + x_4 = 0 \tag{D.18}$$

Solving for $\dot{x}_6$:

$$L_2\dot{x}_6 = -x_3 - R_2x_6 + x_4 \tag{D.19}$$

$$\dot{x}_6 = -\frac{1}{L_2}x_3 - \frac{R_2}{L_2}x_6 + \frac{1}{L_2}x_4 \tag{D.20}$$

KVL for Central Mesh:

$$-x_5 + R_1x_5 + L_1\dot{x}_5 + x_2 + L_2\dot{x}_6 + R_2x_6 = 0 \tag{D.21}$$

Substituing $\dot{x}_6$ and solving for $\dot{x}_5$:

$$L_1\dot{x}_5 = x_1 - x_2 - R_1x_5 - L_2\dot{x}_6 - R_2x_6 \tag{D.22}$$

$$L_1\dot{x}_5 = x_1 - x_2 - R_1x_5 - L_2\left(-\frac{1}{L_2}x_3 - \frac{R_2}{L_2}x_6 + \frac{1}{L_2}x_4\right) - R_2x_6 \tag{D.23}$$

$$L_1\dot{x}_5 = x_1 - x_2 - R_1x_5 + x_3 + x_4 \tag{D.24}$$

$$\dot{x}_5 = \frac{1}{L_1}x_1 - \frac{1}{L_1}x_2 + \frac{1}{L_1}x_3 - \frac{1}{L_1}x_4 - \frac{R_1}{L_1}x_5 \tag{D.25}$$

State Space Equations:

$$\dot{x} = Ax + Bu \tag{D.26}$$

$$\dot{x}_1 = \frac{V_s}{C_1 R_s} - \frac{1}{C_1 R_s} x_1 - \frac{1}{C_1} x_5 \tag{D.27}$$

$$\dot{x}_2 = \frac{1}{C_2} x_5 - \frac{1}{C_2} I_L \tag{D.28}$$

$$\dot{x}_3 = -\frac{1}{C_3} x_5 + \frac{1}{C_3} x_6 \tag{D.29}$$

$$\dot{x}_4 = \frac{1}{C_4} x_5 - \frac{1}{C_4} x_6 + I_L \tag{D.30}$$

$$\dot{x}_5 = \frac{1}{L_1} x_1 - \frac{1}{L_1} x_2 + \frac{1}{L_1} x_3 - \frac{1}{L_1} x_4 - \frac{R_1}{L_1} x_5 \tag{D.31}$$

$$\dot{x}_6 = -\frac{1}{L_2} x_3 - \frac{R_2}{L_2} x_6 + \frac{1}{L_2} x_4 \tag{D.32}$$

State Space Matrix:

$$\begin{pmatrix} \dot{x_1} \\ \dot{x_2} \\ \dot{x_3} \\ \dot{x_4} \\ \dot{x_5} \\ \dot{x_6} \end{pmatrix} = \begin{pmatrix} -\frac{1}{C_1 R_S} & 0 & 0 & 0 & -\frac{1}{C_1} & 0 \\ 0 & -\frac{1}{C_2} & 0 & 0 & \frac{1}{C_2} & 0 \\ 0 & 0 & 0 & 0 & -\frac{1}{C_3} & \frac{1}{C_3} \\ 0 & 0 & 0 & 0 & \frac{1}{C_4} & -\frac{1}{C_4} \\ \frac{1}{L_1} & -\frac{1}{L_1} & \frac{1}{L_1} & -\frac{1}{L_1} & -\frac{R_1}{L_1} & 0 \\ 0 & 0 & -\frac{1}{L_2} & \frac{1}{L_2} & 0 & -\frac{R_2}{L_2} \end{pmatrix} \begin{pmatrix} x_1 \\ x_2 \\ x_3 \\ x_4 \\ x_5 \\ x_6 \end{pmatrix} + \begin{pmatrix} \frac{1}{C_1 R_S} & 0 \\ 0 & \frac{1}{C_2} \\ 0 & 0 \\ 0 & 1 \\ 0 & 0 \\ 0 & 0 \end{pmatrix} \begin{pmatrix} V_s \\ I_L \end{pmatrix} \tag{D.33}$$

APPENDIX E

E.1. STATE SPACE MODEL [19]

The differential equations of a linear system can be written in the form:

$$\begin{cases} \dot{x}=Ax+Bu \\ y=Cx+Du \end{cases} \tag{E.34}$$

This system of first order differential equations is known as the state equation of the system, where $x(t)$ is the state vector and $u(t)$ is the input vector. The second equation is referred to as the output equation. A is called the state matrix, B the input matrix, C the output matrix and D the direct transition matrix. One advantage of the state-space method is that the form lends itself easily to the digital and/or analog computer methods of solution. Further, the state-space method can be easily extended for the analysis of nonlinear systems. State equations may be obtained from an nth-order differential equation or directly from the system model by identifying appropriate state variables[19].To illustrate how is the selection of a set of state variables, an nth-order linear model described by a differential equation is considered:

$$\frac{d^n y}{dt^n} + a_{n-1}\frac{d^{n-1}y}{dt^{n-1}} + \cdots + a_1\frac{dy}{dt} + a_0 y = u(t) \tag{E.35}$$

where $u(t)$ is the input and $y(t)$ is the output. A state model for this system is not unique but depends on the choice of a set of state variables. A useful set of state variables, referred to as phase variables, is defined as:

$$x_1 = y, \quad x_2 = \dot{y}, \quad x_3 = \ddot{y}, \quad \cdots, \quad x_n = y^{n-1} \tag{E.36}$$

Taking the derivatives yields:

$$\dot{x} = x_2, \quad \dot{x_2} = x_3, \quad \dot{x_3} = x_4, \quad \cdots, \quad \dot{x_n} = -a_0 x_1 - a_1 x_2 - \cdots - a_{n-1} x_n + u(t) \tag{E.37}$$

Expressed in matrix form:

$$\begin{pmatrix} \dot{x}_1 \\ \dot{x}_2 \\ \vdots \\ \dot{x}_{n-1} \\ \dot{x}_n \end{pmatrix} = \begin{pmatrix} 0 & 1 & 0 & \cdots & 0 \\ 0 & 0 & 1 & \cdots & 0 \\ \vdots & \vdots & \vdots & \vdots & \vdots \\ 0 & 0 & 0 & \cdots & 1 \\ -a_0 & -a_1 & -a_2 & \cdots & -a_{n-1} \end{pmatrix} \begin{pmatrix} x_1 \\ x_2 \\ \vdots \\ x_{n-1} \\ x_n \end{pmatrix} + \begin{pmatrix} 0 \\ 0 \\ 0 \\ \vdots \\ 1 \end{pmatrix} u(t) \tag{E.38}$$

The output equation is given by:

$$y = [1 \quad 0 \quad 0 \quad \cdots \quad 0]\, x \tag{E.39}$$

For electrical networks, the state variables are directly related to the energy-storage elements of the system. Therefore, the number of independent initial conditions is equal to the number of energy-storing elements.

BIBLIOGRAPHY

[1] U. E. I. Independent Statistics and Analisis, Administration, *International Energy Outlook 2016,* (2016).

[2] N. Hatziargyiou, *MICROGRIDS Architectures and Control* (2014).

[3] U. of Southampton, *Sustainable Energy Research Group,* (2009).

[4] N. Hatziargyriou, *MICROGRIDS – Large Scale Integration of Micro-Generation to Low Voltage Grids,* Proc. CIGRE Gen. Session, Paris, France, Paper no. C6-309 (2006), 10.1109/MPAE.2007.376583.

[5] J. J. Justo, F. Mwasilu, J. Lee, and J. W. Jung, *AC-microgrids versus DC-microgrids with distributed energy resources: A review,* Renewable and Sustainable Energy Reviews **24** (2013), 10.1016/j.rser.2013.03.067.

[6] L. Mackay, A. Dimou, R. Guarnotta, G. Morales-Espania, L. Ramirez-Elizondo, and P. Bauer, *Optimal power flow in bipolar DC distribution grids with asymmetric loading,* 2016 IEEE International Energy Conference, ENERGYCON 2016 (2016), 10.1109/ENERGYCON.2016.7513921.

[7] IEC, *TR 60479-5:2007 - Effects of current on human beings and livestock - Part 5: Touch voltage threshold values for physiological effects,* (2007).

[8] L. Li, J. Yong, L. Zeng, and X. Wang, *Investigation on the system grounding types for low voltage direct current systems,* 2013 IEEE Electrical Power and Energy Conference, EPEC 2013 **6** (2013), 10.1109/EPEC.2013.6802975.

[9] L. Mackay, N. H. Van Der Blij, L. Ramirez-Elizondo, and P. Bauer, *Towards the Universal DC Distribution System,* Electric Power Components and Systems **45** (2017), 10.1080/15325008.2017.1318977.

[10] R. M. Cuzner and G. Venkataramanan, *The status of DC micro-grid protection,* Conference Record - IAS Annual Meeting (IEEE Industry Applications Society) (2008), 10.1109/08IAS.2008.382.

[11] R. J. Earley, M. W., Sargent, J. S., Coache, C. D., & Roux, *National Electrical Code*, Tech. Rep. (Mass: National Fire Protection Association, 1999).

[12] W. Leterme, P. Tielens, S. De Boeck, and D. Van Hertem, *Overview of grounding and configuration options for meshed HVDC grids,* IEEE Transactions on Power Delivery **29** (2014), 10.1109/TPWRD.2014.2331106.

[13] IEC, *International Electrotechnical Commision,* .

[14] E. M. Vandeventer, *Residual Current Protection of a Meshed DC Distribution Grid with Multiple Grounding Points,* .

[15] L. Mackay, N. Gouvalas, T. Hailu, H. Stokman, L. Ramirez-Elizondo, and P. Bauer, *Low Short-Circuit Current Protection Philosophy for DC Distribution Grids,* Under Review **11** (2017).

[16] D. Kumar, F. Zare, and A. Ghosh, *DC Microgrid Technology: System Architectures, AC Grid Interfaces, Grounding Schemes, Power Quality, Communication Networks, Applications and Standardizations Aspects,* IEEE Access **3536** (2017), 10.1109/ACCESS.2017.2705914.

[17] L. Mackay, F. K. Yanez, E. Vandeventer, L. Ramirez-Elizondo, and P. Bauer, *Capacitive Grounding for DC Distribution Grids with Multiple Grounding Points,* DC Microgrids, IEEE 2nd International Conference on (2017).

[18] K. Lacanette, *A Basic Introduction to Filters - Active, Passive, and Switched-Capacitor,* Application Note (2010).

[19] S. I. M. F. Rodrigues and Disserta,, *Dynamic Modeling and Control of VSC-based Multi-terminal DC Network,* (2011).